The correlation of the molecular structure of polyolefins with environmental stress cracking resistance

By

Anour Nasser Shebani

Thesis presented in partial fulfillment of the requirement for the degree of Master of Science (Polymer Science)

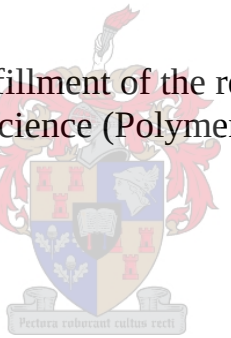

at the

University of Stellenbosch

Study leader: Dr. Albert J. Van Reenen

Stellenbosch
December 2006

DECLARATION

I, the undersigned hereby declare that the work in this thesis is my own original work and that I have not previously in its entirety or in part submitted it at any university for a degree.

Signature:……

Date:…….

Abstract

This study concerns the phenomenon of environmental stress cracking resistance (ESCR) in three impact polypropylene copolymers (IPPCs). The main purpose was to correlate the ESCR with their properties such as microstructure, molecular weight (MW), molecular weight distribution (MWD), crystallinity and morphology.

Initially the selection of a suitable test method and an active stress cracking agent (SCA) were the preliminary concerns. The Bell telephone test was used to evaluate SCAs, while a published procedure for determining ESCR of ethylene based plastics was adapted for the purpose of this study. Isopropanol was selected as SCA. Polymers were fully characterized by FTIR, ^{13}C NMR, DSC and high temperature GPC. Optical microscopy was used to investigate craze formation and crack growth, and scanning electron microscopy (SEM) was used to study the morphology of the polymers.

Since IPPCs are known to have multi-fraction copolymeric structures and each of these fractions has significantly different average properties, fractions were selectively removed from the materials, either by solvent extraction at room temperature, or by TREF fractionation. The effect of removing these fractions on the ESCR was determined. The effect of the molecular composition of the three IPPCs on the ESCR of these materials, as well as the effect of the removal of the selected molecular fractions on the ESCR, morphology and molecular characteristics are discussed and compared. Conclusions are drawn as to the factors controlling ESCR in these materials.

Opsomming

Hierdie studie behels die verskynsel van omgewings-stres-kraakweerstand (ESKW) van drie sogenaamde “impak” propileen kopolimere (IPPCe). Die hoofdoel van die studie was om die ESKW met eienskappe soos mikrostruktuur, molekulêre massa en molekulêre massa verspreiding, kristalliniteit en morfologie te korreleer.

In die begin was die keuse van ‘n geskikte toetsmetode en aktiewe stres-krakingsmiddel (SKM) van belang. Die sogenaamde “Bell telephone test” is gebruik om SKMe te evalueer, terwyl ‘n gepubliseerde metode vir die bepaling van ESKW van etileen-gebaseerde plastieke aangepas is vir die doeleindes van hierdie studie.. Isopropanol is gekies as SKM. Polimere is ten volle gekrakteriseer met behulp van FTIR, ^{13}C KMR, DSC en hoë temperatuur GPC. Optiese mikroskopie is gebruik vir die ondersoeke na kraak-vorming e kraak-groei, terwyl skandeer elektron mikroskopie (SEM) gebruik is om die morfologie van die polimere te ondersoek.

Omdat die IPPCe bekend is as bestaande uit multi-fraksie kopolimeriese strukture, en elk van die fraksies beduidend verskillende samestelling en eienskappe het, is fraksies selektief vanuit die materiale verwyder. Dit het geskied deur beide oplosmiddel-ekstraksie by kamertemperatuur, sowel as deur fraksionering deur kristallisasie (TREF). Die uitwerking van die verwydering van hierdie fraksies mop die ESKW is ondersoek. Die uitwerking van die molekulêre samestelling van die drie IPPCe op die ESKW van hierdie materiale, sowel as die uitwerking van verwydering van fraksies vanuit die materiale op die ESKW, morfologie en molekulêre eienskappe word bespreek en vergelyk. Gevolgtrekkinge word gemaak t.o.v die faktore wat ESKW in hierdie materiale beheer.

Dedicated to:

My Mother, Zohra

and

My Father, Nasser

For their love, support and encouragement and
for giving me the opportunities they didn't have.

ACKNOWLEDGEMENTS

I would like to thank Allah/God for giving me strength, health, opportunity and courage to face my reality. I thank him also for blessing me.

I wish to express my appreciation for my study leader, Dr. Albert J. Van Reenen for his support, advice, and guidance throughout this work. I really appreciate his time and concern.

I sincerely thank the International Centre for Macromolecular Chemistry and Technology in Libya for financial support and encouragement.

I am grateful to Dr. M. J. Hurndall for her assistance and advice on the proofreading of this thesis.

I also would like to express my thanks to all the members of our polyolefins research group at the Institute of Polymer Science at the University of Stellenbosch for their friendship, fellowship, assistance, helpful suggestions, support and encouragement.

I extend my thanks to the people who kindly did my measurements and analysis, especially Jean and Elsa for the NMR analysis, and Esmé Spicer from Geology Department for SEM measurements.

I would like to profoundly thank Dr. K Marcus, from the Materials Engineering Department at the University of Cape Town, for his cooperation and helpful articles.

Lastly and most of all, there are not enough words to thank my family for their continuous love, strong support and unlimited encouragement that I have received over the years. Without them none of this would have been possible. My appreciation is also expressed to all my dear and wonderful friends for their friendship, help and support.

Contents

List of Contents

Chapter 1: Introduction and objectives

Chapter 2: Environmental stress cracking

Chapter 3: Test methods for evaluation of ESCR of plastics

Chapter 4: Experimental work

Chapter 6: Effect of selective removal of fractions on the ESCR

Chapter 7: Conclusions

List of figures

Chapter 2

Chapter 3

Chapter 4

Chapter 5

Chapter 6

List of tables

Chapter 2

Chapter 3

Chapter 4

Chapter 5

Chapter 6

List of abbreviations

ABS	Acrylonitrile butadiene styrene
ASTM	American Society for Testing Materials
BSC	Bottle stress crack test
BTT	Bell telephone test
CTA	Cellulose triacetate
DPM	Dipropylene glycol monomethyl ether
DSC	Differential scanning calorimetry
EPR	Ethylene propylene elastomer
EP rubber	Ethylene propylene random copolymer
EPDM	Ethylene propylene diene rubber
ESC	Environmental stress cracking
ESCR	Environmental stress cracking resistance
ESCR test 1	Bent strip ESCR test / Bell telephone test
ESCR test 2	ESCR test of ethylene based plastics
FNCT	Full notched creep test for testing ESCR of pipes
FTIR	Fourier-transform infrared spectroscopy
HDPE	High density polyethylene
HSP	Hansen solubility parameters
HTGPC	High temperature gel permeation chromatography
ΔH_F	Heat fusion
$\Delta H_{F(100\%)}$	Heat fusion of 100% crystalline polymer
IP	Internal pressure for testing ESCR of bottles
iPP	Isotactic polypropylene
IPPCs	Impact polypropylene copolymers
LDPE	Low density polyethylene
MI	Melt index

$\overline{M_n}$	Number average molecular weight
$\overline{M_w}$	Weight average molecular weight
MW	Molecular weight
MWD	Molecular weight distribution
NMR	Nuclear magnetic resonance spectroscopy
PB	Polybutylene
PBS	Poly butylene succinate
PC	Polycarbonate
PE	Polyethylene
PEEK	Polyether etherketone
PE/EVA	Poly ethylene-co-vinyl acetate
PEs	Polyethylenes
PMMA	Poly methyl methacrylate
PS	Polystyrene
PVC	Polyvinyl chloride
PIB	Polyisobutylene
RH	Relative humidity
RHM / PRHM1	Running hour meter timer
RT	Room temperature
SCA	Stress crack agent
SCB	Short chain branching
SCC	Stress corrosion cracking
SCG	Slow crack growth
SDBS	Sodium dodecylbenzene sulphonate
SEM	Scanning electron microscopy
t	Thickness of the sample in bell telephone test
ΔT	The elution temperature range between each fraction
T_c	Crystallization temperature
TLESCR	Top-load stress crack test for bottles

T_m	Melting point
T_g	Glass transition temperature
TREF	Temperature rising elution fractionation
UV	Ultraviolet
w	Width of the holder in bell telephone test
W	Weight of each TREF fraction
W%	Weight /total weight of sample A x 100
W% / Δ T	Weight fraction percentage divided by the elution temperature range between each fraction
ΣW%	Summation of the [(weight /total weight of sample A x 100)]

Chapter 1
Introduction and objectives

1.1 Introduction

Polymers are well known materials. Unrivaled in the variety of their properties, polymers are used in nearly every industry. Polymers can be naturally occurring or synthetic, the latter making up the bulk of the commercially used materials. [1] The most widely used polymers today are the polyolefins. They account for about half of the total annual plastics production (about 40% worldwide). [2,3] Polyolefins comprise polyethylene (PE), polypropylene (PP), poly(1-butene), poly(1-octene), poly(4-methyl-1-pentene), impact polypropylene copolymers (IPPCs) and ethylene–propylene–diene rubber. [2,4]

The so-called impact polypropylene copolymers (IPPCs) are commercially important. [5] These materials contain, apart from propylene, varying amounts of ethylene. The focus of this study is to determine the difference in the environmental stress cracking resistance (ESCR) of three IPPCs with different ethylene contents. IPPCs are multi-fraction copolymeric structures, and each fraction has significantly different average properties. These fractions include ethylene-propylene (EP) random copolymer or EP rubber, EP segmented copolymers with different sequence lengths of ethylene and propylene and polypropylene homopolymer. [6-9] The effect of these fractions on the ESCR of the materials will be studied by selectively removing some of these fractions and observing the change in ESCR. This change in ESCR can be related to the change in molecular architecture or microstructure, molecular weight, molecular weight distribution, crystallinity and morphology. For example, the presence of EP rubber particles in IPPCs are reported to improve the impact properties, toughness and brittle-ductile transition. [10-11] In IPPCs, impact properties, toughness and the brittle-ductile transition are related to rubber content, rubber particle size, and the interparticle distance. [12] The particle size significantly affects the deformation and failure processes; small particles favour shear yielding while a coarser particle dispersion promotes crazing. [13] Furthermore, the size of particles and interparticle distance govern the ESC process and therefore influence the ESCR. [10]

Although the phenomenon of ESC has been studied for over 50 years, [14-15] there is no mention in the literature of a systematic study of the ESCR of IPPCs. ESC is reportedly one of the most important common causes of polymer failure. [16-19] Since the beginning of recorded history, failure, in general, has been a serious problem in the use of polymeric materials. [20] ESC was first reported in polyolefins by Richard [21] in the 1950s.

ESCR can be defined as the susceptibility of a thermoplastic article to cracking under the influence of certain chemicals and stresses. [22] According to ASTM D883, ESCR is an internal or external crack in a plastic caused by stresses less than its short-time mechanical strength. [23] ESC occurs in amorphous polymers and semi-crystalline polymers. [24] ESCR has enormous industrial and economic implications, [18] and recent reports have shown that ESC is responsible for about 25% of polymer part failures. [25] It can occur any time after manufacturing, especially during storage, transportation, at point of sale or over the long term. [24] It occurs principally in polyolefins and is caused by the combined actions of: mechanical stress, chemical agents or radiation, or both mechanical stress and chemical agents or radiation. [26] The problem of ESC of polymers is prevalent in many different applications. These applications include the packaging industry, such as bottles and containers, the electrical supply industry, such as wire and cable, and the medical industry, such as labware and implant components, etc. [27-28] Scheirs [13] listed the special applications where ESC is likely occur as the following: adhesive bonding and solvent welding, contact between dissimilar polymers, welded assemblies, metal inserts and finally lubricated or moving parts. To reduce failure by ESC plastic product manufacturers should consider: material selection, stress from component processing and the environmental conditions.

There are several standard test methods that have been developed to estimate ESCR of polymers. ESCR tests can be classified into two main types of tests: tests at constant strain (e.g. Bell telephone test) and tests at constant stress (e.g. test methods for determining ESCR of ethylene based plastics). [13,21,25]

1.2 Objectives

The primary objectives of this study were:

1. To find a suitable test method and suitable environmental stress crack agents in order to determine the difference in the environmental stress cracking resistance (ESCR) of three commercial IPPCs with different amounts of ethylene.
2. The correlation of the ESCR with bulk polymer molecular properties like molecular weight, molecular weight distribution and morphology (inclusive of crystallinity and comonomer distribution).
3. Fractionation and characterization on molecular level of the three IPPCs.
4. Correlation of fractional composition and ESCR.
5. Selective removal of fractions from the IPPCs and the study of the effect of these fractions on the ESCR of the materials.

The study would also include studying the craze formation, crack growth with time and finally studying the morphology of these polymers after etching them.

1.3 Structure of the manuscript

Chapter 2 discusses the phenomenon of ESC of plastics. This information includes different definitions of ESC, historical overview, the occurrence of ESC, distinguishing characteristics of ESC, mechanisms of ESC and the most important factors that influence the ESC behaviour. This chapter also describes the failure in semi-crystalline polymers, such as the samples to be tested in this study.

Chapter 3 describes the most important methods available for the evaluation of ESCR of plastics. Several standard test methods are available for evaluation of ESCR. These methods can be classified into two main types of tests: tests at constant strain and tests at constant stress.

Chapter 4 provides experimental detail and material property details.

Chapters 5 and 6 present the results for the objectives as set out in Section 1.2. The results of ^{13}C NMR, HTGPC, DSC, formation of craze, crack growth with time and morphology of the three original IPPCs are discussed in Chapter 5. The results of ^{13}C NMR, HTGPC, DSC analyses, formation of craze, crack growth with time and morphology of the samples after selective removal of fractions are discussed in Chapter 6. Some conclusions are drawn.

Chapter 7 gives a summary of the conclusions reached in earlier chapters.

1.4 References

1. B. Stuart, Polymers Analysis, Biddles Ltd, UK, **2002**, 2.
2. T. Chung, Progress in Polymer Science, **2002**, 27, 39-85.
3. U. Romano and F. Garbassi, Pure and Applied Chemistry, **2000**, 72, 1383-1388.
4. J. Dong and Y. Hu, Coordination Chemistry Reviews, **2005**, 250, 47-65.
5. Z. Xiao, L. Li, D. Zhou, G. Xue, Z. Yuan and Q. Dai, Thermochimica, **2003**, 404, 283-288.
6. H. Tan, L. Li, Z. Chen, Y. Song and Q. Zheng, Polymer, **2005**, 46, 3522-3527.
7. J. Xu and L. Feng, European Polymer Journal (Review article), **2000**, 36, 867-878.
8. J. Xu, L. Feng, S. Yang, Y. Wu, Y. Yang and X. Kong, Polymer, **1997**, 38, 4381-4385.
9. H. Mark, J. Mcketta and D. Othmer, Encyclopedia of Chemical Technology, Second Edition, Executive Editor: A. Standen, Wiley & Sons, USA, **1967**, 14, 299-301.
10. K. Marcus, B. Sole and R. Patil, Macromolecular Symposium, **2002**, 178, 39-53.
11. W. Tam, T. Cheung and R. Li, Polymer Teating, **1996**, 15, 363-379.
12. F. Mirabella, Polymer, **1993**, 34, 1729-1735.
13. J. Scheirs, Compositional and Failure Analysis of Polymer: A Practical Aproach, John Wiley & Sons, UK, **2000**, 546-561.
14. M. Hough and D. Wright, Polymer Testing, **1996**, 15, 407-421.
15. A. Raman, R. Farris and A. Lesser, Journal of Applied Polymer Science, **2003**, 88, 550-564.
16. E. Myer, The Three Amigos of Part Failure, Success, Plastics World, ProQuest Science Journals, **1996**, 54, 25-26.
17. P. Gramann, A. Rios and B. Davis, Failure of Plastics Plumbing Products, The Madison Group: PPRC, Madison, **2004**.
18. R. Galipeau, Plastics Technology Laboratories, Inc., Predicting the Effects of Contact Materials and Their Environments on Thermoplastics Through Chemical Compatibility Testing, Presented at the ANTEC conference, USA, **1995**.
19. F. Al-Saidi, K. Mortensen and K. Almdal, Polymer Degradation and Stability, **2003**, 82, 451-461.
20. W. Brostow and T. Corneliussen, Failure of Plastics, Hanser Publishers, USA, **1986**, Preface.
21. H. Mark and N. Gaylord, Encyclopedia of Polymer Science and Technology, Second Edition, Executive Editor: N. Bikales, John Wiley & Sons, USA, **1971**, 7, 261-289.
22. V. Shah, Handbook of Plastics Testing Technology, Second Edition, John Wiley & Sons, USA, **1998**, 420.
23. BP SOLVAY Polyethylene, Environmental Stress Crack Resistance of Polyethylene, North America, **2001**, Technical publication 9, 1-4.
24. B. Borisova, Investigations on Environmental Stress Cracking Resistance of LDPE/EVA Blends, Ph.D. Thesis, University of Halle Wittenberg, Germany, **2004**, 9-24.
25. J. Jansen, Advanced Material and Processes, **2004**, 162, 50-53.
26. R. Portnoy, Medical Plastics: Degradation, Resistance & Failure Analysis, Understanding Environmental Stress Cracking in Polyethylene by A. Lustiger, Plastic Design Library, **1998**, 65-70.
27. K. Hatada, R. Fox, J. Kahovec, E. Marikhalk, I. Mita and V. Shibaev, Pure and Applied Chemistry, IUPAC Recommendations, UK, **1996,** 68, 2313-2323.
28. A. Siahkali, P. Kingshott, D. Breiby, L. Arleth, C. Kjellander and K. Almdal, Polymer Degradation and Stability, **2005**, 89, 442-453.

Chapter 2
Environmental stress cracking

2.1 Introduction

As was stated in Chapter 1, polymers are important materials, and polyolefins are an important class of polymers, accounting for about half of total annual plastics production and consumption (about 40% worldwide). [1-4] Polyolefins comprise polyethylene (PE), polypropylene (PP), poly(1-butene), poly(1-octene), poly(4-methyl-1-pentene), ethylene–propylene elastomer (EPR) or impact polypropylene copolymer (IPPC) and ethylene–propylene–diene rubber (EPDM). [1,5] They are used in pipes, packaging, wires, cables, etc. [2,6] Polyolefins and polyvinyl chloride (PVC) are also amongst those polymers used in medical applications. [7] Polyolefins in general have an excellent combination of properties such as, low cost, flexibility, strength, lightness, stability, superior processability and is generally easy to recycle. [8] These benefits result from the very nature and structure of these materials. It is possible to produce a large variety of polyolefins. [6] For example, by controlling the monomer, catalysts and process conditions during the polymerization of propylene, it is possible to produce a diverse family of polypropylenes. [9]

Although polyolefins are at the top of the list of commodity polymers, they may fail and suffer from unpredictable behavior during processing, service conditions and environmental conditions. Such factors could shorten the useful lifetime of the materials. Indeed, failure has been a serious problem in the use of polymeric materials since the start of their usage. [9] Associated with an increase in the number of polymer applications with time, this problem will become even more serious. Thus, more focus should be directed to avoiding this problem and extending the lifetime of these materials by improving their performance. This can be achieved in part by understanding the reasons why materials fail.

2.2 Polymer failure

Synthetic polymers including polyolefins do have several disadvantages, including becoming brittle, cracking, failing, etc. Polymeric materials can be affected, *inter alia*, by

environmental conditions, conditions of storage (e.g. time and temperature) and transportation. Failure can be regarded as any change of property that makes the material functionally, structurally and aesthetically unacceptable. [10] Failure could have huge cost implications. Common causes of polymer failure are: environmental stress cracking (ESC), chemical attack, ionizing radiation attack, oxidation, improper processing conditions, incorrect design, excessive performance and bad material selection. [11-15] These can be summarized into four essential factors: the material, the design, processing, and storage, as shown in Figure 2.1.

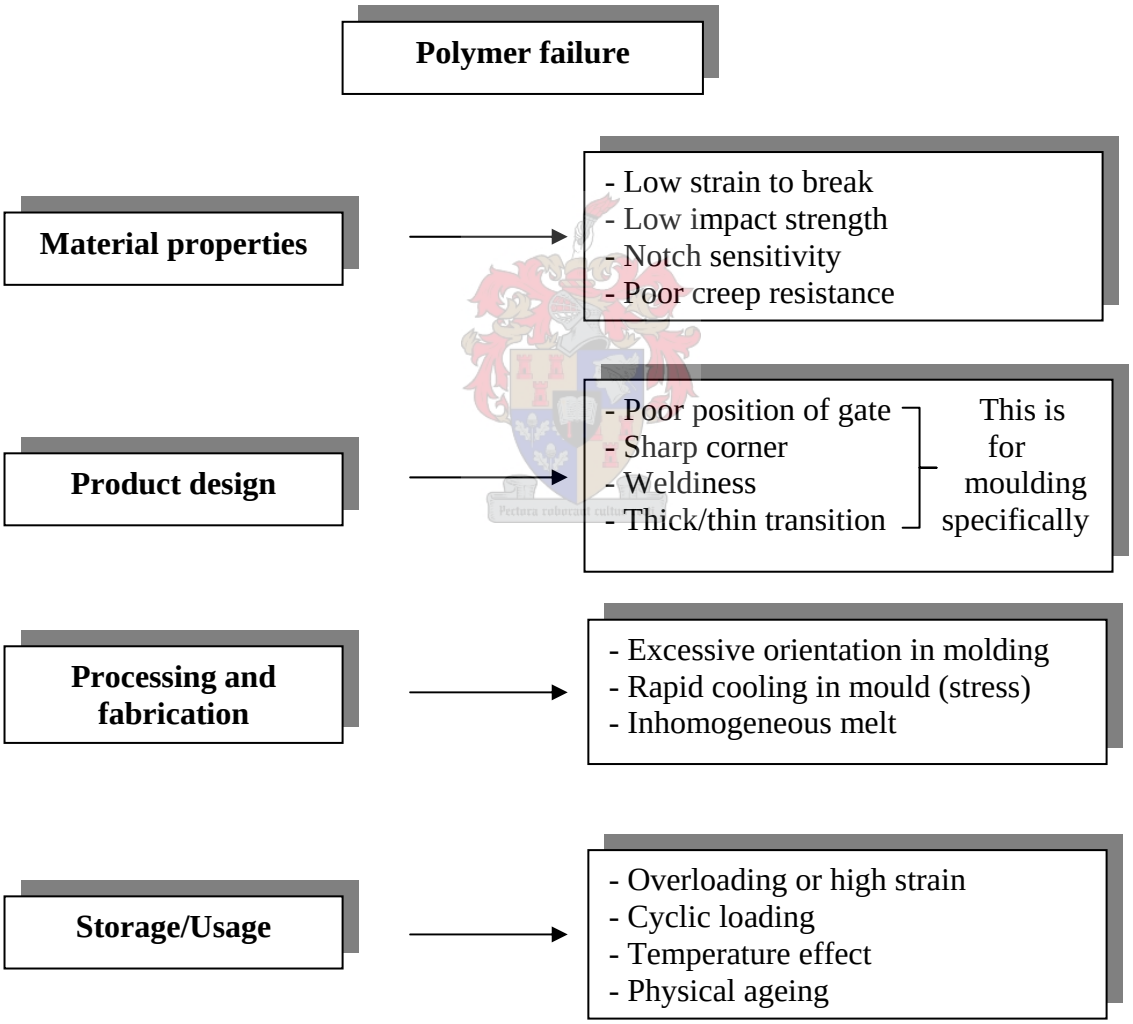

Figure 2.1. Factors that can contribute to the mechanical failure of polymers. [12]

Polymer properties in general are dependent on: molecular weight, molecular weight distribution, crystallinity, orientation and thermal history. Added to this are the wide variety of additives such as fillers, plasticizers, pigments, antioxidants and processing aids. All of these factors have to be taken into account when evaluating failure in plastic materials. One of the most important factors, however, remains molecular composition. [16]

Failure analysis is a very important aspect w.r.t forming a better understanding of the problem of material failure, and to avoid recurrence. Failure analysis can assist in elucidating the failure mechanism, which allows suitable solutions to be sought. The four types of failure that occur in polymers are: mechanical failure, thermal failure, chemical failure and environmental failure. [17-18]

Table 2.1. Relative stability of some unstabilized polyolefins towards various environmental factors [19]

Polymers	Environmental factors			
	Thermal oxidn	Ozone attack	Combustion	Moisture
PE (branched)	Fair	Excellent	Poor	Excellent
PP	Poor	Excellent	Poor	Excellent
Polyisobutylene	Good	Excellent	Poor	Excellent
Polybutadiene	Poor	Poor	Poor	Good
EPR	Fair	Excellent	Poor	Excellent

Many polymers, including some polyolefins, are developed to use outdoors, and they are not supposed to warp, craze, crack, or deteriorate over time. These outdoor polymers are susceptible to various types of environmental factors such as ultraviolet rays (UV), humidity, temperature, microorganisms, ozone, heat and pollution. These are major environmental factors that seriously affect these polymers. This effect can lead to slight crazing and/or cracking or to a complete breakdown of the polymer construction (see Section 2.3). [20] The present study concerns the effect of some environmental factors on some samples of PP “impact” copolymers with different ethylene contents. In fact, as shown in Table 2.1, different polyolefins exhibit different resistance to environmental conditions. [19]

2.3 The effects of the environment

Environmental factors have significant effects on the most polymers. [19,21] The extent of changes in polymer properties can be considered as a sign of a material's long-term environmental stability. The environmental factors shown in Figure 2.2 (moisture, chemicals, high temperatures, irradiation…etc), all tend to weaken or change polymers. [22-23] Most polymers are susceptible to oxidation; oxidation usually leads to increasing brittleness, deterioration in strength and reduction in molecular weight. [2] As the molecular weight decreases most polymer properties also change and this may cause failure.

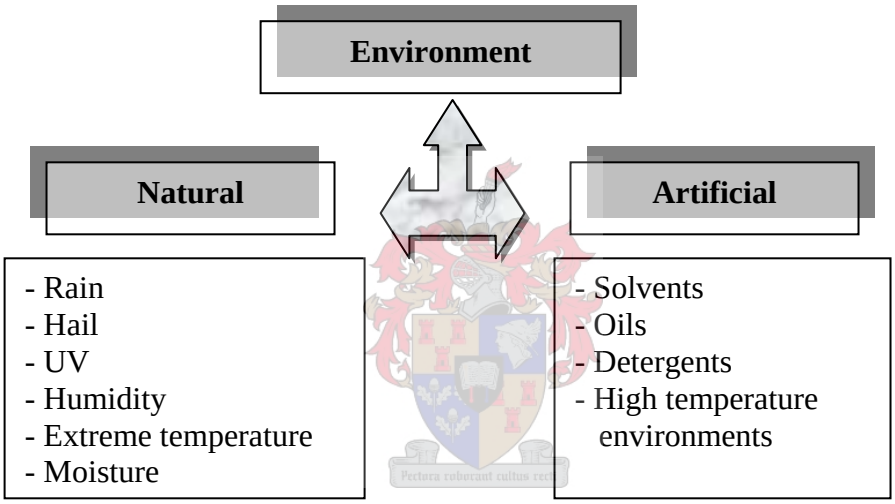

Figure 2.2. Important environmental factors that can affect polymers [24]

Stressed polymeric materials can fail or crack when exposed to certain environmental agents. [24] These agents can be organic liquids such as, fuels, oils and various organic solvents. There are several agents that are surface-active liquids able to lower the polymer surface tension. Upon the exposure to these agents, polymers under stress show a complete breakdown of the polymer construction. [25-26] This is discussed in more detail in Section 2.5.2. For example, although polyolefins including PP resist most organic and inorganic acids, salt solutions, solvents, soaps, detergent and bases below 90^{o}C, they fail or deteriorate in strong oxidizing agents such as fuming nitric acid. [27] The seriousness of the final failure depends largely on a certain factors such as the nature of the environment, the type of polymeric material, the duration of exposure either to the

environment or stresses and indeed the particular grade or formulation. For example, branched polymer chains are considered to be less stable to oxidation than the linear chains. The reason is that the branch points have lower dissociation energy associated with them. The level of crystallinity in a polymer also affects the amount of degradation. High crystallinity, for example, restricts oxygen diffusion into the polymer. [28] It is not always easy to predict the performance of polymeric materials in an unusual environment. It is important to study the effect of the environment on a given polymer to ensure a complete understanding about the failure process in this particular polymer.

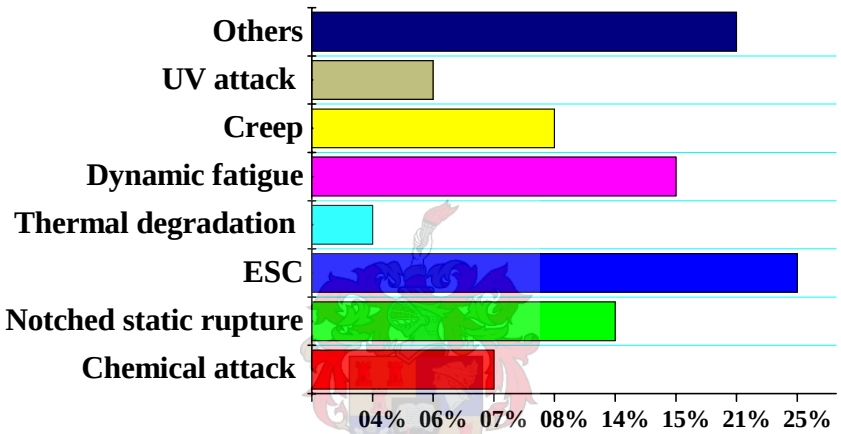

Figure 2.3. Phenomenological causes of failure in polymers [29]

2.4 Environmental stress cracking (ESC)

2.4.1 Introduction

Environmental stress cracking (ESC) is a term for the early failure of a stressed polymer in service, in the presence of active chemical agents. [30] ESC is one of the most important common causes of polymer failure. [31] In metals, this phenomenon is generally termed stress corrosion cracking (SCC). [32] Recent reports have shown that ESC is responsible for about 25% of polymer part failures, as shown in Figure 2.3. [33] ESC is considered as a major problem in terms of long-term service behaviour of polymers. [34] ESC can occur any time after manufacturing, like during storage, transportation or any time during the usage. [10] ESC failure has been encountered in many applications, such as in wires,

cables, and PE bottles. [35] The lifetime of many polymers, like the polyethylenes (PEs), in the presence of stress and active environments is limited. [30]

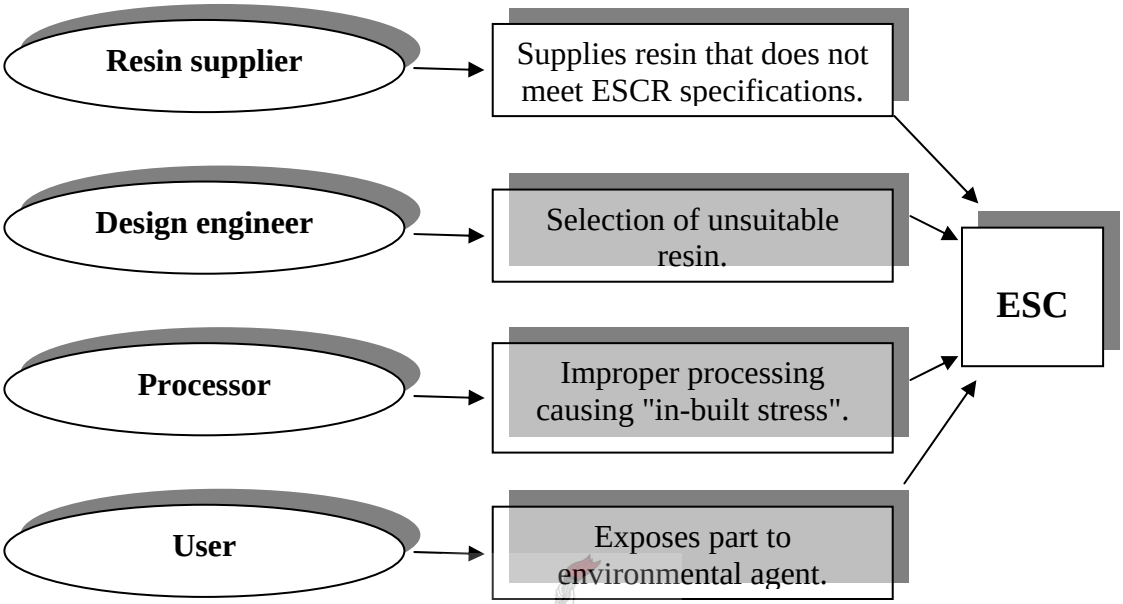

Figure 2.4. Some primary causes of ESC failures in polymers [12]

The synergistic effects of these chemical agents and stresses, which resulting in cracking or failure, is a purely physical occurrence. There is no associated chemical change, degradation or alteration of the material, or any other physical change beyond the development of macroscopically brittle cracks. [36] ESC of polymers is prevalent in many applications, including the packaging industry (bottles and containers), the electrical supply industry (wire and cable), and in the medical supply industry (labware and implant components). [37-38] Some of primary causes of ESC failures are shown in Figure 2.4. In general, to reduce failure by ESC of plastic products three things should be considered: material selection and properties, residual stress (arising from processing) and the environmental conditions.

2.4.2 Definition of ESC

Howard was the first scientist who defined the term ESC. He proposed the following definition of ESC for PE in 1959: "*Failure in surface initiated brittle fraction of a polyethylene specimen or part under polyaxial stress in contact with a medium in the absence of which fracture does not occur under the same conditions of stress*". [39-40]

Galipeau [16] defined ESC as "*the localized cleaving of portions of the intertwined molecular chains in an area of concentrated stress. Most chemicals cannot attack a polymer in an unstressed state. But in the case of ESC, chemicals will attack the area weakened by localized stress, causing a crack or craze*". According to Wright [41] "*ESC is the premature initiation of cracking and embrittlement of a plastic due to the simultaneous action of stress and strain and contact with specific fluids*". Shah [42] defined ESC as the susceptibility of a thermoplastic article to cracking under the influence of certain chemicals and stresses. In other words, ESC manifests itself as cracks that develop when a plastic is subjected to incompatible chemicals and put under stress. ESC, according to ASTM D883 can be defined as "*an internal or external crack in a plastic which is caused by tensile load less than its short time mechanical strength*". [43]

2.4.3 Historical review of ESC.

The phenomenon of ESC has been studied for over 50 years. [44,45] It is reported that ESC was first noted in polyolefins by Richard, early in the 1950s. The term ESC was coined by DeCoste and co-workers. [36] ESC occurs principally in polyolefins and is caused by the combined actions of: mechanical stress, chemical agents or radiation, or both mechanical stress and chemical agents or radiation. [46] Andrews [47] mentions that Howard has reviewed the phenomenology of ESC of polyolefins, while Gent *et al.* have reviewed some aspects of ESC of glassy thermoplastics as part of broader reviews of the crazing and fracture of these materials. This phenomenon has been recognized in other polymers such as poly methyl methacrylate (PMMA), polycarbonate (PC), poly ethylene terephthalate (PET), PVC etc. [48-52] It has been reported [53-54] that most studies on ESC have used a glassy polymer under stress in the presence of an organic penetrant.

The ESC of polyolefins, especially the polyethylenes, have been studied by many groups. [55-62] According to Kawaguchi and Nishimura, [63] Woshinis and Wright studied different types of failure of polymers and found that about one-third of the failures were caused by ESC. They considered ESC as a very interesting phenomenon for both chemists and physicists because this phenomenon involves stress enhanced absorption, permeation, thermodynamics of mixtures, local yielding, cavitation, fibrillation, and fracture. Brown [64] studied the theory behind the ESC of PE and proved that ESC of PE is caused

by stress-induced swelling and plasticization of certain favourably orientated amorphous regions in PE. He believed that the crack resistance normally increases with an increase in MW and with the removal of very low molecular weight materials. DeCoste *et al.* [65] found that when PE is exposed to some chemicals such as alcohols, soaps, and fatty oils under polyaxial stress it fails by cracking. They also pointed out that better crack resistance can be obtained by the selection of a suitable high molecular weight resin or by blending PE with polyisobutylene. Other studies [66] showed that certain PEs can undergo brittle failure under stress in the presence of mobile polar liquids. Nisizawa [67] agreed that the stress cracking or stress failure of polymers such as PE is caused by alcohols as an environmental agent. Bernier and Kambour [68] pointed out that the organic agent plays a controlling role in stress crazing and cracking when a stressed polymer is placed in such an environment. Bandyopadyay and Brown [57] studied the ESC versus to morphology of PE. They showed that failure occurred either in an interlamellar manner within a spherulite, or when lamella matched poorly across an interspherulitic boundary.

This phenomenon was also studied in blends and copolymers. [69-71] Borisova and Kressler [70] studied the stress cracking resistance of a blend of low density polyethylene (LDPE) with random copolymers of ethylene and vinyl acetate (PE/EVA blend) and defined ESC as initiating failure of polyaxially stressed polymer in the presence of certain active agents such as alcohols or soaps, or even wetting agents. They also mentioned that PE can fail in an inert environment at room temperature by slow crack growth. Tatsushima *et al.* [71] investigated ESC in blend films of poly (butylene succinate) (PBS) with cellulose triacetate (CTA) in the presence of sodium hydroxide and found that the addition of CTA into PBS lead to an increase in the ESCR of the blend.

Many workers have focused on the ESC of plastics that are used in medical devices. [72-73] Medical devices should be durable and must be stable under all circumstances as health care devices. Qin *et al.* [73] studied different plastic materials, such as polycarbonate, copolyesters, acrylics, rigid thermoplastic polyurethane and their blends in various chemical agents (certain types of hospital disinfection solutions) that have great impacts on the physical and functional properties of these materials. They found that most of these polymers exhibited the ESC phenomenon. Moskala and Jones [72] considered the study of ESC in medical devices such as luers and stopcocks to be a most important

concern because many modern medical devices are made of plastics, which might fail. For example, using certain chemicals such as isopropanol and lipid solutions might lead to the initiation of crazes or cracks. [45] Wiggins *et al.* [74] studied the effect of strain and strain rate on the fatigue-accelerated biodegradation of polyurethane. They found that polyurethanes can exhibit excellent fatigue resistance and ESC is eliminated if residual stresses are eliminated. They concluded that ESC, at certain rates of strain, can be quite noticeable and that generally an increase in strain will lead to an increase in ESC.

2.4.4 Distinguishing characteristics of ESC

This phenomenon does have several distinguishing characteristics. [75-76] These include:

1. Surface initiation is one of the distinguishing characteristics of ESC. Simply, cracking originates at a surface flaw. Notch-free surfaces have better ESCR.
2. The second distinguishing characteristic of ESC is the appearance of the fracture surface (apparent brittle nature of the fracture). This feature is a "rib and hackle" appearance that is similar to the fracture surface in glass. Figure 2.5 shows a typical ESC surface. [76]
3. Stress is a third distinguishing characteristic of ESC. It is often a combination of externally applied stress in conjunction with internal stresses arising from flow during moulding. Stresses are responsible for final failure.
4. The presence of external sensitizing agents/stress crack agents, such as detergents, is the fourth distinguishing characteristic of ESC. These agents are polar and mobile. These agents do accelerate the failure process of polymers.

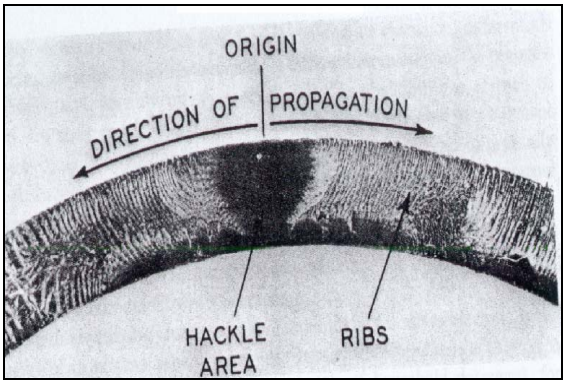

Figure 2.5. Typical ESC surface [76]

Jansen [34] mentioned that ESC failures share several typical characteristics and listed them as the following: brittle fracture, multiple cracks, smooth morphology, craze remnants, stretched fibrils and alternating bands. Most of the distinguishing characteristics are discussed in following sections in more detail.

2.4.5 The occurrence of ESC

ESC is exhibited by most types of polymers. ESC occurs in amorphous polymers (e.g., polystyrene (PS), PC, PVC, etc.) and semi-crystalline polymers (e.g., PE, PP, polybutylene (PB), etc.). [77]

Amorphous polymers are particularly susceptible to ESC, more so than crystalline materials. [78] For example, amorphous polyether ether ketone (PEEK) absorbs 100 times the quantity of environmental stress crack agents than semi-crystalline PEEK does. [79] However, not all amorphous polymers are susceptible to ESC, for example, PVC is remarkably resistant to ESC. [80] Some amorphous polymers exhibit the enhancement of this failure close to their glass transition temperature (T_g). This is because of the increase in free volume as T_g is reached; hence more environment stress crack agent can permeate into the polymer. [77]

On the other hand, semi-crystalline polymers also can undergo ESC under stress in the presence of stress cracking agents. The important factor in semi-crystalline polymers is the presence of tie-molecules that connect amorphous and crystalline regions. [81] Tie-molecules in semi-crystalline polymers play a huge role under these circumstances (load or stress and stress crack agent). They play a vital role in transferring stress from one lamella to the next lamella when strained. [82] The influence of the polymer microstructure on environmental stress crack resistance (ESCR) has been related to the presence of these tie-molecules. [61] The roles of tie-molecules are discussed in more details in the following section. Amongst semi-crystalline polymers, different polymers suffer ESC to different extents. It has been found [83-84] that PP can undergo ESC but does not suffer as much as PE. PP is less resistant to degradation than PE, [78] but has better ESCR. In both amorphous and semi-crystalline polymers ESC is strongly dependent on the concentration of stress crack agent, exposure temperature and time, polymer properties and the level of stress. [77]

2.4.6 A graphic model for failure

Commonly, the failure in semi-crystalline polymers can be either ductile or brittle, depending on the stress (levels and times of exposure), environmental conditions (e.g. stress crack agents, temperature, etc.) and the material itself. [77] Brittle failure occurs by rapid crack propagation without any deformation (little or no energy absorption mechanisms are involved), whereas ductile failure is characterized by extensive gross plastic deformation (significant energy absorption mechanisms are involved in deformation). Kennedy *et al.* [85,86] studied the tensile properties of a wide range of linear PEs and random ethylene copolymers and found that all the copolymers and the higher molecular weight grades of the linear PEs showed ductile behaviour, whereas a ductile to brittle transition was observed in the lower MW linear PEs. Butler *et al.* [87,88] proved the occurrence of brittle failure of low MW HDPE. Lustiger [39] demonstrated that ESC in PE occurs because of interlamellar failure, caused by the relaxation of tie-molecules. This type of failure can be better evaluated through constant tensile stress or load testing. To describe the deformation process in semi-crystalline polymers, it is important to know that there are three types of intercrystalline materials, as shown in Figure 2.6A. These types of materials are:

- cilia: chains suspended from the end of a crystalline chain,
- loose loops: chains that begin and end in the same lamella, and
- tie molecules: bunches of chains that begin and end in adjacent lamellae.

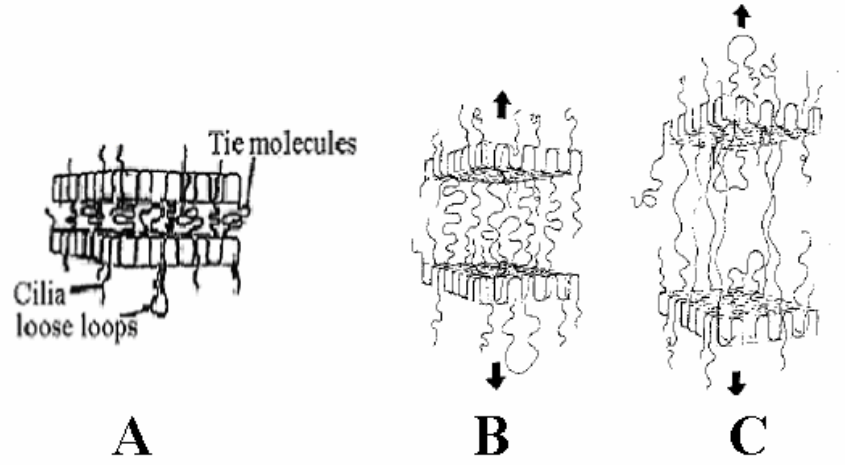

Figure 2.6. Three types of intercrystalline or amorphous polymer chains and initial steps in the deformation of PE [39]

As mentioned earlier, tie-molecules play an important role in the deformation process of semi-crystalline polymers and have been used to explain both ductile and brittle modes of failure. [89] These tie-molecules act to produce ductile deformation. It is presently thought that the material consists of lamellar crystals, separated from each other by a layer of amorphous polymer and held together by tie-molecules through the amorphous phase. [90] If a tensile stress or load is applied normal to the face of lamellae, these tie-molecules stretch in the direction of stress, as shown in Figure 2.6. If such crystalline polymer is subjected to an external stress, it undergoes a re-arrangement of crystalline material. The polymer chains then will align in the direction of the applied stress. [91] The tie-molecules continue stretching and chains traverse adjacent lamellae with time, as shown in Figure 2.7a. At certain point, however, the tie-molecules pulled out no further. At this time the lamellae break up into smaller unit, as shown in Figure 2.7b. These so-called "mosaic blocks" are directly incorporated into new fiber morphology (Figure 2.7b). The reason for this is that the tie-molecules essentially are the "cement" holding the lamellae "bricks" together. Their integrity is critical for ductile-type behaviour to occur. [39]

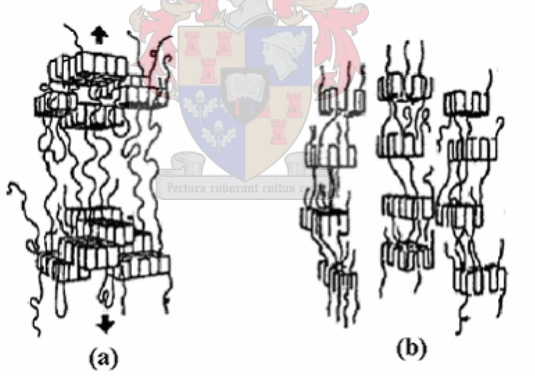

Figure 2.7. Steps in the ductile deformation of PE [39]

On the other hand, the brittle-type of failure occurs over longer periods of time at lower stress levels than the ductile deformation discussed above. Brittle failure is a complete fracture of the specimen of polymer in a direction perpendicular to the direction of loading. [92] The first steps in brittle deformation are similar to those illustrated in Figure 2.6. However, the stress necessary to achieve large-scale fiber pull out is not attained because the material is under lower stress level. Therefore, the loading situation can be expected to remain as shown in Figure 2.6 for a relatively long time, although under long-

term low level stress, tie-molecules can begin entangle and relax. After a finite period of time, most of the tie-molecules untangle, so that ultimately the load can not be supported by the few tie-molecules remaining, and, as a result, the materials fails in a brittle manner. Thus, the material passes from the state in Figure 2.6 to that of Figure 2.8. [39] The stress-cracking agents penetrates voids plasticization the materials and promotes lamellae separation, as shown in Figure 2.8. They accelerate the brittle-failure process. They will lubricate the tie-molecules and that will facilitate their pull out from the lamellae.

There are two important factors that should be taken into account in this process. First, the total energy needed for brittle failure to occur is really made up of two components: crack initiation energy and crack propagation energy. [80] Polymers in general fail in the manner which corresponding to the lowest energy necessary to produce failure. If the energy to produce brittle failure is higher than the energy necessary to produce tough failure, so the sample will fail in a tough manner and vice versa. Second, the resistance of this failure will depend upon the number of tie-molecules. [64] The higher the concentration of tie-molecules present the greater the ESCR will be. Lu *et al.* [93-94] claimed that the number of tie-molecules and the strength of the crystals are the most important and controlling factors.

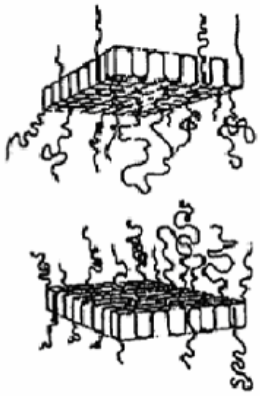

Figure 2.8. Final step in the brittle failure of PE [39]

Ductile deformation is preferred for two reasons. First, brittle failure occurs suddenly and catastrophically without any warning, while the presence of plastics deformation for ductile failure gives warning that failure is imminent, allowing preventive measures to be

taken. Second, ductile materials are tougher than brittle materials and more energy is required to induce ductile failure. [95] The deformation process (ductile or brittle) depends on stress levels, time considerations, polymer morphology, molecular orientation, molecular weight, molecular weight distribution, degree of crystallinity, drawing conditions, etc.

2.4.7 Mechanism of ESC

ESC can be a three-stage process: initiation of a craze, crack growth, followed by propagation of the crack to failure. [96] These three stages can be described as follows:

2.4.7.1 First stage

The first stage is craze initiation. Crazes are planar crack-like defects, where the two faces of the craze are bridged by thin or secondary fibrils. [97-98] These crazes contain highly voided material having a fibrilar structure. These voids will increase the permeability and allow the chemicals from the environment to penetrate into the polymer, causing plasticization or craze initiation. Initiation is thought to be a three-stage process. [98] These stages are:

1. The development of regions of microporosity.
2. These microporosities agglomerate into stable voids.
3. An extension process whereby the void areas form the characteristic craze geometry. That is why ESC is named either environmental stress *crazing* or *cracking.* [99] ESC can be used to describe the crazing that occurs under stress in the presence of certain chemical agents.

2.4.7.2 Second stage

The second stage is the crack growing stage. It is a propagation step, the growing craze breaks down to form a crack and then the crack propagates or grows. [100] The propagation of the craze can be split into three considerations: kinetics, interfacial stress and breakdown. As the crack propagates, more crazes are produced at the crack tip and so on. These crazes act as initiation sites for cracks. [98] The newly formed crazes grow again due to the chemical agents from the environment along the craze, leading to further

plasticization of the craze tip and weakening of the craze fibrils. Crazes break down again to form cracks. These steps will repeat themselves until final failure occurs. The diffusion and rate of absorption of the chemical agents/stress crack agents into the polymer structure play a dominant role in this step. These agents are able to move more rapidly than a growing crack. The faster the stress crack agents are absorbed the faster the polymer will be subjected to this failure.

2.4.7.3 Third stage

The final stage is the occurrence of final failure, and the lifetime of a material is limited in this step. A complete breakdown of the polymeric part occurs in this stage.

An important fact about the craze is that craze morphology and breakdown are largely dependent on the molecular weight of the material. The craze width and length increases with up to a limiting value, whereafter dimensions remain stable. [98] For example, at low molecular weight, the interpenetration and entanglement of coils are so small that fibril formation is extremely difficult, whereas at high molecular weight, there are large number of entanglements per chain which give strong fibrils (more resistance to slippage and disentanglement). The critical molecular weight is that at which craze dimensions become stable.

2.5 Important factors influencing ESC behaviour

Many factors are known to play a dominant role in influencing of the ESC behaviour of a polymer. Stress crack agents, temperature, level of stress or strain in/on polymers, polymer morphology, molecular weight, molecular weight distribution, co-monomer content, type of co-monomer, orientation, environmental conditions, etc., may all be considered as important factors which can affect the ESC behavior of a polymer. [12,37,39]

Li [101] claims that ESCR can be affected by two main factors. These factors are polymer properties and non-polymer factors. He listed the non-material factors as the following; molecular weight, residual stress, temperature, design and the interacting solvent. However, the most important factors influencing the ESC behaviour of the polymer are listed in Figure 2.9.

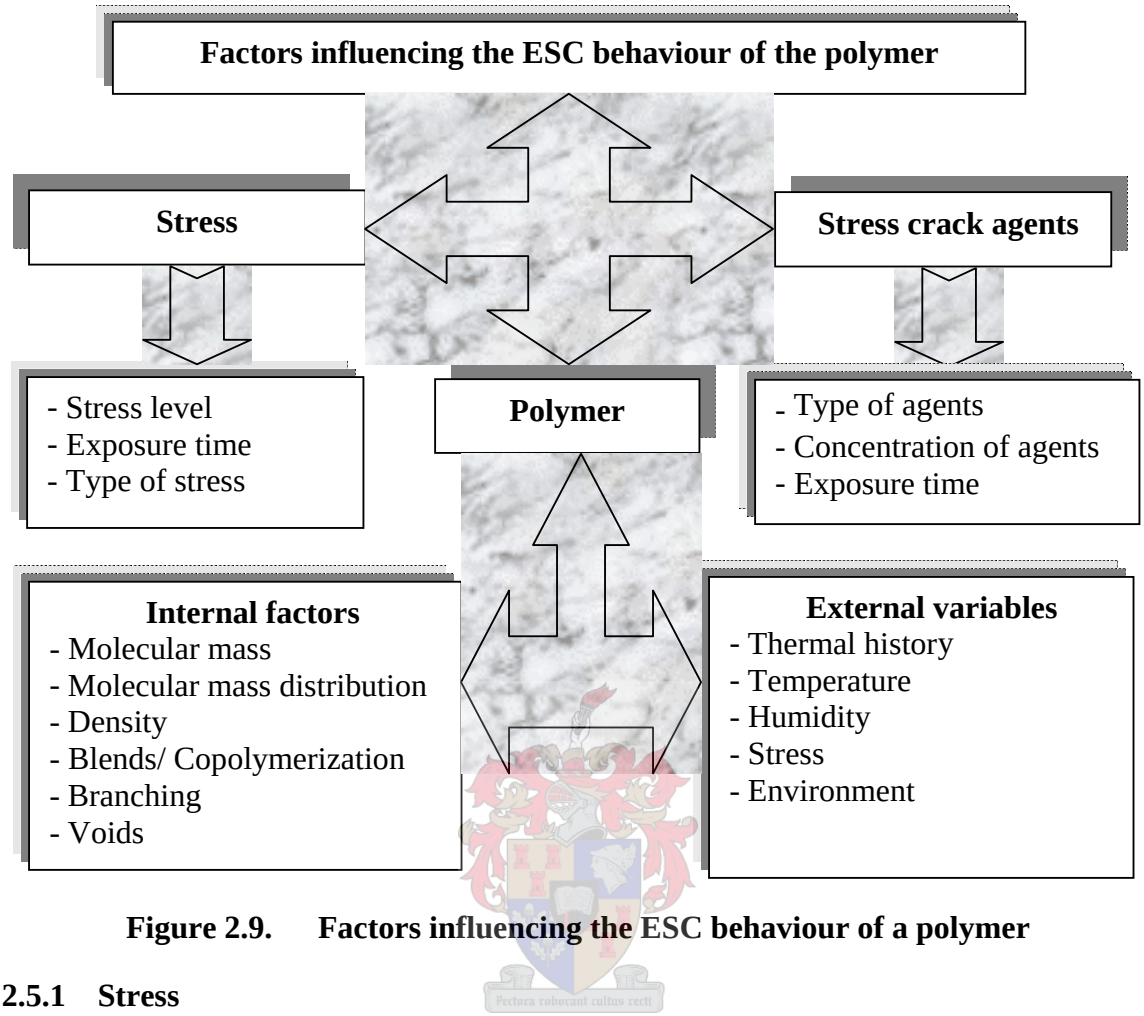

Figure 2.9. Factors influencing the ESC behaviour of a polymer

2.5.1 Stress

Stress can be defined as the internal distribution of forces within a body that balance and react to the loads applied to it. Most stresses accelerate polymer deterioration in many ways (e.g. autoxidation of polyolefins can be accelerated by introducing the sample to stress). The ESC failure that occurs in polyolefins is a typical example of deterioration under stress. [20] In most cases these stresses are left in or added to the polymer during moulding or in use. [48] These stresses can be internal or external, or both. [34,48] External stresses can be considered as tensile stress [77] and may be due to improper packing or storage, incorrect use, etc. Although it is hard or even impossible in some cases to predict residual stresses, they are an important concern in order to prevent polymeric materials from failure. In most thermoplastics, particularly PE, these stresses must be polyaxial for ESC to occur rapidly, except if the material is of low molecular weight. Brown [64] proved that stress cracking initiated more rapidly under polyaxial stresses than uniaxial stresses.

The higher the stress, the shorter the time for failure to occur. [52,96] Arnold [102] claims that at intermediate stresses, the time of failure depends on the ability of stress crack agents to flow into the growing cracks and accelerate the propagation step. At low stress, these agents are able to flow into a growing crack and maintain contact during propagation, causing failure, while at high stress, failure is due to the high applied tensile stress, before ESC occurs.

2.5.2 Stress crack agents

All chemicals that are absorbed by a plastic in a short time can be considered as active stress cracking agents (SCAs) for that particular plastic. [77] The effectiveness of these agents is dependent on temperature, time of exposure, and the chemical concentration. According to studies [37] these agents are usually mobile and polar liquids, but they may be gaseous or in paste or gel form. These agents move far more rapidly than the growing crack. [103] Diffusion of these agents into the polymer due to stress might result in an increase in the chain mobility, therefore, reducing the activation energy of the deformation process. [31] Furthermore, they lower the cohesive forces between crystalline and amorphous regions. [77] In general, the diffusion in polymers will be dependent on a number of factors such as the molecular size, physical state of the diffusant (e.g. viscosity may influence the craze growth rate; the higher the viscosity the slower the craze rate), the morphology of the polymer, the compatibility or solubility limit of the solute within the polymer matrix, and the volatility of the solute. [104-105]

The solubility parameters of the SCAs and the polymer play a significant role in ESC. ESC in polymers involves both the solubility and rate of absorption of the SCA. ESCR decreases when the solubility parameters of the SCA and the polymer are similar. Calculating solubility parameters, particularly the Hansen solubility parameters (HSP), has proven to be useful to predict ESC. There are more than 800 chemicals with known HSP values. [106-107]

Hansen and Just [108] found that the solubility parameter of a stress cracking agent is a measure the cohesive attraction between liquid molecules. The HSP quantitatively represent the nonpolar (atomic) bonding, the permanent dipolepermanent dipole (molecular) bonding, and the hydrogen (molecular) bonding, as shown in Figure 2.10. If

the solubility parameter of the polymer matches that of the chemical agents or stress cracking agents, then the diffusion of these agents will occur and ESC (ductile behaviour) is likely to take place. Solubility relations have been correlated with HSP and can be calculated as described in reference 108.

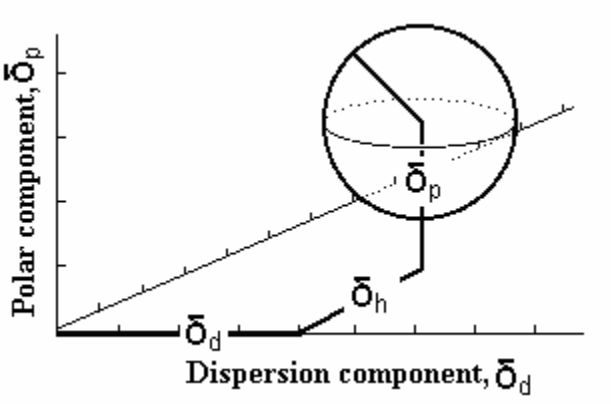

Figure 2.10. Hansen solubility parameters [108]

Polymers will swell more as the concentration of the penetrating liquid is increased. [109] The effect of increasing the amount of chemicals that diffuse into the polymer include the following: [110]

- the introduction of surface compressive stress which can hinder the craze formation,
- localized diffusion along voided zone (promotes crazing),
- easier void formation with a pre-plasticized surface layer (earlier craze formation),
- plasticization at front of growing flaws, thus hindering their development, and
- overall softening of the material, giving a substantial reduction in strength.

Stress crack agents can be organic liquids such as aromatic and halogenated hydrocarbons, ethers, ketones, aldehydes, esters and nitrogen and sulphur containing compounds. They can also be aliphatic hydrocarbons and liquids with strong hydrogen bonds such as water and alcohols. [77] These agents may be hydrophilic, like typical surfactants, or hydrophobic, like the silicones. [76] Borisova [77] considered the following solvents as typical SCAs causing ESC in most amorphous polymers: petroleum ether, carbon tetrachloride, toluene, acetone, ethanol and chloroform.

Table 2.2. Classification of materials as SCA for PE

Active (surface active)	Inactive (not surface active)
Alcohols	Water
Liquid hydrocarbons	Polyhydric alcohols
Organic esters	Sugars
Metallic soaps	Hydrolyzed protein
Sulphated and sulphonated alcohols	Rosin
Silicone fluids	Selected asphalts
	Selected saponins
	Acid and neutral inorganic salts

Wright [110] divided SCAs into three categories: mild, moderate and severe. All chemicals that are significantly absorbed by a polymer in a short period under simple immersion conditions have a high probability of being severe SCAs for that particular polymer. Dipropylene glycol monomethyl ether (DPM) is the best example of a severe ESC agent for acrylonitrile butadiene styrene polymers (ABS). An important fact associated with this type of agent is that solubility is not essential for severe stress cracking. On the other hand, most ESC problems encountered in-service are due to moderate SCAs. Following stress free immersion polymers may reveal no significant weight gain and no detectable change in mechanical properties. They would be classed as chemically compatible, but in the presence of stress will result in cracking. The time to crack depends upon the level of stress or strain. Mild agents are chemicals or fluid that reduces the lifetime of a polymer from say 20 years to 10 years then for most products this would not be regarded as a serious matter even if the case could not be retrospectively identified. Mild agents are often difficult to detect and are therefore difficult to avoid. Some gases such as helium, nitrogen, and hydrogen have been shown to be mild craze growth enhancers in polystyrene at 25 ^{o}C. [111] According to Borisova [77] these agents are surface-active liquids which are able to lower the polymer surface energy but do not cause any swelling or dissolving of the polymer. In fact, some of these agents may have a huge effect on a polymer; while others produce no effect at all on the same polymer. For example, certain

SCAs were tried on PEs and were classified in terms of their ability to cause cracking (active or inactive), as shown in Table 2.2. [65,66]

2.5.3 Polymer properties

The resistance of polymeric materials to ESC depends on the factors shown in Figure 2.9. Amongst these factors are the properties of the polymer itself, and can be divided into the following two important types: [37, 103]

1. Internal factors: these factors include MW, MWD, branching, degree of crystallinity, blends, voids and crosslinking.
2. External factors: these factors include thermal history, humidity, and temperature.

Other factors include: the type of polymer grade, the additives, the lamellar orientation, and the production of polyolefins either by metallocene or Ziegler-Natta catalysts.

2.5.3.1 Internal factors

Molecular weight

Many physical properties of a polymer, including the resistance to ESC, vary depending on the molecular weight. Materials with low molecular weight stress crack easily, while those with high molecular weight may not crack at all, or only after a much longer time. [112-113] Longer chains have more entanglements and therefore make SCA migration more difficult. [114] Additionally, the longer the polymer chain, the greater the number of tie-molecules and therefore, the increased ESCR. Hence, higher molecular weight improves ESCR. [115] In fact, during exposure, PEs ranging in molecular weight from 67,000 to 158,000 exhibited an increase in the rate of crack growth as the molecular weight decreased. [116] On the other hand, the narrower the molecular weight distribution is, the better the ESCR would be, while broadening the molecular weight distribution has the opposite effect, so that narrow molecular weight distribution and high molecular weight are desirable. [116] Yoon *et al.* [117] mention that polyolefins with narrow molecular weight distribution and a sufficient degree of long chain branching combines the excellent mechanical properties of polyolefins such as impact properties, tear resistance, ESCR, and tensile properties.

Crystallinity

Crystallinity is an indication of the amount of crystalline regions in a polymer with respect to the amorphous content. Higher density or crystallinity means higher tensile strength and greater propensity to stress cracking over time. Thus, as density decreases, ESCR generally increases. [39,43,103,117] Crystalline polymer is a mixture of regions of different degree of order ranging all the way from completely ordered crystallites to complete amorphous regions. As the stress on sample changes due to applied stress, the amount of these regions changes continuously. Also, in crystalline polymers the relatively large crystallize are bound together in such away that large stress concentrations inevitably develop. [118]

According to Soares *et al.* [61] related the influence of crystallinity on ESCR to the formation of tie-molecules. It would be expected that the more crystalline materials, the fewer amorphous intercrystalline tie molecule that hold it together. [39] The tie-molecules bind the lamellae and provide the strength, so, as the number of tie-molecules increases, strength and ESCR increases. This can be dependent on the density of the tie molecules and the strength of the crystals. [61]

Polymer density or crystallinity can be controlled by the level of the short chain branching (SCB). In general increasing the SCB, up to a limit, will enhance the probability of tie-molecule formation. The amount of SCB present in the molecular chain depends on the polymerization conditions. [114] It has been found [60] that an increased degree of branching in PE causes a substantial decrease in crack growth rate, simply because highly branched polymers have a higher density of tie-molecules and lower crystallinity. Thus, as SCB increases, so does ESCR due to the decrease in crystallinity. The type of α-olefin comonomer also plays an important role. For the same comonomer content, longer SCBs (higher α-olefins) increase ESCR. Increasing the size of SCBs decreases the chance for this co-crystallization to occur and, hence, the increase in the formation of tie-molecules. [61] So, the higher comonomer content and longer comonomer SCBs (higher α-olefins) provide less crystallinity and better ESCR. Lustiger [117] stated that “it would be expected that the more crystalline the material, the fewer amorphous intercrystalline tie-molecules that hold it together”.

Blends and copolymers

Blends and copolymers may exhibit better ESCR compared to the individual homopolymers. For example, ethylene/acrylate copolymers exhibit better ESCR than the homopolymer of ethylene. [20] Lagaron *et al.* [118] explained the difference in ESCR between the homopolymer and the copolymer as follows "the large difference in ESCR between homopolymers and copolymers might be understood by comparing the molecular relaxation behaviour of these materials. A copolymer did not show the same molecular stress as a homopolymer when strained to the stress level, which implies that a higher molecular mobility (molecular relaxation) might occur in the latter sample". The ESCR of polymers, including polyolefins, particularly PE, can be improved by blending with rubber or elastomeric material. [71,75] Spenadel [75] proved that blending of some elastomeric materials such as polyisobutylene (PIB), butyl rubber (copolymer of isobutylene and isoprene), a copolymer of ethylene and propylene (EPM) and a terpolymer of ethylene, propylene and a non-conjugated diene (EPDM), to PE can improve its resistance to ESC. This improvement in ESCR was found to increase as the rubber concentration increased. With some polymers the addition of rubber doubles the ESCR, while with others a hundredfold improvement can be achieved. Spenadel reported that the butyl rubber was found to be a most effective elastomer for PE, and the PIB rubber was better than EPDM and EPM. DeCoste *et al.* [65] agreed that a blend of PE with PIB showed improvement in ESCR. PIB has a plasticizing effect on PE, and when used in large enough percentages, it produces highly flexible and rubber-like materials. The main reason for this improvement is the low moduli of the blends, and their greater tendency to relax under stress. [75]

Voids

Voids can be one of the most common causes of product failures. It is important to know that voids and cracks can cause internal stress to a polymer and lead to premature failure because they allow the SCA to diffuse into that particular polymer. Voids generally act as stress concentration points and are the likely places where cracks begin. These voids seem to generate points of stress concentration and potential crack initiation sites, especially in higher void levels. Under increased stress/strain voids grow and

coalescence, until finally a complete failure occurs. For example, ductile failure occurs as a result of the nucleation, growth and coalescence of voids in the polymer. In most cases, the rate of nucleation of the voids, rate of growth of the voids and the mechanism of coalescence are the most important factors controlling the polymer failures if the voids are present in this particular polymer. The effect of these factors increases with the increase in the level of stress. However, voids will obviously cause a dramatic decrease in ESCR. [37,76,103]

Crosslinking

Crosslinked materials demonstrate better properties, such as improved resistance to heat, less creep, better chemical resistance, and ESCR than their linear counterparts. In general the effects of crosslinking on ESCR are precisely what might be predicted from extremely high molecular weight. In fact, crosslinking affects increases in molecular weight and improved strength at interface boundaries. [37,103] For example, crosslinked PE has significantly improved performance compared to high performance linear resins, as shown in Table 2.3. [119]

Table 2.3. Comparison between linear and crosslinked PE [119]

Properties	Linear PE	Crosslinked PE
Range of chemical compatibility	Excellent	Excellent
Impact resistance	Good	Excellent
Weatherability	Excellent	Excellent
Stress crack resistance	Fair	Excellent
Initial material cost	Excellent	Good
Recyclability	Poor	Poor
Abrasion resistance	Good	Excellent

2.5.3.2 External factors

Thermal history and processing conditions can influence ESCR behavior of polymers. [77] For example, thermal history plays a dominant role in the formation of crystals and the development of residual stresses. The amount of crystallinity in a polymer is dependent on the thermal history of the polymer, while the residual stress levels increase with an

increase in the thermal gradients through the thickness of the material. It is well known that the degree of crystallinity can be affected by the cooling rate. The cooling rate affects both the degree of crystallinity and therefore the spherulite texture. The polymer becomes amorphous by heating to above its melting point (T_m). It will then crystallize during slow cooling (enough time for crystalline area to develop), while if quench it, it may not be as crystalline as in slow cooling (not enough time for crystalline area to develop as in slow cooling). Quenching tends to reduce somewhat the overall crystallinity and to limit severely the sizes of the crystallites and spherulites. [37] It leads to increase the ESCR. This increase in ESCR is due to the formation of small lamellae, a large amorphous interspherulite boundary and an increase in the number of tie-molecules, whereas slow cooling has the opposite effect; it allows large crystals to form. [103] In fact, slow cooling tends to augment crystalline content, produce large spherulites, and small amorphous interspherulite boundaries. As spherulitic growth tends toward the extreme, the amorphous materials remaining in crystal interfaces presumably becomes strained, due to competition of crystallization forces from adjacent regions, and voids may develop. This leads to decrease the ESCR. [37] DeCoste *et al.* [65] found that the crack resistance in quenched in PEs samples was better than PEs that had been annealed. He claimed that the difference observed between quenching and annealing is probably associated with the degree of crystallinity that obtained. Ebnesajjad [11] pointed out that fast cooling or quenching at the end of the fabrication process serves to reduce the crystallinity content and increase the amorphous content which results in an increase in ESCR.

ESCR is extremely sensitive to temperature. In general, increasing/decreasing the ambient temperature has a profound effect on cracking performance. There is a general exponential decrease in time to failure with increasing temperature. It is well accepted that stress cracking is governed by crack growth rates which can be accelerated by increasing temperatures. Temperature can also affect the chemical resistance. As temperature increases, resistance to attack decreases. Thus, a higher temperature will result in a shorter time to material failure. Lustiger [39] reported that the crack-growth data generated for PE suggests that for every 7 °C increase in temperature, the crack-growth rate is doubled. The effect of temperature on ESCR is quite complex, however, an increase in temperature does not always lead to shorter time to failure. Borisova and

Kressler [70] studied the effect of temperature on ESCR in LDPE/EVA blends and found that the time to failure was shorter at 50 ^{o}C than at 30 ^{o}C and at 70 ^{o}C. They explained this by saying "it could be the result of semi-crystalline material of EVA melting (above T_m of EVC), and thus the particles are deformed more easily under the influence of stress".

On the other hand, some polymers are affected by humidity. For example, properties such as mechanical properties of polymers vary because of their environmental conditions, such as temperature, humidity and so forth. [120] Ishiyama *et al.* [121] studied the effect of humidity on ESC behaviour in PMMA and proved that the crazing behavior is strongly influenced by water sorption. He found that at low and medium humidities (relative humidity (RH) of about 54%), the number of craze initiation sites (craze density) increased with increasing humidity, and the lengths of crazes decreased gradually. In contrast, at high humidity (RH about 98%), a few long crazes grew rapidly, and the specimen broke in a short period. These results indicate that ESC occurs in engineered polymer structures even by water vapour in air. He concluded his study by saying that the sorbed water in the craze at the crack tip strongly affects the craze strength.

2.5.3.3 Other factors

Different polymer grades exhibit varying degrees of ESCR. For example, some grades of PE have very good resistance against ESC, while some have a marginal effect. Spenadel [75] found that low-density polyethylene (LDPE) that contains 3.4% vinyl acetate provides the best stress cracking resistance of any of the other grades when blended with butyl rubber.

Additives such as pigments, fillers, stabilizers and plasticizers can have an effect on the ESC behaviour of a polymer. Spenadel [75] studied the effect of fillers and plasticizers in PE and PE/rubber blends and found that the addition of additives to these polymers had the effect of increasing the MI, broadening the MWD and reducing ESCR. The effect of fillers on ESC was also found in some PVC applications such as installed pipes. These fillers may improve initial performance but they can affect the long-term performance of these pipes, and exhibit ESC. [120] On the other hand, pigment also has an effect on polymer properties, including ESCR. Borisova [77] claimed that increasing the pigment

content usually decreases the ESCR. Lustiger [122] showed that increasing the organic pigment content leads to a decrease in ESCR behaviour, while an inorganic pigment content has the opposite effect. Lustiger [122] has listed all the factors that have profound effect on ESC of a polymer, including the additives, as shown in Table 2.4. Finally, stabilizers can be effective in one polymer and ineffective or even act as a sensitizer in another polymer. For example, a nickel complex of 2,4-pentanedione was found to increase the outdoor stress-crack life of PP while reducing that of PE. [123]

In the case of lamellar orientation, the lamellae would be more susceptible to interlamellar failure if they oriented perpendicular to the direction of the stress than if they oriented parallel to the stress. This can be minimized in the case of a spherulitic PE, since the lamellae in spherulites are oriented radially. [39] Raman *et al.* [45] found that the oriented specimens cracked at lower stress than their unoriented counterparts. They mentioned the influence of the direction of propagation of the cracks by saying "in oriented polymers the crack always formed parallel to the film orientation".

Finally, polymers that are produced using metallocene or Ziegler-Natta catalysts exhibited different ESCR. Although not much attention has been given to this difference, some studies [124] have discussed it. Metallocene technology allows producing controlled polymers and improving their properties. Unlike other polyolefins, the structure, molecular weight and molecular weight distribution, of metallocene catalyzed polymers are relatively easy to control. For example, metallocene catalysts can be used to produce PE with narrow molecular weight distribution and a uniform distribution of comonomer incorporated into the polymer chain. [125] These characteristics provide an enhancement on polymer properties including ESCR of final products. Apparently, metallocene technology has the ability to control polymer properties such as crystallinity, a polymer's melting characteristics, flexibility, ESCR, level of extractables, and mechanical properties. As a result of all the above advantages an improvement in ESCR of polyolefins can be achieved by controlling the following factors: molecular weight and molecular weight distribution, and chain branching or crystallinity, as described in Section 2.5.3.1. This was proved by Soares *et al.* [61] when they said that metallocene catalysts have the ability to produce a high ESCR polymer. For example, it is possible to

incorporate the α-olefin comonomer in the high molecular weight end of the molecular weight distribution. [61] Then high ESCR polymers can be produced.

Table 2.4. Material changes and ESCR behaviour [122]

ESCR decreases with increasing
• Spherulite size • Melt index (MI) • Organic pigment • Crystallinity • Molecular weight distribution (MWD)
ESCR increases with increasing
• Average molecular weight ($\bar{M}_w$ or $\bar{M}_n$) • Inorganic pigment content • Cooling rate after extrusion (may be transient effect)
ESC varies with
• Comonomer content • Various additives

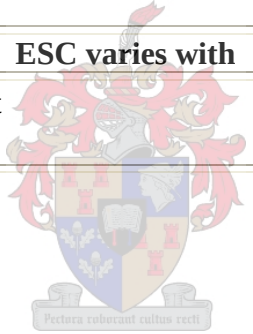

2.6 References

1. C. Greenwood and W. Banks, Synthetic High Polymers, Oliver and Boyd, UK, **1968**, 1.
2. J. Fried, Polymer Science and Technology, Prentice Hall PTR, USA, **1995**, 2.
3. T. Chung, Progress in Polymer Science, **2002**, 27, 39-85.
4. U. Romano and F. Garbassi, Pure and Applied Chemistry, **2000**, 72, 1383-1388.
5. J. Dong and Y. Hu, Coordination Chemistry Reviews, **2005**, 250, 47-65.
6. C. Maier and T. Calafut, Polypropylene; The Definitive User's Guide and Databook, Plastic Design Library, a Division of W. Andrew Inc., USA, **1998**, 109-111.
7. S. Shang and L. Woo, Selecting Materials for Medical Products: From PVC to Metallocene Polyolefins, Medical Device & Diagnostic Industry Magazine MDDI, **1996**.
8. R. Crawford, Plastics Engineering, Third Edition, Elsevier Butterworth-Heinemann, Amasterdam, **1999**, 1-3.
9. W. Brostow and T. Corneliussen, Failure of Plastics, Hanser Publishers, USA, **1986**, Preface.
10. B. Borisova, Investigations on Environmental Stress Cracking Resistance of LDPE/EVA Blends, Ph.D. Thesis, University of Halle Wittenberg, Germany, **2004**, 9.
11. S. Ebnesajjad, Volume 2: Fluoroplastics; Melt Processible Fluoropolymers, The Definitive User's Guide and Databook, Plastic Design Library, USA, **2003**, 371-372.
12. J. Scheirs, Compositional and Failure Analysis of Polymer: A Practical Approach, John Wiley & Sons, UK, **2000**, 546-548.
13. E. Myer, The Three Amigos of Part Failure, Success, Plastics World, ProQuest Science Journals, **1996**, 54, 25-26.
14. P. Gramann, A. Rios and B. Davis, Failure of Plastics Plumbing Products, The Madison Group: PPRC, Madison, **2004**.
15. R. Galipeau, Plastics Technology Laboratories Inc., Predicting the Effects of Contact Materials and their Environments on Thermoplastics through Chemical Compatibility Testing, Presented at the ANTEC conference, USA, May **1995**.
16. J. Jansen, Advanced Materials and Processing, **2001**, 59, 56-60.
17. J. Jansen, Using Failure Analysis to Assure Product Quality, Automotive Plastics, ProQuest Science Journals, **2001**, 59, 34-39.
18. V. Shah, Handbook of Plastics Testing Technology, Second Edition, John Wiley & Sons USA, **1998**, 420.
19. R. Brown, Handbook of Polymer Testing, Rapra Technology Ltd., USA, **1999**, 275.
20. W. Hawkins, Polymer Stabilization, John Wiley & Sons, USA, **1972**, 21-23.
21. J. Moalli, Plastics Failure: Analysis and Prevention, Plastics Design Library USA, **2001**, 1-2.
22. A. Alves, L. Nascimento and J. M. Suarez, Polymer Testing, **2005**, 24, 104-113.
23. A. Vegt, From Polymers to Plastics, DUP Blue Print, Netherlands, **2002**, 156-159.
24. T. Osswald and G. Menges, Materials Science of Polymers for Engineering, Hanser Publishers, Germany, **1996**, 372-375.
25. A. Volynskii and N. Bakeev, Solvent Crazing of Polymers, Elsevier Science B. V., Netherlands, **1995**, 22.
26. W. Woishnis and D. Wright, Advance Materials and Processes, **1994**, 12, 39-40.
27. A. Blaga, Properties and Behavior of Plastics, National Research Council Canada (NRC): Institute for Research in Construction, **1973**.
28. M. Howe-Grant, Encyclopedia of Chemical Technology, Fourth Edition, Executive Editor: J. Kroschwitz, John Wiley & Sons, USA**, 1996**, 7, 820-821.
29. H. Parvatareddy, J. Wang, D. Dillard and T. Ward, Composites Science and Technology, **1995**, 53, 399-409.

30. Rapra Environmental Stress Cracking (ESC) Web Site, http://www.esc-plastics.com/index.asp, **2005**.
31. J. Lagaron, J. Pastor and B. Kip, Polymer, **1999**, 40, 1629-1636.
32. F. Al-Saidi, K. Mortensen and K. Almdal, Polymer Degradation and Stability, **2003**, 82, 451-461.
33. N. Kuipers, A. Riemslag, R. Lange, M Janssen, A. Bakker and R. Marissen, Polymer Engineering and Science, **2004**, 44, 1319-1328.
34. J. Jansen, Advanced Materials and Processes, **2004**, 162, 50-53.
35. K. Cho, M. Lee and C. Park, Polymer, **1997**, 38, 4641-4650.
36. H. Mark and N. Gaylord, Encyclopedia of Polymer Science and Technology, Fourth Edition, Executive Editor: N. Bikales, John Wiley & Sons, USA, **1992**, 6, 299-303.
37. H. Mark and N. Gaylord, Encyclopedia of Polymer Science and Technology, Second Edition, Executive Editor: N. Bikales, John Wiley & Sons, USA, **1971**, 7, 261-289.
38. A. Siahkali, P. Kingshott, D. Breiby, L. Arleth, C. Kjellander and K. Almdal, Polymer Degradation and Stability, **2005**, 89, 442-453.
39. R. Portnoy, Medical Plastics: Degradation, Resistance & Failure Analysis, Understanding environmental stress cracking in polyethylene by A. Lustiger, Plastic Design Library, **1998**, 65-70.
40. S. Turner, Mechanical Testing of Plastics, Second Edition, Godwin, UK, **1983**, 163-175.
41. D. Wright, Environmental Stress Cracking of Plastics, Rapra Technology Ltd., UK, **1996**, 3.
42. V. Shah, Handbook of Plastics Testing Technology, Second Edition, John Wiley & Sons, USA, **1998**, 252-255.
43. BP SOLVAY Polyethylene, Environmental Stress Crack Resistance of Polyethylene, North America, **2001**, Technical publication 9, 1-4.
44. M. Hough and D. Wright, Polymer Testing, **1996**, 15, 407-421.
45. A. Raman, R. Farris and A. Lesser, Journal of Applied Polymer Science, **2003**, 88, 550-564.
46. K. Hatada, R. Fox, J. Kahovec, E. Marikhalk, I. Mita and V. Shibaev, Pure and Applied Chemistry, UK, IUPAC Recommendations **1996,** 68, 2313-2323.
47. E. Andrews, Developments in Polymer Fracture, Applied Science Publishers Ltd, UK, **1979**, 55-114.
48. H. Wang, B. Pan, Q. Du and Y. Li, Polymer Testing, **2003**, 22, 125-128.
49. V. Truong, P. Allen and D. Williams, European Polymer Journal, **1987**, 23, 181-189.
50. D. Faulkner, Journal of Applied Polymer Science, **1986**, 32, 4909-4917.
51. S. Bishop, D. Isaac, P. Hinksaman and P. Morrissey, Polymer Degradation and Stability, **2000**, 70, 477-484.
52. E Moskala, Polymer, **1998**, 39, 675-680.
53. R. Haward, The Physics of Glassy Polymers, Applied Science, UK, **1973**, 532-533.
54. J. Arnold, Materials Science and Engineering A197, **1995**, 119-124.
55. P. Hittmair and R. Ullman, Journal of Applied Polymer Science, **1962**, 19, 1-14.
56. C. Singleton, E. Roche, and P. Geil, Journal of Applied Polymer Science, **1977**, 21, 2319-2340.
57. S. Bandyopadhyay and H. Brown, Polymer, **1978**, 19, 589-592.
58. H. Okamoto and Y. Ohde, Polymer, **1982**, 23, 8, 1204-1210.
59. A. Lustiger, R. Markham and M. Epstein, Journal of Applied Polymer Science, **1981**, 26, 1049-1056.
60. J. Yeh, J. Chen and H. Hong, Journal of Applied Polymer Science, **1994**, 54, 2117-2126.
61. J. Soares, R. Abbott and J. Kim, Journal of Polymer Science: Part B: Polymer Physics, **2000**, 38, 1267-1275.
62. J. Lagaron, J. Pastor, W. Reed and B. Kip, Polymer, **1999**, 40, 2569-2586.

63. T. Kawaguchi and H. Nishimura, Polymer Engineering and Science, **2003**, 43, 419-429
64. H. Brown, Polymer, **1978**, 19, 1186-1188.
65. J. DeCoste, F. Malm, and V. Wallder, Industrial and Engineering Chemistry, **1951**, 43, 117-121.
66. A. Renfrew and P. Morgan, Polyethylene: The Technology and Uses of Ethylene Polymers, Iliffe, UK, **1975**, 200-201.
67. M. Nisizawa, Journal of Applied Polymer Science, **1971**, 15, 829-833.
68. G. Bernier and R. Kambour, Macromolecules, **1968**, 1, 393-400.
69. S. Saeda and Y. Suzko, Polymer for Advanced Technologies, **1995**, 6, 593-601.
70. B. Borisova and J. Kressler, Macromolecular Materials and Engineering, **2003**, 288, 509-515.
71. T. Tatsushima, N. Ogata, K. Nakane and T. Ogihara, Journal of Applied Polymer Science, **2003**, 87, 510-515.
72. E. Moskala and M. Jones, Evaluating Environmental Stress Cracking of Medical Plastics, Medical Plastics and Biomaterials Magazine MPB, **1998**.
73. C. Qin, Y. Ding, V. Zepchi, H. Dhyani, and K. Hong, Environmental-Stress Crack Resistance of Rigid Thermoplastic Polyurethanes, Medical Plastics and Biomaterials Magazine MPB, **1997**.
74. M. Wiggins, J. Anderson and A. Hiltner, Journal of Biomedical Materials Research, Part A, 66A, **2003**, 3, 463-475.
75. L. Spenadel, Journal of Applied Polymer Science, **1972**, 16, 2375-2386.
76. E. Bear, Engineering Design for Plastic, John Wiley & Sons, USA, **1964**, 742-790.
77. B. Borisova, Investigations on Environmental Stress Cracking Resistance of LDPE/EVA Blends, Ph.D. Thesis, University of Halle Wittenberg, Germany, **2004**, 11-17.
78. B. Stuart, Polymer Analysis, Biddles Ltd. UK, **2002**, 126-132.
79. D. Wright, Environmental Stress Cracking of Plastics, Repra Technology Ltd., UK, **1996**, 81.
80. R. Lenk, Plastics Rheology, Maclaren and Sons UK, **1968**, 163-165.
81. R. Clough, N. Billingham and K. Gillen, Polymer Durability; Degradation, Stabilization and Lifetime Prediction, American Chemical Society, USA, **1993**, 210.
82. Z. Spitalsky and T. Bleha, Polymer, **2003**, 44, 1603-1611.
83. K. Saunders, Organic Polymer Chemistry, Second Edition, Chapman and Hall, UK, **1973**, 65.
84. C. Harper, Modern Plastics Handbook, chapter 1: Thermoplastics, A. Baker and J. Mead, McGraw-Hill, USA, **1999**, 1.62-1.63.
85. M. Kennedy, A. Peacock and L. Mandelkern, Macromolecules, **1994**, 27, 5297-5310.
86. M. Kennedy, A. Peacock, M. Failla, J. Lucas and L. Mandelkern, Macromolecules, **1995**, 28, 1407-1421.
87. M. Butler, A. Donald, W. Bras, G. Mant, G. Derbyshire and A. Ryan, Macromolecules, **1995**, 28, 6383-6393.
88. M. Butler, A. Donald and A. Ryan, Polymer, **1998**, 39, 39-52.
89. G. Ashraf, Brunel University, Environmental Waste Management and Plastics Recycling - An Overview, Takveen – Khwarzimic Science Society, UK, **2004**.
90. A. Galeski, Progress in Polymer Science, **2003**, 28, 1643–169.
91. F. Billmeyer, TextBook of Polymer Science, John Wiley & Sons, USA, **1984**, 289.
92. W. Brostow and D. Corneliussen, Failure of Plastics, Hanser Publishers, USA, **1986**, 179.
93. A. Ward, X. Lu, Y. Huang and N. Brown, Polymer, **1991**, 32, 2172-2178.
94. X. Lu and A. Windle, Polymer, **1995**, 36, 451-459.
95. W. Callister, Materials Science and Engineering, Fifth Edition, John Wiley & Sons, USA, **2000**, 185-201.

96. P. Hinksman, D. Isaac and P. Morrissey, Polymer Degradation and Stability, **2000**, 68, 299-305.
97. S. Basua, D. Mahajana and E. Giessenb, Polymer, **2005**, 46, 7504-7518.
98. J. Kocsis, Polypropylene an A-Z Reference, Environmental Stress Cracking of Polypropylene by R. Chatten and D. Vesely, Kluwer Academic Publishers UK, **1999**, 207-214.
99. K. Cho, M. Lee and C. Park, Polymer, **1998**, 36, 1357-1361.
100. G. Williams, Fracture Mechanics of Polymer, Ellis Horwood, Chichester, **1984**, 189.
101. X. Li, Polymer Degradation and Stability, **2005**, 90, 44-52.
102. J. Arnold, Materials Science and Engineering, **1995**, A197, 119-124.
103. R. Sanderson, Honours Course in Polymer Science, University of Stellenbosch, South Africa, **2004**.
104. I. Garrido, J. Rienda and G. Frutos, Macromolecules **1996**, 29, 7164-7176.
105. E. Földes, Journal of Applied Polymer Science, **1993**, 48, 1905-1913.
106. C. Hansen, Polymer Degradation and Stability, **2002**, 77, 43-53.
107. C. Hansen, Progress in Organic Coating, 2004, 51, 109-112.
108. C. Hansen and L. Just, Industrial Engineering Chemistry Research, 2001, 40, 21-25.
109. L. Masaro and X. Zhu, Progress in Polymer Science, **1999**, 24, 731-775.
110. D. Wright, Environmental Stress Cracking of Plastics, Repra Technology Ltd., UK, **1996**, 7.
111. H. Mark, N. Bikales, G. Overberger and G. Menges, Encyclopedia of Chemical Technology, Second Edition, Executive Editor; A. Standen, John Wiley & Sons, USA, **1971**, 16, 97-105.
112. R. Brown, Handbook of Polymer Testing, Repra Technology Ltd., USA, **1999**, 361.
113. V. Wallder, Aging Problem of Plastics, Bell Laboratories Record, **1968**, 151-154.
114. G. Wypych, Handbook of Material Weathering, Third Edition, ChemTec Publishing, Canada, **2003**, 20.
115. W. Hawkins, Polymer Stabilization, John Wiley & Sons, USA, **1972**, 369.
116. W. Yoon, Y. Kim, I. Kim and K Choi, Korean Journal of Chemical Engineering, **2004**, 21, 147-167.
117. A. Lustiger, Understanding Environmental Stress Cracking in Polyethylene, Medical plastics and Biomaterials Magazine MPB, **1996**, 1-5.
118. J. Lagaron, N. Dixon, D. Gerrard, W. Reed and B. Kip, Macromolecules, **1998**, 31, 5845-5852.
119. F. Billmeyer, TextBook of Polymer Science, John Wiley & Sons, USA, **1984**, 323.
120. Pinker Material Hydro Conduit, INFO Series, Hydrostatic Design Basis for Thermoplastic Pipes, Rinker Materials Corporation, **2003**.
121. C. Ishiyama, T. Sakuma, M. Shimojo and Y. Higo, Journal of Polymer Science: Part B: Polymer Physics, **2002**, 40, 1-9.
Thermoplastic Pipes, Rinker Materials Corporation, **2003**.
122. W. Brostow and D. Corneliussen, Failure of Plastics, Chapter 16: Environmental Stress Cracking: The Phenomemon and its Utility, by A. Lustiger, Hanser Publishers USA, **1986**, 321.
123. W. Hawkins, Polymer Stabilization, John Wiley & Sons, USA, **1972**, 204.
124. B. Judy, Metallocenes, Plastics World, ProQuest Science Journals, **1996**, 54, 107.
125. W. Kaminsky, O. Sperber, and R. Werner, Coordination Chemistry Reviews, **2006**, 250, 110–117.

Chapter 3

Test methods for the evaluation of ESCR of plastics

3.1 Introduction

One of the aims of testing plastics is to provide a framework for evaluating the suitability of a plastic for a certain application in terms of its stress crack behaviour. Although there are many test methods available to test and measure material properties, the proper selection of testing methods is not always easy. The methods are usually chosen based on the following criteria: the purpose of testing, the characteristics of the service application, the consequences of failure and the cost of testing. [1-3] The primary goal of testing is to obtain information on the limitations of materials, while the second goal it to evaluate materials that have failed in use and to use the information to make material corrections to meet the original requirements. [4-5] The testing performed should be chosen to confirm, or exclude, the hypothesized failure mode, as well as gain an understanding of what can be altered and improved to prevent failures in the future. This is the ultimate goal of failure analysis.

3.2 ESCR testing

Several standard test methods have been developed to determine the ESCR of polymers. [6-7] A sample that fails early on during the test is deemed to have a low ESCR. Failure times will obviously differ depending on the material's response to a load under the test conditions. [8] Most polymers are sensitive to the test conditions. In most cases, accelerated testing is carried out on products to characterize ESCR. It is important to note that ESCR testing is extremely sensitive to some environmental conditions. ESCR can be accelerated by such factors as temperature, humidity, level of stress, concentration of SCA or even making notches in the sample that is being tested. For example, a higher applied temperature will result in a shorter time to failure of a given test specimen if all other conditions remain the same. The results of accelerated tests can really only be valid if the failure is similar to the failure that occurs in the normal service environment. ESCR tests can be classified into two main types of tests: tests at constant strain and tests at constant stress. [9-11] Wang *et al.* [6] mentions that in these methods, it is important to

decide on the level of strain because too high strain will result in overly fast failure, while strain that is too low will cause very long experiments. Moskala and Jones [12] listed the most common tests for evaluating stress crack resistance of plastics as the following: ASTM D 1693 (ESC of ethylene plastics), ISO 4600 (Resistance to ESC Ball/Pin impression method), ISO 6252 (Resistance to ESC constant tensile stress method), ISO 4599 (Resistance to ESC Bent-Strip Method), Critical Strain, and Fracture Mechanics.

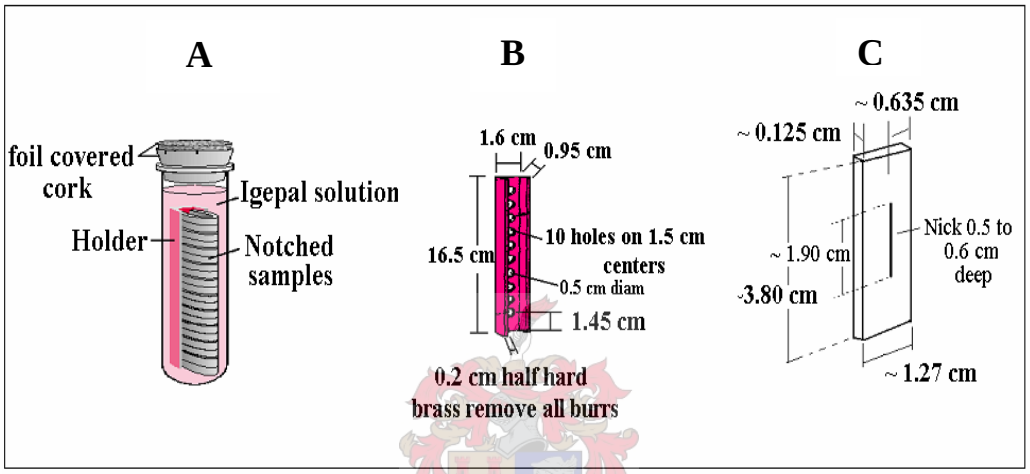

Figure 3.1. A) Specimen apparatus for bent strip test ASTM D 1693, B) holder (stressing element) and C) sample dimensions before stressing [9]

3.2.1 Tests at constant strain

3.2.1.1 Bell telephone test (BTT) or bent strip test (ASTM D 1693)

The bent strip test was developed in USA by Bell laboratories in the late 1940s. [5,10] In this method the sample should be notched and bent in a holder (stressing element) into a controlled U-shape as shown in Figure 3.1. The holder with the samples is placed in test tubes containing SCA. This test should be performed at constant temperature by placing the test tubes in an oil bath. Samples are considered as having a good ESCR if all the samples do not fail. [10] Time to 50% failure is sometimes used as a reference point. Failure in this type of test is deemed to be the appearance of a crack visible to the naked eye. The duration of this test, according to some workers, should not be less than 48 h. [10] The maximum surface strain can be calculated by the following equation:

$$\varepsilon_{max} = (t/t - w)100 \text{ ..... } (1)$$

Where t is the thickness of the samples and w is the width of the holder. [13]

3.2.1.2 Three point bending test

This test can be performed in two different types of gauges as shown in Figure 3.2. Gauge A allows for regulation of deflection and gauge B has constant deflection. In test A, the convex surface of the sample is in contact with the SCA fluid, while in test B samples are deformed and afterward immersed in the SCA. After a period of time samples can be removed and cooled down to room temperature, by rinsing with distilled water. Finally, craze and crack and tensile properties of these samples can be investigated. [10,13]

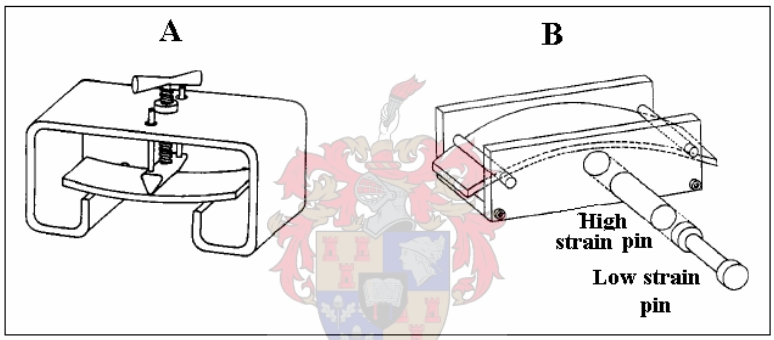

Figure 3.2. Three point bending apparatus for testing the ESCR under constant strain [13]

3.2.2 Tests at constant stress

3.2.2.1 Constant tensile load test

Brown and Lu [14] described this method for measuring the slow crack growth behaviour of PEs. This test is now given as an ASTM standard test method (ASTM F 1473). They tried this test on different PE samples in order to study the slow crack growth (SCG) and found this test very sensitive to changes in the molecular structure and morphology of PE. They also found that the resistance to SCG depends on the tie-molecules and strength of crystals, as discussed in Chapter 2. In this method a constant load test is applied on a notched specimen under planar strain conditions in air at various temperatures. This method can also be used estimate the same fracture process that occurs during the long-

term failure of PEs. The main advantage of this method is that it can accelerate the fracture process faster than any other test method, using a constant load in air. As shown in Figure 3.3, once the specimen fails the timer will be switched off. It is also easy to monitor the rate of crack growth by using an optical microscope. [10] Lu *et al.* [15] also used the same test but in the presence of a SCA (Igepal CO-630). Using SCA in this test resulted in a reduction in the lifetime of tested polymers or testing time and using a lower concentration of SCA was showed to be more effective (e.g. 50% Igepal was more effective than 100% Igepal).

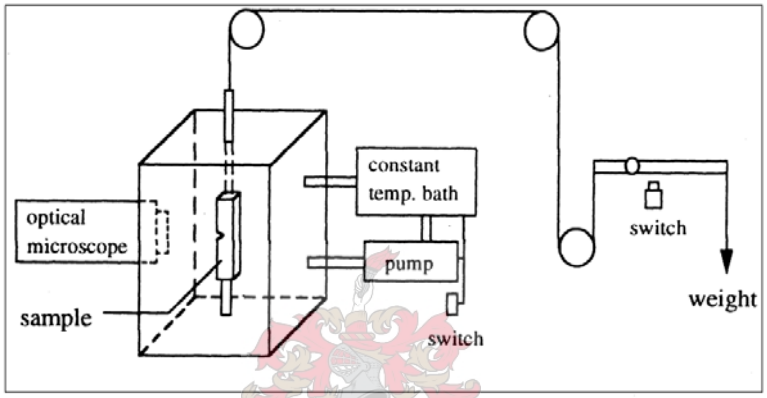

Figure 3.3. Apparatus for testing ESCR at constant load [10]

3.2.2.2 Monotonic creep tests

Wright and Hough [13,16] developed this method as shown in Figure 3.4A. This type of test is similar to the slow-rate testing technique used by the metal industry for many years. This method can generate a strain-stress curve (strain from extensometer and stress from water container actual weight) for the specimen. Furthermore, the critical stress, time and strain can be obtained from this test. These critical stress, time and strain invite the use of the method for investigating viscoelastic criterion for initiation of ESC. [10] In this method, the strain response to a constant stress rate is monitored. The method employs a tensile creep machine with the weight pan replaced by a blow-moulded vessel. Water is supplied by a peristaltic pump to a container (70 liters) which then that exerts a load on the tested specimen. The rotational speed of the pump is continuously variable and this provides a means of applying a known stressing rate to the tested specimen. The effective range of stressing rate was found to be 0.1-10 MPa/hour. Specimen strain is monitored

via a Moiré fringe extensometer as shown in Figure 3.4B. A Moiré fringe extensometer employing diffraction gratings of 250 lines/mm with four photodiodes, this provides a digital electronic pulse for each micrometer of extensometer displacement. With a gauge length of 66 mm this translates to a recorded tensile strain increment of 1.5 x 10^{-6}. Within the gauge length, as shown in Figure 3.4B, is incorporated a glass tube sealed with a grommet at each end. This contains the SCA. [13] High resolution and discrimination can be considered as major advantages of this test. [16]

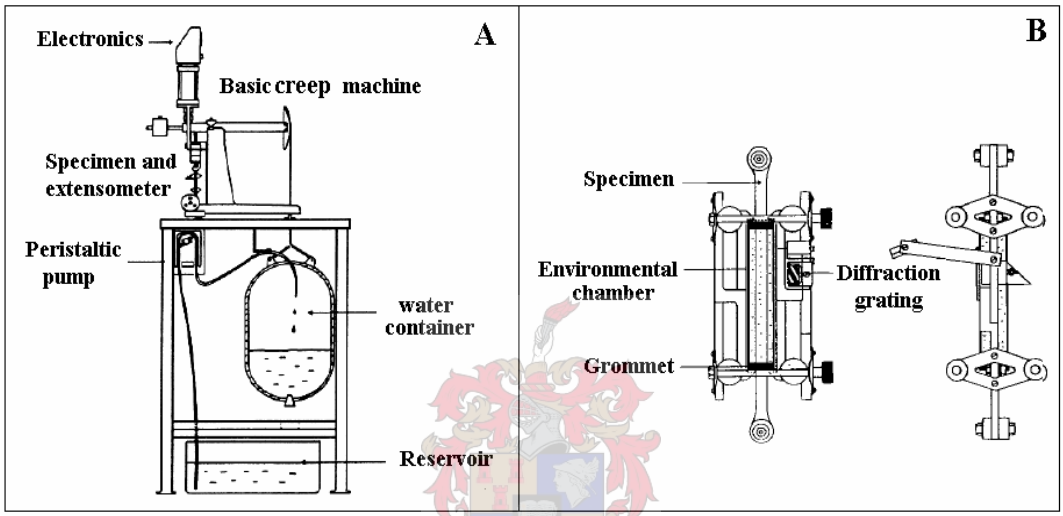

Figure 3.4. (A) Monotonic creep testing machine and (B) Rapra Moiré fringe extensometer with environmental chamber attached to specimen [10]

3.2.2.3 Test methods for determining ESCR of ethylene based plastics.

This method was used in this study in an adapted form to test three samples of IPPCs with different ethylene contents. Crissman [17] proposed this method for determining the ESCR of ethylene plastics under different stresses and temperatures.

Table 3.1. Optimum conditions for test method used for determining ESCR of ethylene based plastics.

Condition	Value
Nominal specimen thickness	From 1-1.25 mm
Bend radius	5.5 mm
Applied stress	5 kPa
Temperature	75 ^{o}C

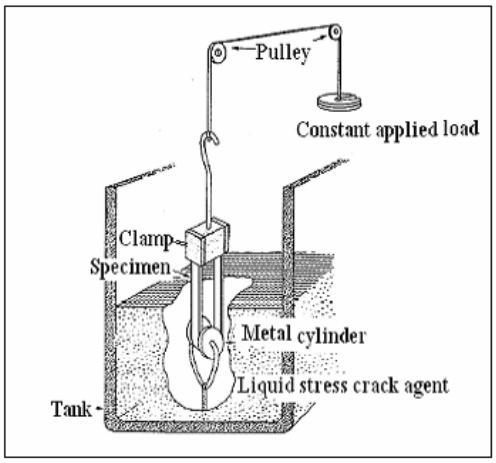

Figure 3.5. Schematic of the test method used for determining the ESCR of ethylene based plastics in this study [17]

This test has been most commonly accepted by industry to measure the ESCR of ethylene based plastics. [10] This method incorporates features of the following two methods: ASTM of ethylene based plastics (D 1693) and the test for environmental stress rupture of polyethylene under constant strain (D 2552). The advantage behind this combination is to reduce the time required to collect data. The reproducibility of this test can be affected by the curvature of the bent specimen (depends on the stiffness of the specimen) and the fact that the strain might not be kept constant during the time of testing. [17,10] Moreover, if a notched specimen is required in order to accelerate this test, it is difficult to ensure a comparable sharp notch that is reproducible from specimen to specimen. As shown in Figure 3.5, the sample to be tested is constrained in a fixed geometry by bending it around a cylindrical metallic form and clamping it properly in a tank containing SCA. Then constant stress can be applied at a fixed temperature. The optimum conditions for this method are listed in Table 3.1.

3.3 Other methods

There are other ESCR test methods used in industry to predict the service life of some products such as bottles, pipes and geomembranes. [18-25] For example, a variety of tests exist to check the ESCR of plastic bottles. The most common bottle test methods are: the bottle stress crack (BSC) test (ASTM D2561), the top-load stress crack (TLESCR) test,

and the internal pressure (IP) test. [18] The TLESCR test can be done by placing a weight on the cap of the bottle. This additional load is meant to check the integrity of the bottle when it is stacked, as during warehousing. The IP test is similar to the BSC test. In this test the vapour pressure of the stress cracking fluid is supplemented by an external pressurized air source (for more information see reference 18). However, Strebel [18] compared these methods and concluded that the IP test is a quicker and more reproducible method for measuring the ESCR of blow moulded polyethylene bottles. This test also provides the same relative ESCR ranking of materials as can be achieved with the BSC test.

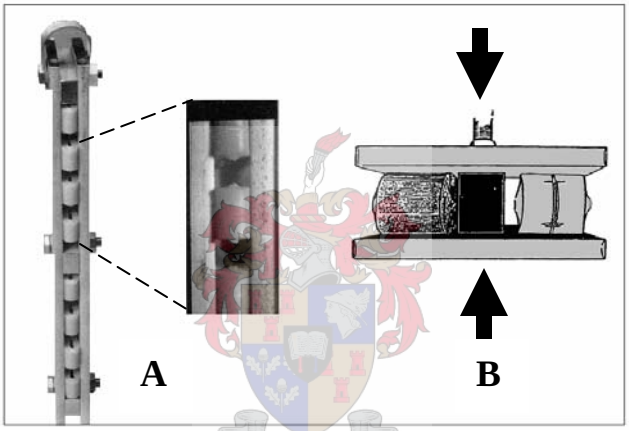

Figure 3.6. A) Compressed ring test for determination of ESCR of pipe and B) the notched area must be positioned parallel to the direction of compression [19]

Some methods are available to evaluate the resistance of pipes to ESC. The common ESCR method used is the compressed ring test or standard test method for determination of ESCR of PE pipe, as shown in Figure 3.6A. [19-20] It determines the PE pipe's resistance to stress cracking in the presence of a SCA at elevated temperatures. This test is believed to be more realistic than the bent strip ESCR test (ASTM D1693) since the test specimens are actual pieces of pipe rather than compression-moulded specimens. A ring specimen of pipe, having a controlled imperfection at one location, is exposed to a SCA while compressed between two parallel plates (compression plates). Eight specimens can be mounted between the two parallel plates with notched areas. The notched area must be positioned parallel to the direction of compression as shown in Figure 3.6B. The second test method for ESCR of PE pipes is the PE notch tensile (PENT) test or ASTM F1473.

This method is shown in the Figure 3.7. The typical test conditions are 80 ^{o}C and 2.4 MPa. The typical samples or specimens measure 10x25x100 mm. These specimens should be notched before the test and the depth of the notch in every specimen is dependent on its thickness. The final failure is a complete separation at the notch, and then the time of failure must be recorded for each specimen. [5] There is another standard test method to test PE pipe grade material. This test is the fully notched creep test (FNCT). It is similar to the PENT test but with shorter failure time. This is due to the specimen design and the presence of SCA instead of air. Specimens should be notched on all four sides and a typical specimen measures 10x10x100 mm. The typical test conditions are 80-95 ^{o}C and 4-5 MPa. The final failure is recorded when a complete separation at the notch has occurred.

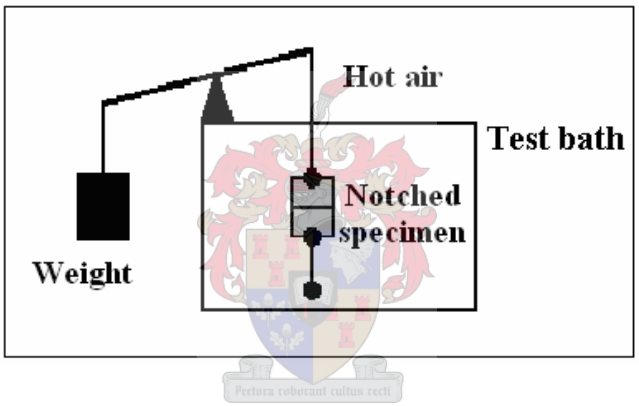

Figure 3.7. PENT test apparatus for ASTM F 1473 [5]

There are some procedures for testing a geomembrane material. [21] The most common method is the single point notched constant tensile load test (NCTL) test. This test is also known as the standard test method for evaluation of stress crack resistance of polyolefin geomembranes using the notched constant load test, ASTM D5397. [22-23] This method is shown in Figure 3.8.

The typical conditions of this test are listed in Table 3.2. The specimen to be tested must be notched and subjected to a constant load in the presence of SCA. The final failure is recorded and it can be indicator of SCG performance. [5] The results of a series of such tests conducted at different stress levels are presented by plotting stress level against failure time for each stress level on a log-log axis. [24-25]

Table 3.2. Typical test conditions for NCTL test [24]

Temperature	50 °C
Concentration of stress crack agent (Igepal)	10%
Notch depth	20% of the sample's thickness
Applied load	30% of the sample's yield stress

Finally, the main differences between constant strain and constant stress methods are listed below.

1. Constant strain methods are widely used due to their simplicity and inexpensive equipment required for the test.
2. The reproducibility of results of constant strain methods is not really good due to:

   - human error because the final failure is recorded visually,
   - the curvature of a specimen is very dependent on the stiffness of the material, and
   - the strain cannot remain constant and stress will decay with time. This is due to stress relaxation.
3. Constant stress methods are more accurate. This is because failure is detected by optical microscopy.
4. The test procedure in constant stress methods is shorter than in the constant strain methods (less time and cost). [10]

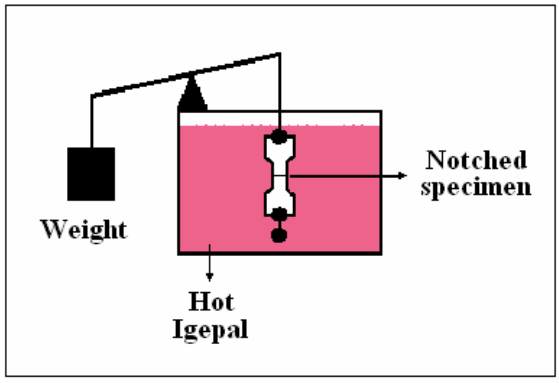

Figure 3.8. NCTL test apparatus for ASTM D 5397 [5]

3.4 References

1. R. Brown, Handbook of Polymer Testing; Physical Methods, Rapra Technology Ltd., UK, **1999**, 285.
2. H. Mark, N. Bikales, C. Overberger and G. Menges, Encyclopedia of Polymer Science and Engineering, Second Edition, Executive Editor: A. Standen, John Wiley & Sons, USA, **1989**, 16, 570-576.
3. A. Maxwell and A. Turnbull, Practical Guide to Selection of Environment Stress Cracking Test Methods for Plastics, NPL Materials Centre National Physical Laboratory, Teddington, Middlesex, **2000**, 1-20.
4. G. Wypych, Handbook of Material Weathering, Third Edition, ChemTec Publishing, USA, **2003**, 689.
5. BP Solvay Polyethylene, Environmental Stress Crack Resistance of Polyethylene, North America, **2001**, Technical Publication 9, 1-4.
6. H. Wang, B. Pan and Q. Du, Polymer Testing, **2003**, 22, 125-128.
7. J. Lagaron, J. Pasror and B. Kip, Polymer, **1999**, 40, 1629-1636.
8. R. Portnoy, Medical Plastics: Degradation, Resistance & Failure Analysis, Understanding Environmental Stress Cracking in Polyethylene by A. Lustiger, Plastic Design Library, USA, **1998**, 65-70.
9. H. Mark and N. Gaylord, Encyclopedia of Polymer Science and Technology, Second Edition, USA, Executive Editor: N. Bikales, John Wiley & Sons, USA, **1971**, 7, 261-289.
10. Bistra Borisova, Investigations on Environmental Stress Cracking Resistance of LDPE/EVA Blends, Ph.D. Thesis, University of Halle Wittenberg, Germany, **2004**, 18-24.
11. J. Scheirs, Compositional and Failure Analysis of Polymers: A Practical Aproach, John Wiley & Sons, UK, **2000**, 556-561.
12. E. Moskala and M. Jones, Evaluating Environmental Stress Cracking of Medical Plastics, Material Testing, Medical Plastics and Biomaterials Magazine MPB, **1998**.
13. D. Wright, Environmental Stress Cracking of Plastics, Repra Technology Ltd., UK, **1996**, 13-21.
14. N. Brown and X. Lu, Polymer Testing, **1992**, 11, 4309-4319.
15. X. Lu, Z. Zhou and N. Brown, Polymer Engineering and Science, **1997**, 37, 1896-1900.
16. M. Hough and D. Wright, Polymer Testing, **1996**, 15, 407-421.
17. J. Crissman, Journal of Testing and Evaluation, **1983**, 11, 273-278.
18. J. Strebel, Polymer Testing, **1995**, 14, 189-202.
19. A. Lustiger, R. Markham and M. Epstein, Journal of Applied Polymer Science, **1981**, 26, 1049-1056.
20. W. Brostow and R. Corneliussen, Failure of Plastics, Chapter 16: Environmental Stress Cracking: The Phenomenon and its Utility by A. Lustiger, Hanser Publishers, USA, **1986**, 320-321.
21. I. Peggs, Stress Cracking in HDPE Geomembranes: “What It Is and How to Avoid It”, Geosynthetics Asia ’97, Asian Society for Environmental Geotechnology, New Delhi/India, **1997**, 83-90.
22. ASTM D5397, "Standard Test Method for Evaluation of Stress Crack Resistance of Polyolefin Geomembranes Using Notched Constant Tensile Load Test," American Society for Testing and Materials, Philadelphia, PA, **1995**.
23. W. Müller, Certification Guidelines for Plastic Geomembranes Used to Line Landfills and Contaminated Sites, Federal Institute for Materials Research and Testing. Second Edition, Translated by D. Etter, **1999**, 21.
24. Y. Hsuan, Geotextiles and Geomembranes, **2000**, 18, 1-22.
25. Y. Hsuan and R. Koerner, Geosynthetics International, **1995**, 2, 831-843.

Chapter 4
Experimental

4.1 Polymers

The three propylene impact copolymer (IPPC) samples used in this study were supplied by Sasol (South Africa). The samples had different ethylene contents, as shown in Table 4.1.

The first sample (sample A) is an easy-flow copolymer with low ethylene content (6.5%). This polymer can be used in paint containers, domestic food storage containers, outdoor stadium seating and furniture components. [(1)] The second sample (sample B) is a medium-flow IPPC, with medium ethylene content (9.5%). Typical applications for this type of polymer are household and domestic articles, outdoor furniture and stadium seating, crates and containers, electrical appliance components and buckets/pails. [(2)] The third sample (sample C) is an easy-flow IPPC with high ethylene content (12%). These polymers are used to make bottle crates, transport and storage containers, folding boxes, buckets and some garden tools. [(3)]

Table 4.1. The materials used in this study

No	Samples	Type	Supplier
A	IPPCs with low ethylene content (6.5%)	CMV348(2348MC)	Sasol, South Africa
B	IPPCs with medium ethylene content (9.5%)	CKR448(2448K)	Sasol, South Africa
C	IPPCs with high ethylene content (12%)	CMR648(2648M)	Sasol, South Africa

4.1.1 Sample properties

These polymers are generally extruded into pellets and formulated with antistatic additives. They contain a nucleating agent that ensures rapid crystallization, resulting in an improved impact as well as shorter cooling times. The major properties of these polymers are listed below in Table 4.2 (typical values at 23 ^{o}C for uncoloured products).

Table 4.2. Properties of the IPPC samples used in this study [1-3]

Properties	Sample		
	A	**B**	**C**
Mass density, g/cm^3	0.91	0.91	0.91
Melting point (DSC*), ^{o}C	163	163	163
Tensile strength at yield (50 mm/min), MPa	29	27	21
Elongation at yield (50 mm/min), %	6.5	6.0	6.0
Ultimate elongation (50 mm/min), %	>50	>50	>50
Modulus of elasticity in tension (1mm/min), MPa	1450	1450	1150
Izod notched impact resistance 23 ^{o}C, kJ/m^2	7.5	20	45
Charpy impact resistance 23 ^{o}C, kJ/m^2	NB	NB	NB
Ball indentation hardness, MPa	62	50	44
Shrinkage, %	1.5	1.4	1.5
Vicat softening point, ^{o}C	153	150	144

DSC* = Differential scanning calorimetry

4.2 Chemicals

- Teepol Blue 825 (0.5% from Acorn Products (Pty) (Ltd), ethanol (EtOH, 99.9% from Saarchem) and sodium dodecylbenzene sulphonate (SDBS) (25%, from Rhodia) were used as SCAs to accelerate the ESCR tests. All these chemicals were tried in different concentrations in order to find the most active SCA for the IPPCs.

- The above chemicals/SCAs were shown to be not active enough for IPPC samples. So, ispropanol (PC grade, chemically pure) from Sasol Solvents was used (as received) in this study after the above evaluation as an SCA for testing the ESCR of the IPPCs.

- Mylar polyester film with a thickness of 125 μm, from Wire System Technology (South Africa), was used in this study to avoid any possible adhesion between the moulded polymers and the press plates during film preparation.

- Potassium permanganate (Riedel-deHaên AG D-3026) and sulphuric acid 98% AR (Kimix) were used in this study as etchants to etch the samples in order to study their morphology. Methanol (99.5%, from Saarchem) and distilled water were used to wash the samples after the etching process. The whole process of etching (preparation of etching reagent and procedure of etching process) is discussed in Section 4.7.

4.3 Special equipment

The following pieces of equipment used in this study were manufactured to affect a standardized test method for determining ESCR of ethylene based plastics.

1. A stainless steel tank and stainless steel clamp were designed and made as shown in Figure 4.1 These devices were made of stainless steel as some experiments were to be carried out in the presence of chemicals at high temperature.

A) Stainless steel tank

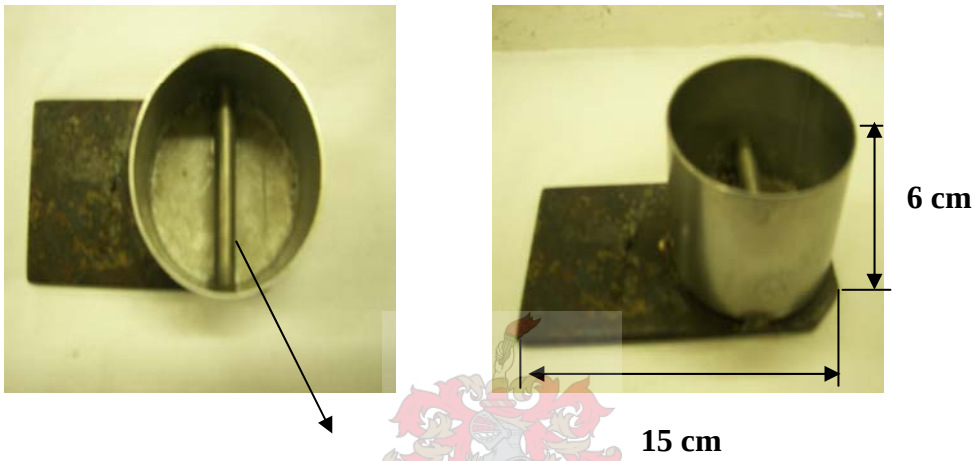

B) Stainless steel clamp

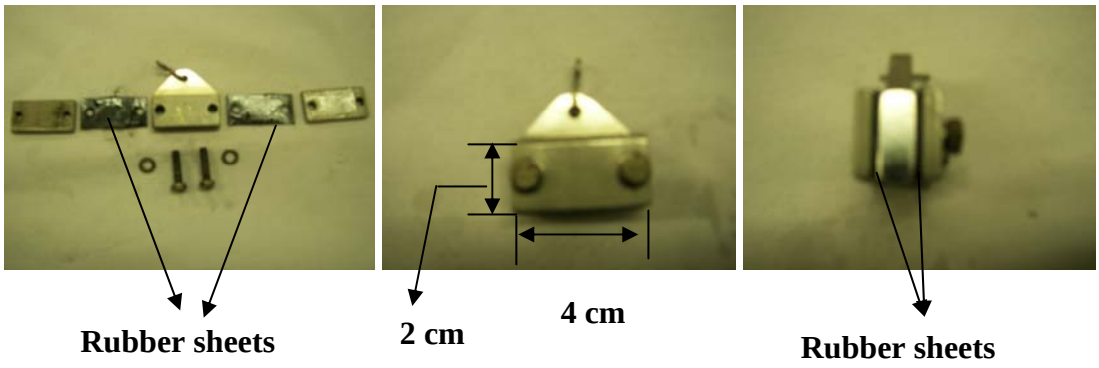

Figure 4.1. Special equipment used to determine ESCR using ESCR test 2

2 The running hour meter (RHM / PRHM1) timer (designed & manufactured by ICON Electronics c.c.) was used to record the failure time. This device has the following features:

a. It can monitor running hours up to 9999 hours.

b. The accuracy is rated at ± 0.05 %.

c. a single setpoint is available to switch a relay after a pre-set number of hours.

d. Once the setpoint is reached the user can reset the counter. The relay will then de-energise until the next service interval is reached.

e. The device includes two counters: number of hours since the last reset and a 6 digit total counter.

f. All data is stored in a non-volatile memory so that the number of hours lapsed will NOT be reset after a power failure (the device will continue counting where it left off). [4]

Table 4.3 Dimensions of the tests specimen

Type of test	Specimen length, cm	Specimen width, cm	Thickness, cm	Length of notch, cm
ESC test 1	4.0	~ 1.3	0.12-0.17	2.0
ESC test 2	16±0.5	1.5	0.14-0.22	No notch
Craze formation	16±0.5	1.5	0.14-0.22	0.5
Crack growth	16±0.5	1.5	0.14-0.22	0.5

4.4 ESCR tests

4.4.1 Sample preparation

Pellets were compressed into films by compression moulding using a heated hydraulic press (Apex Construction Ltd., UK). Polymer pellets (15 g) were moulded into films of different thickness, depending on the type of test, as shown in Table 4.3. The pellets were placed or sandwiched between two polished, rigid, metal plates (having an area of 20 x 17 cm). To avoid adhesion between the samples and the press plates, Mylar sheets were used to cover the metal plates. The metal plates were inserted between the heating plates and heated to 200 °C under minimum pressure for 3 min. Then a pressure of 20 MPa was applied and the plates were maintained at 200 °C for 5 min to melt the pellets. The 20 MPa pressure was removed and then applied three times at 200 °C for 1 min. Then the samples were rapidly quenched in a mixture of

ice and water. The film was removed from the plates and cut into rectangular pieces of test specimens.

Later, these test specimens were cut with a specific geometry, using a razor blade and notched to fixed dimensions depending on the type of test they were to be subjected to. Sample dimensions varied with the type of test specified, as illustrated in Table 4.3.

4.4.2 ESCR test 1

The Bell telephone test/Bent strip test (ASRM D 1693) was performed in order to study the ESCR of the three samples of IPPC with different ethylene contents. Four rectangular test specimens from each polymer (4 cm length, ~1.3 cm width, and 0.12-0.17 cm thickness) were cut from the films that were prepared as described in Section 4.4.1.

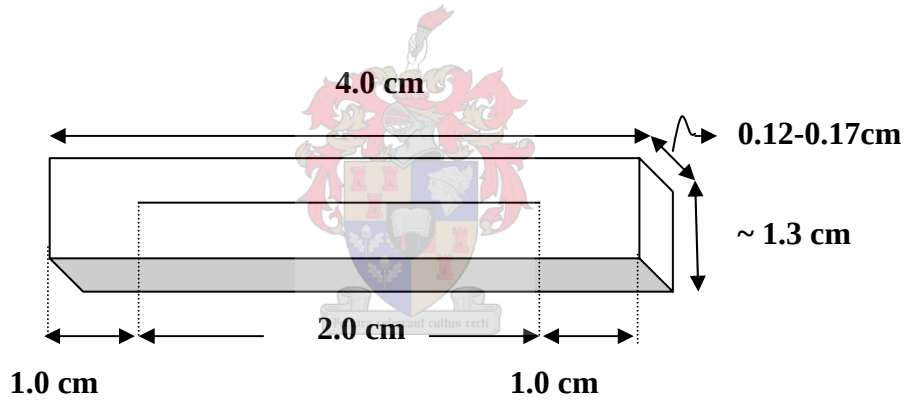

Figure 4.2. Geometry of the test specimen used ESCR test 1

A controlled notch was cut horizontally across each specimen. This serves as a crack initiation point. A notch was cut in the middle (2 cm) of each specimen with a fresh razor blade, as shown in Figure 4.2. These test specimens were bent, with the notches pointing upward, and mounted into a U shaped metal channel. In this step the test specimens were folded into a semi-circle to produce a multi-axial stress condition. This holder was placed into a glass tube filled with isopropanol to submerge the samples. All specimens were completely covered by isopropanol. Finally, the tubes were well sealed and placed in an oil bath at 50 ^{o}C. Failure can be defined as the appearance of any crack visible to the naked eye. [5,6]

Usually the crack resistance is reported as the percentage of the specimens tested that resist cracking after an arbitrary test period of sufficient duration to represent an approximate equilibrium condition. [7]

Generally, in this type of test, susceptibility to stress cracking is gauged by the total number of specimens that crack in a given time, or by the time required for a given percentage of the specimens to fail. [8] The number of samples that exhibit cracking is recorded as a function of time. A picture of the test assembly is shown in Figure 4.3.

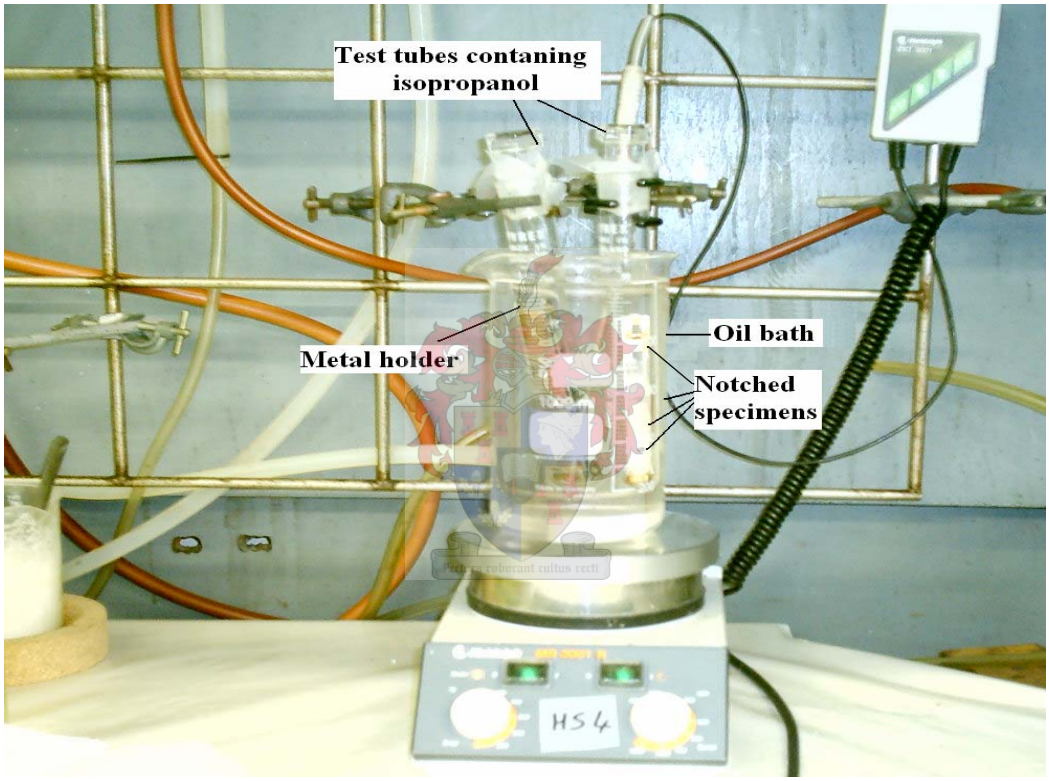

Figure 4.3. Bell Telephone test (ESCR test 1)

4.4.3 ESCR test 2

This test method, for determining ESCR of ethylene based plastics, was also performed in order to evaluate the ESCR of the IPPC samples. This test is classified as a constant stress or load test. It incorporates combined feature of both ASTM D 1693 and ASTM D 2552. The apparatus used for this test is shown in Figure 4.4. Typically the test specimens were strips having a length of 16±0.5 cm, a width of 1.5 cm and a thickness that varied from 0.14-0.22 cm, as shown in Figure 4.5.

The un-notched test specimen in Figure 4.5 was constrained in a fixed geometry by bending it around a cylindrical metallic form welded in the bottom of the stainless steel tank. This cylindrical metallic form has a specific radius of curvature in order to ensure that all the test specimens conformed to the same geometry for the duration of the test. In fact, the bend radius should not to be too small, according to Crissman (about 5.5 mm). [9] The reason for this is that the specimens stiffness becomes a significant variable. The respective specimens were clamped at their ends by a stainless steel clamp. After adding the isopropanol, the stainless steel tank was well covered. Simultaneously, by means of a pulley, the test specimens were subjected to a predetermined constant applied stress (15 MPa).

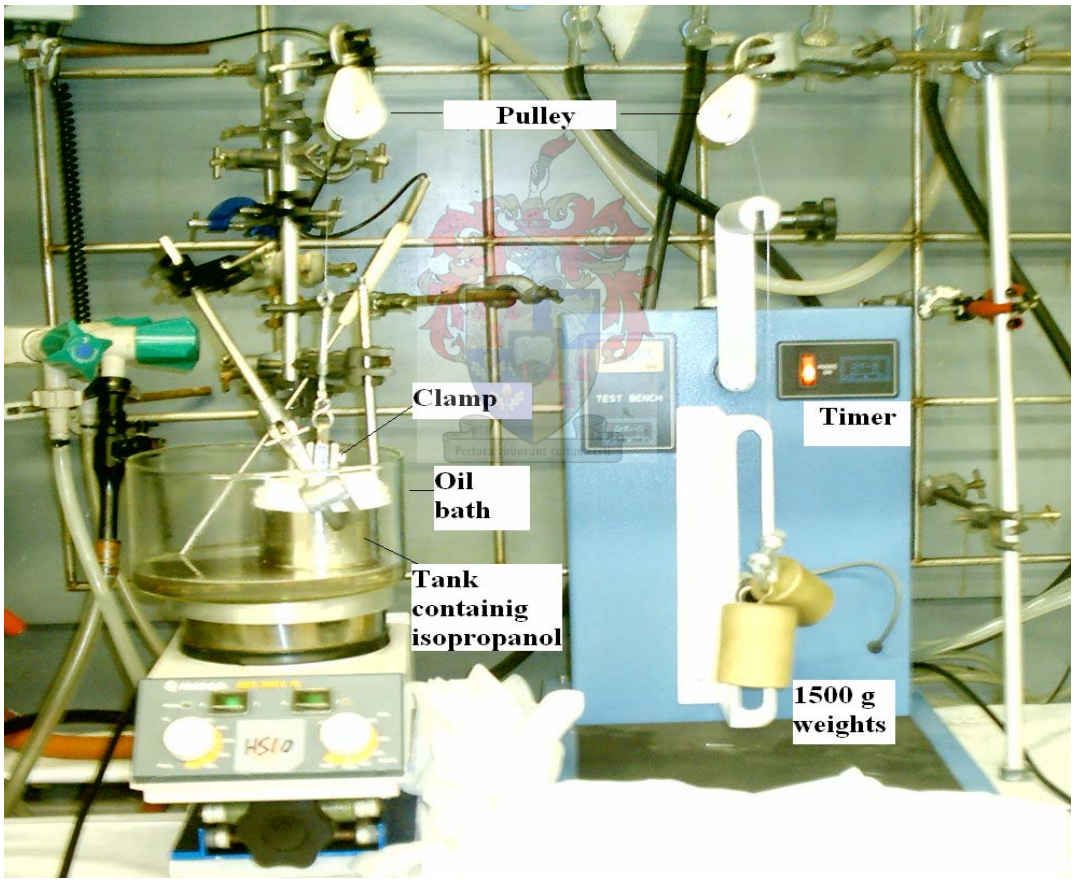

Figure 4.4. Test method for determining ESCR of ethylene based plastics setup

Three samples from each polymer were tested at a temperature of 60 ^{o}C (oil bath). According to Crissman [9], the principal advantage of this method over either ASTM D 1693 and ASTM D 2552 is the shorter time required to conduct the test. The failure

time for the all specimens was recorded using a running hour meter with a set point timer (RHM/PRHM1).

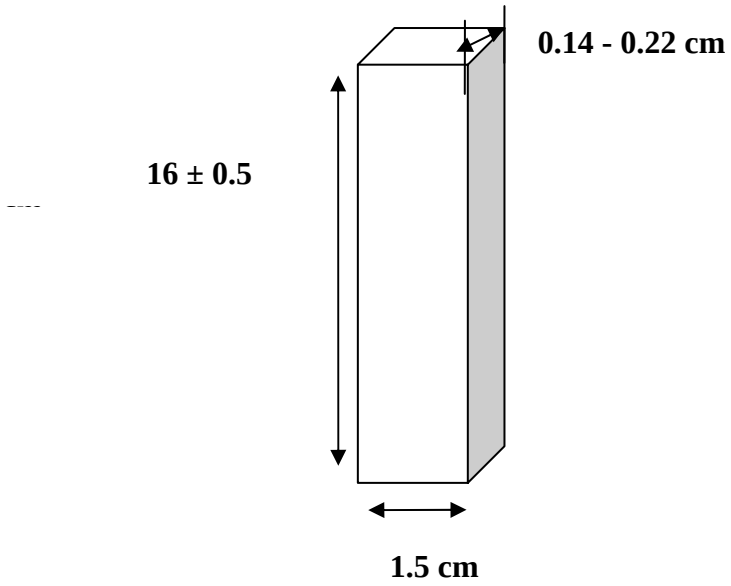

Figure 4.5. Geometry of the test specimens used in ESCR test 2

4.5 Study of the formation of crazes

Optical microscopy was used to investigate the time of craze formation. It was important to investigate craze formation of the IPPC samples in order to understand the failure process. The failure process of most polymers is usually associated with craze formation and governed by craze growth and craze breakdown. An understanding of the craze widening and failure processes is, therefore, important in order to gain insight into the mechanics of failure in materials.

Crazing is a unique morphological feature of polymers and morphologically different from true cracks. [(10)] Notched test specimens of each polymer were subjected to a constant stress (16.5 MPa) for different times (from 1 h to 10 h). Typically, the test specimens were strips having a length of 16±0.5 cm, a width of 1.5 cm, a 0.5 cm notch in the middle of specimen and a thickness that varied from 0.14-0.22 cm, as shown in Figure 4.6. The test method in Section 4.4.3 (test method for determining ESCR of ethylene based plastics) was performed in this investigation in pure isopropanol at 60 ^{o}C. Figure 4.6 shows geometry of the test specimen that used to investigate the craze formation.

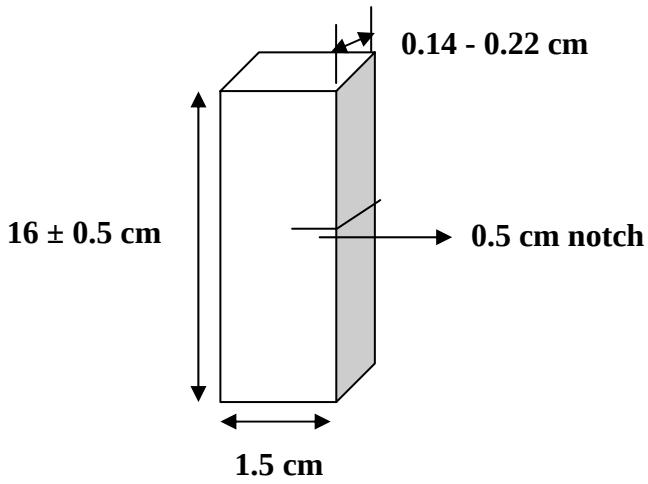

Figure 4.6. Geometry of the test specimen used for the test method for determining ESCR of ethylene based plastics to investigate the craze formation

4.6 Study of crack growth

The crack growth of IPPC samples was measured as a function of time. Test specimens from each polymer (with a length 16 ± 0.05 cm, a width of 1.5 cm, 0.5 cm notch in the middle and a thickness that varied from 0.14-0.22 cm, as shown in Figure 4.6) were subjected to the constant stress (15 MPa) in the presence of isopropanol at 60 ^{o}C. The test method for determining ESCR of ethylene based plastic (ESCR test 2) was used as a standard test method, as shown in Section 4.3.3. Five test specimens of each polymer were subjected to this stress for different periods of time to determine the increase in crack length or notch with time. This time was given according to the obtained ESCR results from ESCR test 2 (Section 4.4.3).

4.7 Morphology

The most common used technique for studying morphology of polymers is by etching. In this study, permanganic etching of polyolefins was used in order to prepare samples for the study of the morphology. This technique for polyolefins has been used by several groups. [11-14]

4.7.1 Preparation of etching reagent

Potassium permanganate (7g) was dissolved in 100 mL concentrated sulphuric acid. The solution was prepared by adding potassium permanganate very slowly to the beaker containing sulphuric acid, with rapid agitation. After adding all the potassium permanganate, the beaker was closed properly and stirred until all the potassium

permanganate was dissolved (yielded a dark green solution). All samples were etched at room temperature.

4.7.2 Procedure of etching process

Specimens from each polymer, with approximate dimensions of length 2 cm, width 1 cm and thickness 0.14-0.22 cm, were cut from the films prepared as described in Section 4.4.1. Each sample was immersed in 10 mL of the etching reagent in a beaker for a period of 150 minutes. Afterwards, the films were washed first with methanol (three times) and secondly with distilled water (three times). Finally, the films were dried in a vacuum oven at 45 ^{o}C for 3 h.

4.8 Characterization

4.8.1 Fourier-transform infrared spectroscopy (FTIR)

Fourier-transform infrared spectroscopy (FTIR) was used to determine the copolymer composition. Infrared spectra of the three original samples were recorded on a Perkin Elmer FTIR spectrometer (model Paragon 1000 PC). The Perkin-Elmer FTIR Spectrometer Paragon 1000 PC is a single-beam Fourier-transform IR spectrometer with FS-DTGS-Detector, 32bit processor and IRDM software (resolution better than 1 cm^{-1}). All samples were recorded from 350 to 4 700 cm^{-1} by using a photo-acoustic detector (PAS).

4.8.2 Nuclear magnetic resonance spectroscopy (NMR)

^{13}C NMR spectra of all the samples were measured and recorded on a Varian VXR 300 MHz spectrometer at 120 ^{o}C. The samples were dissolved in a 9:1 mixture of 1,2,4-trichlorobenzene:C_6D_6. C_6D_6 at δ = 128.02ppm was used as a internal secondary reference. Typical conditions were: 45^{o} pulse and 0.82 s acquisition time.

4.8.3 High-temperature gel permeation chromatography (HTGPC)

Number average molecular weight ($\overline{M_n}$), weight average molecular weight ($\overline{M_w}$) and molecular weight distribution (MWD), were determined by using high-temperature gel permeation chromatography (HTGPC). A PL-GPC 220 high-temperature chromatograph was used with a differential refractive index detector. The flow rate was 1 ml/min and temperature was 160 ^{o}C. Column packed with a polystyrene/divinylbenzene copolymer (PL gel MIXED-B) from Polymer

Laboratories were used. The length and diameter of these columns were 300 mm and 7.5 mm, respectively. Particle size was 10 μm. The concentration of the samples was 2 mg/ml. 1,2,4-Trichlorobenzene, stabilized with 0.0125% 2,6-di-tert-butyl-4-methylphenol, was used as solvent. The calibration was done with monodisperse polystyrene standards (EasiCal from Polymer Laboratories).

4.8.4 Differential scanning calorimetry (DSC)

The degree of crystallinity was determined by differential scanning calorimetry (DSC). A TA instrument Q100 DSC system was used. It was first calibrated by measuring the melting temperature of indium metal according to a standard procedure. All measurements were conducted under a nitrogen atmosphere, and at a purge gas flow rate of 50 ml/min. The samples were heated from 25 to 220 ^{o}C at 10 ^{o}C/min, held isothermally at 220 ^{o}C for 1 minute and cooled to -30 ^{o}C at a rate of 10 ^{o}C/min, during which time the cooling crystallization curve was recorded. At -30 ^{o}C the temperature was kept constant for 1 minute, after which the melting curve was recorded between -30 and 190 ^{o}C at a heating rate of 10 ^{o}C/min. The weight of samples varied from 2 to 5 mg.

4.8.5 Optical microscopy

A Zeiss Axiolab optical microscope (magnification x 50 μm) with a high resolution camera CCD-IRIS (Sony) was used to examine the damage zone, to investigate the craze formation and to look at the mode of crack of the specimens under reflective light conditions.

4.8.6 Scanning electron microscopy

Scanning electron microscopy (SEM) was used to look at the surfaces of the samples after the etching process. Imaging of the surfaces of the samples was accomplished using a Leo® 1430VP scanning electron microscope. Prior to imaging the samples were sputter-coated with gold.

4.9 References

1- Product data sheet (CMV348), Sasol Polymers Polypropylene Business, **2004**.
2- Product data sheet (CKR448), Sasol Polymers Polypropylene Business, **2004**.
3- Product data sheet (CMR648), Sasol Polymers Polypropylene Business, **2004**.
4- Icon Electronics home page, www.icon-electronics.com, Created in **2002**.
5- B. Borisova and J. Kressler, Macromolecule Material and Engineering, **2003**, 288, 509-515.
6- J. Lagaron, N. Dixon, L. Gerrard, W. Reed and B. Kip, Macromolecules, **1998**, 31, 5845-5852.
7- J. DeCoste, F. Malm and V. Wallder, Industrial and Engineering Chemistry, **1951**, 43, 117-121.
8- H. Mark, and N. Gaylord, Encyclopedia of Polymer Science and Engineering, Second Edition, Executive Editor: A. Standen, John Wiley & Sons, USA, **1971**, 7, 287.
9- J. Crissman, Journal of Testing and Evaluation, **1983**, 11, 273-278.
10- J. Fried, Polymer Science and Technology, Prentice Hall PTR Inc., USA, **1995**, 161-163.
11- R. Olley, A. Hodge and D. Bassett, Journal of Polymer Science: Polymer Physics Edition, **1979**, 17, 627-643.
12- K. Naylor and P. Phillips, Journal of Polymer Science: Polymer Physics Edition, **1983**, 21, 2011-2026.
13- A. Freedman, D. Bassett, A. Vaughan and R. Olley, Polymer, **1986**, 27, 1163-1169.
14- R. Olley, Science Progress, **1986**, 70, 17-43.
15- J. Scherirs, Compositional and Failure Analysis of Polymer: A Practical Approach, John Wiley & Sons, UK, **2000**, 108-126.

Chapter 5

Results, discussion and conclusion (original samples)

5.1 Evaluation of stress crack agents

Various chemicals were used in efforts to find an active SCA for the three IPPC samples using the test method for determining ESCR of ethylene-based plastics (ESCR test 2). Teepol, ethanol, sodium dodecylbenzene sulphonate and isopropanol were used as potential SCAs in order to determine the ESCR of the three samples. All these chemicals were liquids which could be added directly to tubes containing stressed specimens. All, except isopropanol, were used as aqueous solutions of different concentrations (10%, 50%, 90% and 100% by volume). Teepol, ethanol and sodium dodecylbenzene sulfonate did not show any effect on these polymers. So, for our purposes, they could not be considered as SCAs for these samples (not active enough for IPPCs). PP generally resists most organic and inorganic acids, and bases below 90 ^{o}C, salt solutions, solvents, soaps, wetting agents and alcohols. [1-2] On the other hand, pure isopropanol showed a marked effect on the three samples. Isopropanol can, therefore, be considered as a low active SCA, producing cracking in IPPCs, and was therefore selected for all further tests.

5.2 ESC experimental results

5.2.1 ESCR test 1

Four notched specimens of each polymer were used in this test. The results showed that the three samples (A, B and C) did not fail during the 500 h of testing at 50 ^{o}C. This result in general indicates high ESCR for all three IPPCs. The length of the notch in sample C increased from 2.0 cm to 2.5 cm (0.5 cm/500 h). Samples A and B showed less of an increase in the length of the notch (0.2 cm/500 h and 0.3 cm/500 h, respectively), as shown in Table 5.1. These preliminary results indicate that the ESCR seems to decrease from A to B to C, as the ethylene content increases.

It is also important to note that the crack starts in a direction perpendicular to the notch on both sides of the notch. Once the specimen is bent, the slit opens up and strains polyaxially. Cracking in the three tested samples were initiated by crazing. Crazing initiation depends on the level of stress on a specimen. Although no complete breakdown

of the samples occurred during this test, cracks in this type of test generally propagate at right angles to the slit. This may occur directly across the specimen or may take place at either end of the slit. [3]

Table 5.1. Crack length and crack rate in the three samples (ESCR test 1)

Sample	Length of crack Or notch at time 0 h, cm	Length of crack or notch after 500 h, cm	Crack rate, cm/h
A	2	2.2	0.2
B	2	2.3	0.3
C	2	2.5	0.5

ESCR test 1 condition: isopropanol as a SCA at 50 ^{o}C.

5.2.2 ESCR test 2

Table 5.2 shows typical ESCR data obtained from ESCR test 2 under a predetermined constant applied force (calculated to give a stress of about 15 MPa) at 60 ^{o}C. All the tests were carried out using unnotched specimens. These results complimented the results that obtained for ESCR test 1. The ESCR data was analyzed both as recorded, and then as "normalized" data. The latter was done as the specimens were not of the same thickness. Thicker samples would obviously have a larger cross-sectional area and as the force remained constant, would experience a lower stress. The original calculations were done assuming a sample thickness of 0.15 cm, and results were therefore adjusted by a calculating the real stress and normalizing it to a stress experienced by a sample of 0.15 cm thickness. These results are shown in the last column of Table 5.2. The use of "normalized" failure times (Table 5.2) has effect on the trends illustrated, but allows for greater accuracy in determining average ESCR behaviour.

As in ESCR test 1, these tested samples showed a high resistance to ESC. This resistance decreased from A to B to C, as the ethylene content increases. ESCR test 2 is more effective and accurate than ESCR test 1, especially for testing high ESCR polymers (e.g. IPPCs). In ESCR test 2, the exact failure time for each sample was recorded precisely, by using the timer that is described in Section 4.3, while in ESCR test 1 it is difficult or even impossible to record the exact time of failure, even if all the samples failed. ESCR test 1 is reported to be less frequently used nowadays. [4-5] ESCR test 1 is easy to use to

estimate ESCR of polymers with poor ESCR due to its simplicity and the inexpensive equipment necessary for the test. On the other hand, high ESCR polymers such as IPPCs can be tested without difficulty by ESCR test 2. ESCR test 2 is an attractive method as it is simple, costs little, shows no decay in the stress with time due to stress relaxation, and is accurate in determining the precise failure time. [6]

Table 5.2. ESCR data of samples A, B and C obtained by ESCR test 2

Sample		ESCR for each specimen (hh:mm)	Average ESCR (h)	ESCR for each specimen (hh:mm) after normalization	Average ESCR (h) after normalization
Sample A					
	Thickness (cm)				
Specimen 1	0.14	85.08	**93.78**	91.16	**86.86**
Specimen 2	0.16	94.90		88.97	
Specimen 3	0.19	101.36		80.02	
Sample B					
Specimen 1	0.15	27.31	**32.93**	27.31	**26.12**
Specimen 2	0.22	36.01		24.55	
Specimen 3	0.20	35.48		26.51	
Sample C					
Specimen 1	0.15	17.31	**15.27**	17.31	**15.58**
Specimen 2	0.14	13.49		14.45	
Specimen 3	0.15	15.00		15.00	

ESCR test 2 conditions: isopropanol as a SCA, 50 ^{o}C and 15 MPa.

As in ESCR test 1, these tested samples showed a high resistance to ESC. This resistance decreased from A to B to C, as the ethylene content increases. ESCR test 2 is more effective and accurate than ESCR test 1, especially for testing high ESCR polymers (e.g. IPPCs). In ESCR test 2, the exact failure time for each sample was recorded precisely, by using the timer that is described in Section 4.3, while in ESCR test 1 it is difficult or even impossible to record the exact time of failure, even if all the samples failed. ESCR test 1 is reported to be less frequently used nowadays. [4-5] ESCR test 1 is easy to use to estimate ESCR of polymers with poor ESCR due to its simplicity and the inexpensive

equipment necessary for the test. On the other hand, high ESCR polymers such as IPPCs can be tested without difficulty by ESCR test 2. ESCR test 2 is an attractive method as it is simple, costs little, shows no decay in the stress with time due to stress relaxation, and is accurate in determining the precise failure time. [6]

The appearance of a typical ESC surface near a crack area can be illustrated by using optical microscopy, as shown in Figure 5.1. Figure 5.1 demonstrates clearly the appearance of the ribs (light area) and hackles (dark area) marks. The crack propagation takes place in a direction that approaches the rib marks on the concave side and leaves on the convex side. [3]

Figure 5.1. Typical ESC surface of sample B (magnified to 50 x 50μm)

The properties of IPPCs can be correlated to their molecular architecture. IPPCs are known to have multi-fraction copolymeric structures. Each of these fractions has significantly different average properties. These fractions are: EP random copolymer (EP rubbery material), a series of EP "blocky" copolymers with different sequence lengths of ethylene and propylene, and PP homopolymer. Some ethylene units could crystallize and form crystalline PE. The difference in properties of individual IPPCs originate from the difference in the composition of the fractions, for example, the different weight percentage of EP random copolymer and/or PP homopolymer and/or EP blocky copolymer component and/or the ethylene content and its distribution. [7-10]

The amount and the distribution of ethylene can be a critical factor for certain properties such as impact properties and crystallinity. [11-13] The ethylene may present as partially crystalline or amorphous regions. [14] An increase in the ethylene content in these copolymers can be associated with an increase in ductility and toughness for the copolymer, and a decrease in stiffness or Young's modulus. This could result in a decrease in the ultimate force or strength, [15-16] leading to a decrease in ESCR.

An important factor in the failure process of IPPCs is the role of the presence the rubbery ethylene/propylene (EP) copolymer. These rubbery materials control craze growth and initiate numerous, small energy absorbing crazes. The crazes act as stress concentrators and they are able to absorb energy up to failure. The main energy dissipation mechanisms can be multiple crazing (source of toughness), shear yielding and void formation. The presence of EP rubber is always associated with an increase in toughness and ductility. [14] The copolymerization of propylene with ethylene is known to be one of the most useful and effective methods for improving the toughness and properties of PP. [7]

The properties of IPPCs in general are dependant on composition, inclusive of monomer sequence distribution and tacticity distribution. [8,17] The composition and sequence structure of these polymers can be determined by IR and ^{13}C NMR spectroscopy, as discussed in the following section.

5.3 Characterization of IPPC samples (A, B and C)

5.3.1 FTIR

IR spectra of samples A, B and C are shown in Figure 5.2. The shape (single or double peak) of the ethylene absorption band at approximately 720-740 cm^{-1} indicates whether the polymer samples contain more random or more blocky type copolymers. [18-21] The three IPPCs samples appear to have a blocky structure as indicated by the characteristic band at approximately 720-740 cm^{-1} (Figure 5.3). The bands at about 720-731 cm^{-1} for sample A, 720-740 cm^{-1} for sample B and 724-736 cm^{-1} for sample C arise from the methylene rocking vibration for $(-CH_2-)_n$ sequences (with $n \geq 5$), of methylene units. It is clear that the ethylene distribution of the three samples is different, as is the apparent ethylene content.

Although there is no real agreement in the literature about the concentration range where these polymers can develop PE-type crystallinity, some crystallizable ethylene sequences might be present in these three samples. The ethylene contained in sequences of $-(CH_2)_n-$ with $n>5$ increases from A to B to C if we take the intensities of these characteristic bands is indicating this fact. We know from the characterization of these materials that the overall ethylene content increases from A to B to C, it now appears as if the

crystallizable ethylene sequences also increase as the ethylene content increases. The actual length of these sequences cannot be ascertained by IR, as the technique cannot distinguish between methylene sequences lengths when longer than five repeat units. [22]

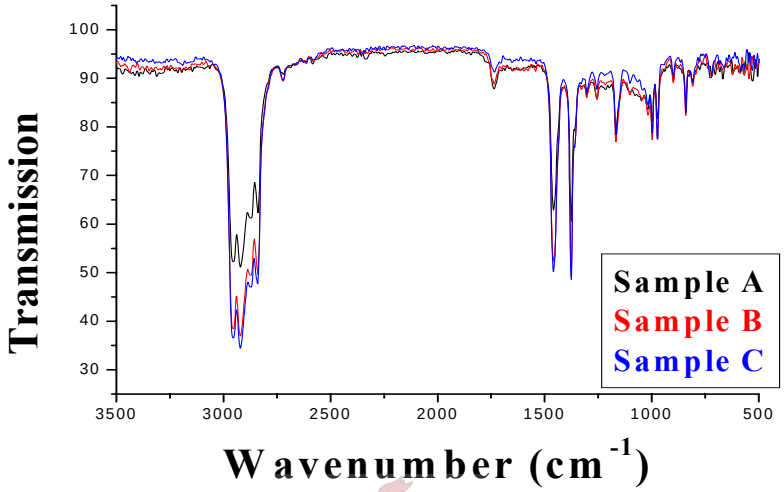

Figure 5.2. IR spectra of the three IPPC samples

The other important bands are also shown in Figure 5.3. The bands at 998 and 841 cm^{-1} are due to methyl rocking modes and are associated with the threefold helix of isotatic PP (iPP). These bands indicate that there are long PP segments that can crystallize. The band at 972 cm^{-1} is associated with methyl rocking vibrations of amorphous PP. The band at 1168 cm^{-1} is associated with the rocking vibration of the ($–CH_3$) group, and is thus a measure of propylene content. Propylene is therefore present in both crystalline form (iPP) and amorphous form (amorphous PP and EP copolymers/EP rubber).

The IR spectra of these IPPCs illustrate the complex nature of these materials, and also show quite clearly that there are differences in composition between the materials, particularly with respect to the way that the ethylene is distributed. [23-25] The differences between the three samples lie mainly in the three aspects: difference in the amount of EP rubber (EP copolymer), crystalline PP and ethylene-type crystal. These differences are somehow responsible for the different in the ESCR.

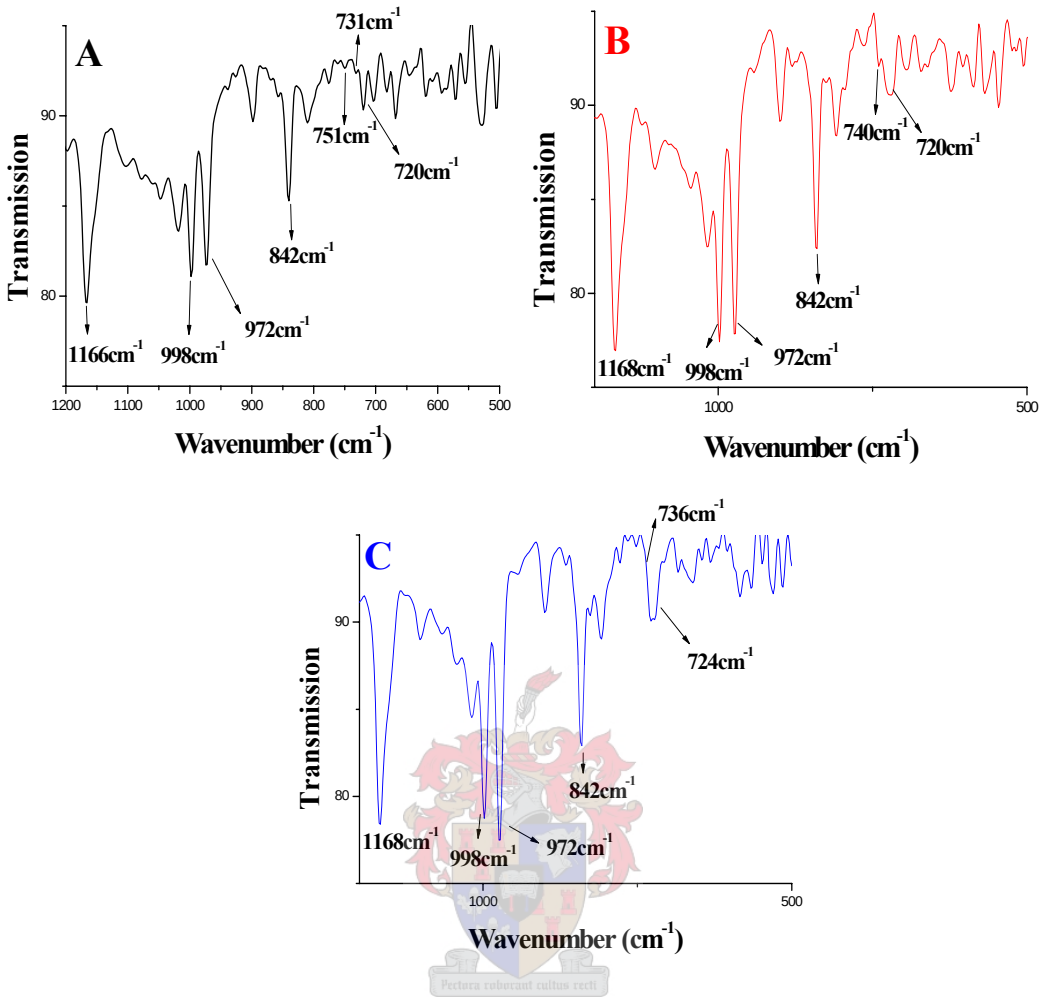

Figure 5.3. IR spectra of IPPC samples A, B and C

5.3.2 ^{13}C NMR

The ^{13}C NMR spectra of the three original samples A, B and C are given in Figure 5.4. The peak assignments are reasonably easy, and can be done according to literature. [9,17,22,23,26,27] The three major peaks at around 21, 28 and 45 ppm (peaks 1,2 and 4 in Figure 5.4) correspond to the three different carbon atoms in the constitutional base unit of PP (methyl (CH_3), methine (CH) and methylene (CH_2)). The other peaks of varying intensity (peaks 3 and 5, as well as those indicated by the area 6 in Figure 5.4) are those associated with the presence of ethylene. It can be seen that the main difference in the three ^{13}C NMR spectra is the difference in ethylene content, as evidenced by the relative intensities of these peaks in the spectra. This illustrates very clearly that the ethylene content increases from polymer A to B to C.

Table 5.3. ^{13}C NMR assignments of the three tested samples (A, B and C)

Peak number	Chemical shift (ppm)			Tacticity, %		
	Sample A	Sample B	Sample C	Sample A	Sample B	Sample C
1	20.45	21.58	21.08	60.26	69.92	67.36
2	27.49	28.66	28.15			
3	28.61	29.79	29.28			
4	45.14	46.32	45.80			

Peak numbers 1, 2, 3 and 4 are shown in Figure 5.4
All samples dissolved in 9:1 mixture of 1,2,4- trichlorobenzene:C_6D_6

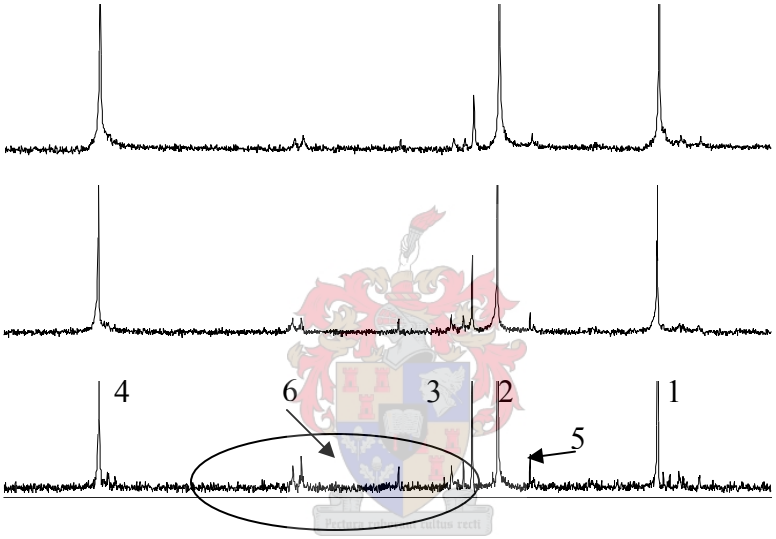

Figure 5.4. ^{13}C NMR spectra of the three original IPPC samples (A, B and C)

The isotacticities (*mmmm*%) of the three samples are evaluated and found to be 60.26% for sample A, 69.92% for B, and 67.36% for C. This indicates that the tacticity of the PP segments is similar for samples B and C, and that it is generally higher for B and C than for sample A. The crystallinity due to long sequence lengths of propylene is therefore expected to be higher for samples B and C. In addition, the increase in the ethylene content from A to B to C, indicates that there are probably more PE-like crystalline areas present in sample C than in the other two samples, which could result in an increase in the overall crystallinity of this sample. This would, of course, only be true if the ethylene is contained in crystalline rather than amorphous areas. It was expected that both

morphology and physical properties of IPPCs would depend strongly on the ethylene content and the molecular structure (distribution of ethylene). [13, 23]

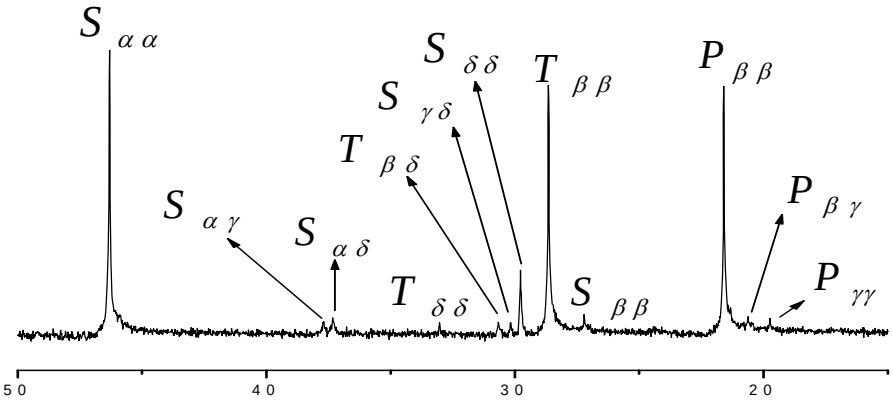

Figure 5.5. ^{13}C NMR spectrum of IPPC sample A

The detailed assignment of the peaks of the ^{13}C NMR spectra is illustrated in Figure 5.5, using sample A as example. Assignments were made were according to Carman & Wilkes and Randall & Cheng. [9,17,22,23,26,27] This helps considerably in elucidating the true composition and sequence structures of the three IPPCs. Table 5.3 lists the assignments of the peaks, chemical shifts and integration of each carbon atom in the ^{13}C NMR spectra of each sample. The nomenclature assigning the peaks for various carbons of sample A is shown in Figure 5.5. Assignments for the methylene carbons in Figure 5.5 are identified by the letter S and a pair of Greek letters that indicate its distance in both directions from the nearest tertiary carbons. A methyl carbon is identified by the letter P and a tertiary carbon is labeled by the letter T.

The four assignments $S_{\delta\delta}$, $S_{\alpha\alpha}$, $T_{\beta\beta}$ and $P_{\beta\beta}$ in Figure 5.5 result from long and continuous PE segments and PP segments. The intensities of these peaks were generally stronger in sample C than in samples B and A, which indicate that both continuous propylene and ethylene sequences are present in sample C in larger amounts compared to A and B. The assignment $S_{\delta\delta}$ at 28.61-29.79 ppm showed clearly that the ethylene content (EEEEE sequences) increased from A to B to C, according to the integrals of these peaks. Finally, some small peaks such as $S_{\alpha\delta}$, $T_{\delta\delta}$ and $T_{\beta\delta}$ also appeared. This means that segments such as EEP, EPE and PPE exist between the PP segments.

Table 5.4. Assignment of the ^{13}C NMR peaks, chemical shifts and integration in three IPPCs

^{13}C NMR			Peak integration (%) of		
Assignments	**Chemical shifts (ppm)**	**Sequences type**	**A**	**B**	**C**
$S_{\alpha\alpha}$	45.14-46.32	PPPPP	18.53	21.28	19.03
$S_{\alpha\gamma}$	37.70-37.90	PPEP	01.02	01.68	02.13
$S_{\alpha\delta}$	37.08-37.70	EEP	01.60	01.70	02.09
$T_{\delta\delta}$	33.03-33.20	EPE	00.46	00.82	00.80
$T_{\beta\acute{\delta}}$	30.40-30.78	PPE	00.79	01.04	01.35
$S_{\gamma\delta}$	30.00-30.31	PEPP	00.47	01.24	00.98
$S_{\delta\delta}$	28.61-29.79	EEEEE	03.74	04.35	05.78
$T_{\beta\beta}$	27.49-28.66	PPPPP	19.15	19.57	20.34
$S_{\beta\beta}$	27.20-27.40	PPEPP	00.89	01.22	00.73
$P_{\beta\beta}$	20.45-21.58	PPPPP	18.13	17.90	19.03
$P_{\beta\gamma}$	20.60-20.98	PPPPE	01.55	00.21	00.96
$P_{\gamma\gamma}$	19.90-20.70	PPPEP	01.01	00.43	00.16

The results in Table 5.4 confirm the IR results about the presence of four types of component in these polymers: EP amorphous or rubbery materials, EP "blocky" copolymer, crystalline PE or continuous ethylene units and PP homopolymer or very long continuous propylene units. Table 5.4 also confirms the increase in the long ethylene sequences and crystalline PP from A to B to C, as the ethylene content increases. The total distribution of ethylene is different from sample A to B to C. In samples B and C the presence of isolated ethylene units are higher than in A. In A, roughly 35% of the ethylene is in the form of long crystallizable ethylene sequences, while the figures are about 38% for B and about 41% for C. Also, the crystalline propylene (PPPPP) content (or iPP) is almost similar for samples B and C and slightly lower for A. These units are about 55.8% in sample A, 58.4% in B and 58.7% in C. So, not only does C have more ethylene than A and B, but the percentage of "crystallizable" ethylene segment and

crystalline PP is also higher than in B and A. According to Tan *et al.* [7] the low miscibility of EP "blocky" copolymer with long PE and PP sequences leads to poor compatibility and toughness. This is probably why the ESCR value for sample C is so much lower than both A and B. On the other hand, a high propylene content and low ethylene content, as shown by sample A, suggests better compatibility of the EP type copolymers. [28]

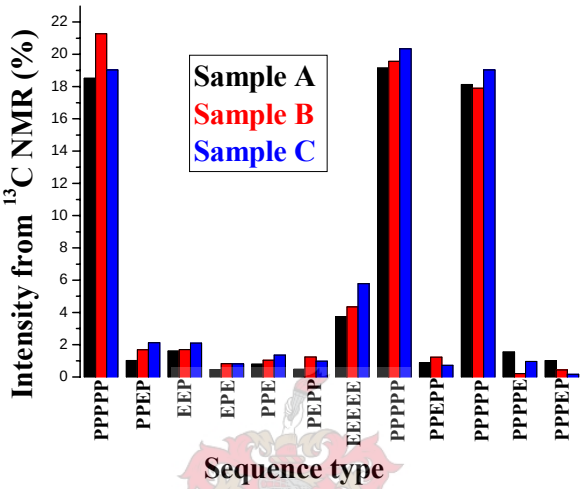

Figure 5.6. The percentage of sequence types in samples A, B and C

It is difficult to draw definite conclusions about the structure-property relationships by just looking to the IR and NMR results. We need to look at bulk material properties as well: molecular weight and distribution, crystallinity and morphology. Since these properties greatly affect the polymer properties, it is necessary to compare these thoroughly.

5.3.3 DSC

According to Scherirs [29], crystallinity of polymers as obtained from DSC data can be a good indicator of the rate of cooling, the density, the optical properties and finally the ESCR. DSC results confirmed the increase in crystallinity in these samples from A to B to C. The crystallinity increased from A (25.06%) to B (36.12%) to C (40.50%), as shown in Table 5.5. The crystallinity was measured by dividing the heat of fusion required to melt a known weight of each polymer samples (the area under the melting peak) by the heat of fusion for a 100% crystalline PP by using the following equation (equation 2):

$$\Delta H_F / \Delta H_{F(100\%)} x100 \quad \ldots\ldots\ldots\ldots\ldots\ldots\ldots (2)$$

Where ΔH_F is the heat fusion of the sample, as determined from the DSC curve, and $\Delta H_{F(100\%)}$ is the heat fusion of 100% crystalline PP. According to Park *et al.* [30] the $\Delta H_{F(100\%)}$ of a folded chain of iPP has a value of 208.3 J/g. The values for crystallinity presented in Table 5.5 are therefore not completely accurate, as part of the heat of fusion could be due to polyethylene-like crystals.

Table 5.5. Characterization of IPPCs by DSC

Sample	T_m (°C)	T_c (°C)	ΔH (J/g)	Crystallinity, %
A	165.30	123.95	52.19	25.06
B	164.75	123.51	75.23	36.12
C	164.67	123.30	84.37	40.50

DSC cooling curves of the three samples showed two exothermic peaks for the crystallization, as shown in Figure 5.7 for sample C and Appendix B for samples A and B. The larger, dominant peak (123.30-123.95 °C) is due to the crystallizing of the homopolymer PP crystal. [31] Only a single peak was detected in the melting endotherms for each sample, which indicates that sequences of stereoregular propylene units of longer than 80 units were present. [31] The other (weak) peak at 84-87 °C probably corresponds to the crystallization of the ethylene sequences. Whatever the cause of the weaker crystallization peak, the melting confirmations of the structures that are formed is not large enough to visibly affect the melting endotherms.

Pizzoli *et al.* [32] found that sequences of 10-20 ethylene units are known to be responsible for the development of about 10% crystallinity. So, it is therefore possible that the ethylene units in the three tested samples could crystallize and result a minor increase in the overall crystallinity. Although increasing the ethylene content resulted in an increase in the overall crystallinity, there is no effect on the T_m and T_c. The overall increase in crystallinity comparing A to C might be ascribed to tacticity of the PP segments, but as B and C have very similar tacticity (B is higher than C), the difference in crystallinity is most likely due to the crystallization of ethylene sequences (less EP rubber).

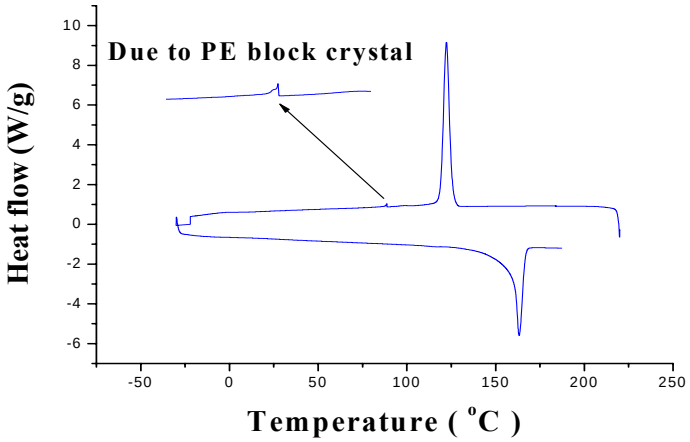

Figure 5.7. DSC curves of sample C

The difference in the values of ESCR of these polymers can be related to the difference in crystallinity, which is related to the ethylene content. The effect of crystallinity on ESCR has been reported in several papers. [33-37] As the crystallinity decreases, ESCR generally increases. Increasing the crystallinity of a material will eventually result in an increase in stiffness and a reduction in the material's permeability and elasticity, and will also reduce stress cracking resistance. As expected, as the crystallinity increased from A to B to C, the ESCR decreased.

In crystalline polymers the relatively large crystallize are bound together in such away that large stress concentrations inevitably develop. [38] Highly crystalline polymer might have more of these large crystallites than a less crystalline polymer. On the other hand, ESCR could be dependant upon the number of tie-molecules. [37,39] The tie-molecules bind the lamellae and so provide the strength, and when their numbers decrease the strength will be reduced. Thus, as the number of tie-molecules increases there is more binding strength among different lamellae, proportional to the applied stress and ESCR increases. In the three tested IPPCs, the decrease in the ESCR could be due to the decrease in the number of tie-molecules.

Sample A with low crystallinity is expected to have a higher number of tie-molecules than B and C. According to Lustiger [33] it would be expected that the more the crystalline the material, the fewer amorphous intercrystalline tie-molecules that hold it together.

An increase in crystallinity can have a marked effect on stress cracking, but whether the value of ESCR increases or decreases is dependant on the conditions involved. [35,40] Polymers are, by nature, sensitive to the conditions of testing (the type and the speed of the testing method). As mentioned in Chapter 3, there are two types of testing: test at constant strain and test at constant stress. It has been found [40] that under constant stress test, as in ESCR test 2, the HDPE showed superior stress crack resistance to the less crystalline LDPE, while under constant strain the opposite effect was observed. This fact is not true in the case of IPPCs because the least crystalline sample (sample A) showed superior ESCR comparing to C (higher crystallinity) when using constant stress conditions (ESCR test 2).

5.3.4 GPC

Table 5.6 shows the results of GPC molecular weights (MWs) for the three samples. These results include the average number molecular weight ($\overline{M_n}$), the weight average molecular weight ($\overline{M_w}$) and polydispersity (MWD). The range of $\overline{M_w}$ in the three samples varies from 240.06 x 10^3 to about 368.91 x 10^3, while the range of MWD was between 3.81 to 4.45. The difference in the MWs of samples B and C are not significant ($\overline{M_w}$ = 240.06 x 10^3 for B and 270.98 x 10^3 for C and $\overline{M_n}$ =61.015 x 10^3 for sample B and 60.899 x 10^3 for sample C). Sample A has a higher molecular weight ($\overline{M_w}$ and $\overline{M_n}$) than B or C, while the MWD of A and B is a little lower than for C.

Table 5.6. MWs of the three IPPC samples determined by GPC

Samples	$\overline{M_w}$ x 10^3	$\overline{M_n}$ x 10^3	MWD
Sample A	368.91	96.748	3.81
Sample B	240.06	61.015	3.93
Sample C	270.98	60.899	4.45

The general thought is that higher molecular weight (longer molecular chains) of the polymer, the higher is its ESCR. The longer the molecular chain, the higher the likely number of tie-molecules. Longer chains also have more entanglements and therefore

make the isopropanol migration somehow more difficult into polymers. The migration of isopropanol can be also effected by the chain ends and free volume. So, as the stress crack resistance is higher for A than for B and C, it could be thought that the higher molecular weight could play a role, but the higher molecular weight for C than B (albeit only slightly higher) would then be indicative that molecular weight is not the only factor causing the difference, as the ESCR for C is significantly lower than that of B. Although the molecular weight distribution is a potential contributor to variations in stress crack behaviour and can be critical factor, [35,40] there is no major difference in the molecular weight distribution for these samples.

So, from the DSC and GPC results, we can conclude that crystallinity appears to be an important factor in determining ESCR of these polymers.

5.4 The formation of crazes

The reason behind studying the crazes formation is because ESC of most polymers proceeds by initiation and growth of crazes which break down to form cracks. Crazing has been observed in IPPC. [41] ESCR test 2, with test specimens prepared as described in Section 4.5, was used at constant stress (16.5 MPa) and 60 ^{o}C to observe the formation of crazes in these samples. Crazes were studied as a function of time and the frequency of analysis depended on the ESCR results presented in Table 5.2. Optical microscopy clearly indicated craze formation in the deformation zone.

Figure 5.8 illustrates the principal features of a craze in sample A. The craze as shown in Figure 5.8 shows a different morphology to that of true cracks. It shows highly oriented fibrillar or microfibrillar structures running from the top to the bottom of the craze. Figure 5.8 shows the first stage of craze initiation in sample A, where stress induced voiding leads to the development of regions of microporosity. These microspores (crazes) agglomerate into stable voids in the following stage. This stability is due to the presence of portions of materials inside the craze, which are polymer fibrils connecting the upper and the lower surfaces of the craze. With the action of external tension, the craze fibrils become more and more slender. The final stage of craze initiation is an extension process whereby the voided areas form the characteristic craze geometry. The craze grows and finally breaks down to from a crack and so on. All these stages repeat themselves until

the final failure occurs. The main difference between these stages is the decrease in the diameter of polymer fibrils that connect the upper and the lower surfaces of the craze as the crazes and cracks grow.

Figure 5.8. Optical micrograph of a crazed region in sample A (magnification 50 x 50μm)

These different stages of crazing are shown in Figure 5.9. Figure 5.9 shows the crazing in the three IPPCs, but at different stages. The craze in sample A was at an early stage of craze formation, when the regions of microporosity are formed. Sample C illustrates the end of the second stage when the microspores agglomerate into stable voids. The crazes in sample B shows the end of the breakdown stage when the crazes break down to form a crack. The density of craze initiation is controlled by the stress level and the nature of the SCA (isopropanol). [42] In fact, it appears as if isopropanol induced softening or plastization led to the formation of crazes. Li [43] said that the research results indicate that chemicals tend to accelerate a crazing process which happens much slower in the air. According to Hansen [44] if there is massive absorption, the polymer dissolves, while lesser degrees of absorption can lead to softening and plasticization and at least sometimes to ESC.

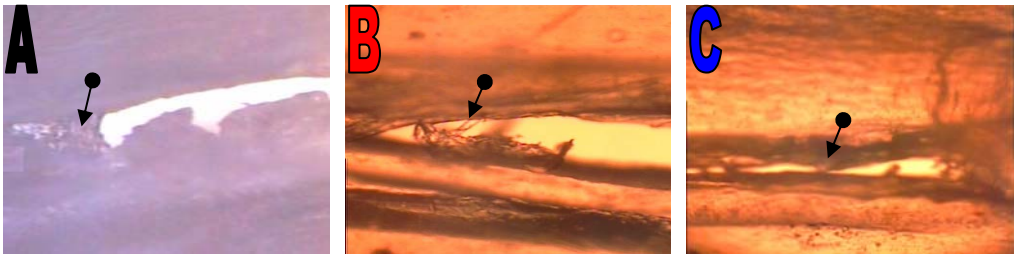

Figure 5.9. Optical micrograph of crazes in samples A, B and C at different stages (magnification 50 x 50μm)

No evidence or sign of craze formation was seen during the first hour in the three samples, as shown in Table 5.7. Crazing started in sample C due to static loading during the second hour, indicating that sample C has the lowest resistance to craze formation. Sample B deformed only in the fifth hour when crazes were formed. Sample A showed no deformation before 10 hours. This indicates that sample A has the highest resistance to craze formation. This is consistent with the differences in total time taken to breakdown.

Table 5.7. Time of the craze formation of the three tested samples

Samples	**Craze formation**									
	1 h	**2 h**	**3 h**	**4 h**	**5 h**	**6 h**	**7 h**	**8 h**	**9 h**	**10 h**
A	No	No	No	No	No	No	No	No	No	**Yes**
B	No	No	No	No	**Yes**	----	----	----	----	----
C	No	**Yes**	----	----	----	----	----	----	----	----

ESCR test 2: isopropanol as a SCA, 60 ^{o}C and 16.5 MPa

Four points were realized and should be mentioned in this part of this study. First, the main cause of ESC in these polymers immersed in isopropanol could be related to craze formation. It seems that there is sufficient isopropanol-induced softening or plastization to ensure the appearance of crazes, as stated above. Once crazes occurred, voids can then act as an easy diffusion path for the isopropanol, thus promoting further craze formation.

Second, according to the results of ESCR test 2 and the craze formation does not pose immediate danger to these polymers. Crazes can continue to sustain loads after they are formed. For example, crazes in sample C were formed during the second hour and final failure was observed only after 15 hours.

Third, although crazes must be time dependent, there is an induction period during which no crazes are visible; after this time the craze density and average craze length increase with time. This induction time seems to be dependant on the level of the applied stress and temperature.

Finally, the craze in sample A with the lowest percentage crystallinity and highest molecular weight formed after a longer period of time than the craze in samples B and C (higher percentage of crystallinity and lower molecular weight). Crazes are highly dependant on molecular weight [41], but as shown in the previous section, the effect of molecular weight is less in samples B and C. Crazing seems to occur more readily in those more crystalline polymers where a modification of the interphase regions might occur (less intersphrulite fibrils and tie molecules).

5.5 Crack growth

An attempt was also made to study the change in the crack length with time. Notched samples (prepared as described in Section 4.5) of each IPPC were studied by using ESCR test 2 under conditions of 15 MPa and 60 ^{o}C. At time 0 h the notch or crack was 0.5 cm length for the three polymers. Then five specimens of each polymer were subjected to the stress for different times in order to study the change in the length of these notches with time. The analysis times for each sample were determined according to the ESCR results in Table 5.2. The results of this test are represented in Table 5.8.

Table 5.8. Time under stress versus the crack growth of the three IPPCs

Sample A							
Time under stress, (h)	0	20	40	52	70	90	~115
Crack growth, (cm)	0.5	0.6	~0.66	0.7	0.9	1.4	2.0 (final failure)
Sample B							
Time under stress, (h)	0	6	10	15	20	30	~39
Crack growth, (cm)	0.5	0.6	0.7	0.8	0.9	1.3	2.0 (final failure)
Sample C							
Time under stress, (h)	0	2	4	6	8	15	~18
Crack growth, (cm)	0.5	0.6	~0.7	0.8	0.9	1.4	2.0 (final failure)

ESCR test 2: isopropanol as SCA, 60 ^{o}C and 15 MPa

The results showed that the crack length increased with time in the three samples, as shown in Table 5.8. For example, the crack length in sample C increased from 0.5, 0.6, 0.8, 0.9 and 1.4 cm after 0, 2, 6, 8 and 15 h, respectively, as shown in Figure 5.10. Sample A and B showed almost the same increase in the length of crack but after a longer period of time. Table 5.8 and Figure 5.11 shows that the mode of failure was almost the same for all the samples and the rate of the failure process was in keeping with the final failure times.

The crack growth in the three samples showed two distinct stages, as shown in Figure 5.11. These stages are a linear slow growth followed by a linear fast growth. The reason for the increasing speed of crack propagation, once a crack has started, according to the Griffith theory, is that as the crack grows in length, the stress required for propagation continually decreases. [42] So, the effective stress is increased, as the area is decreased, but the force remains the same. The force remains constant while the crack length increases in a controlled manner, until eventually a critical length is reached, then the velocity of crack growth becomes too high and the crack resistance decreases. In the slow crack propagation stage (stage 1, as shown in Figure 5.11) in the three samples, the crack goes beyond 0.9 cm, after that the crack velocity increased rapidly. So, 0.9 cm seems to be the critical crack length before the velocity of crack growth increases and crack resistance decreases. At this point, the ductile type deformation ends and brittle deformation begins. The final stage of failure seems to be brittle. The rapidity with which the crack grows in this stage indicates that the material's toughness has been reduced which seems to be more characteristic of a brittle material. [15] The later this “ductile-brittle” transition is, the better the resistance to ESC [35], for example sample A. All the polymers seem to be normally ductile but they eventually fail in a brittle manner when placed in isopropanol under a stress.

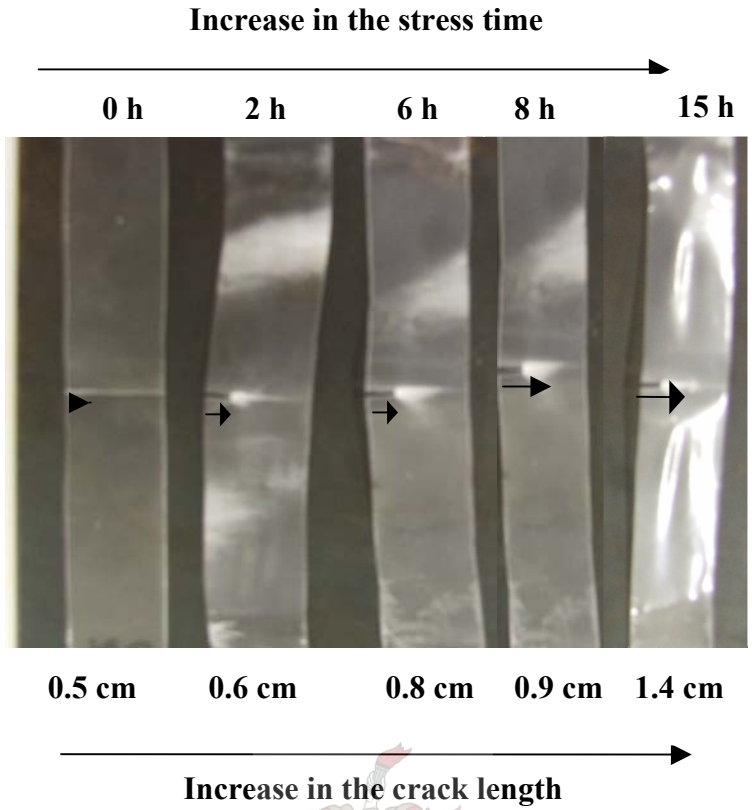

Figure 5.10. Increase in the crack length of sample C with increase in time

In addition, the difference in the velocity of crack growth can be due to the effect of the remnants of the craze material which holds together the polymer surface before the crack propagates through it. This seems to decrease from stage 1 to stage 2 in the three samples, as the crack propagates. The effect of the remnants of the craze material seems to decrease with time due to the increase in the diffusion of isopropanol into the tested samples and their resistance to temperature seems to decrease with time.

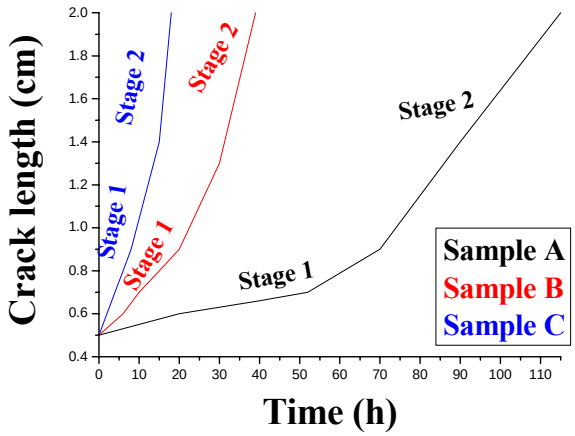

Figure 5.11. Crack length versus time for the three IPPC samples

Crazes (like those shown in Figures 5.8 and 5.9) act as initiation sites for cracks. So it is obvious that these crazes break down to form a crack. These crazes were transformed into cracks via the breakage of the fibrils, as shown in Figure 5.12. Figure 5.12 shows the typical feature of cracking in these polymers. Crack initiation depends on the presence of isopropanol and particularly on the affinity for the polymer for isopropanol and the diffusion rate of the isopropanol. [45] Crazes seem to play a dominating role and control the crack initiation and propagation since they are the defects at which cracks initiate and as these cracks propagate, more crazes are produced at the crack tip. The breakdown stage seems to be the governing stage. In general, crazing in the breakdown stage is dependent on time, stress, molecular weight, environment condition and thermal history. [41] In this study, with exception to the molecular weight of sample A, all these factors are almost constant. This means that the molecular weight of sample A could make a difference between the breakdown stage in sample A and breakdown stage in samples B and C. The breakdown stage gets shorter in samples B and C, as the molecular weight decreased, resulting in a decrease in the time to crack formation and propagation in these particular polymers.

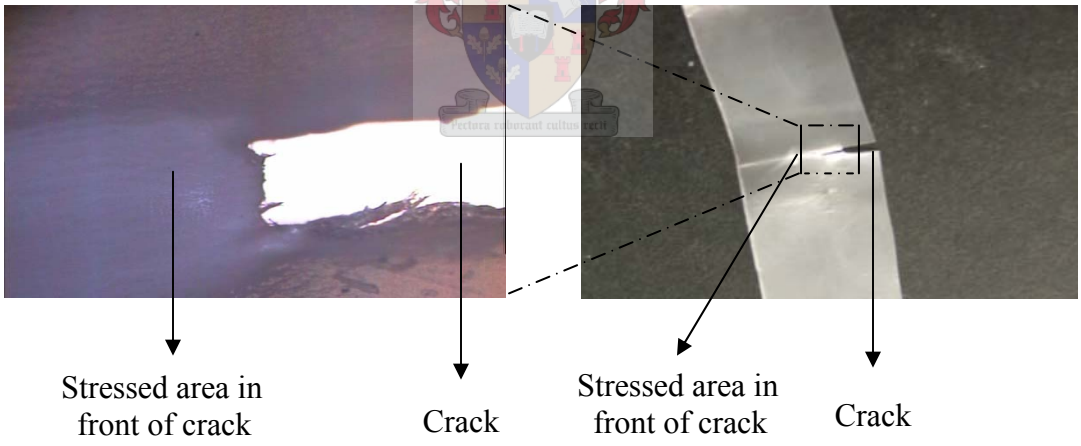

Figure 5.12. Optical micrograph and photograph of crack region in sample C, using ESCR test 2; isopropanol as a SCA, 4 h, 15 MPa and 60 ^{o}C

Molecular weight also has an influence on the craze size because increasing MW increases the strain hardening rates (a key factor of stabilizing craze microstructure) and strengths of craze fibrils. So, higher molecular weight tends to reduce craze tip stress. [41] This indicates that sample A can strain harden to higher levels and gives high craze

strength, while samples B and C would be expected to show less strain hardening. The greater the number of aligned chains in the direction of stress, the more strain hardened the material would be. It does appear, therefore, as if the higher molecular weight of sample A could indeed be a contributing factor to the overall ESCR of the sample, compared to B and C.

5.6 Morphology

Potassium permanganate was slowly added to the sulphuric acid, not vice versa, in order to minimize the likelihood of formation of the unstable and explosive manganese heptoxide. [46] According to Olley [47] this reagent must be prepared by shaking the powder into the vigorously stirred acid. This stirring is important in order to avoid any local concentration of the dangerously explosive manganese heptoxide that might form. The active species is believed to be O_3MnOSO_3H. [46] All the samples described in Section 4.7.2 were etched at the same conditions of temperature (room temperature), concentration (7% w/v) and time (150 min). The etched samples were examined by optical microscopy and SEM. SEM images were much clearer than the optical microscopy images and good enough for measuring the size of the rubber particles and the interparticle distances (to see the difference see Appendixes C and D).

The white areas in Figure 5.13 are particles present in the microstructure of IPPCs which are probably the EP rubber. The results in Table 5.9 are average values of particle size and interparticle distance of EP rubber particles. Three samples from each polymer were etched and examined by SEM. Then the values of the three samples were taken as an average value. This was done by using the instrument software to measure the average size of the particles and interparticle distances. EP rubber has been found to affect the morphology in these polymers. [48] The difference in the morphology in the three samples is due to the increase in the ethylene content and the presence of EP rubber particles.

The most obvious information that could be gleaned from these images is that the increase in the content of ethylene coincides with an increase in the number and a decrease in the size of the EP rubber particles. As is clearly shown in Figure 5.13, there are differences in both the size of the particles and the interparticle distances in the three

samples. The average particle size in sample C (0.166 μm) is smaller than in samples B (0.431 μm) and A (0.464 μm). The large average interparticle distance can be seen in the micrograph of sample B (1.265 μm), while sample A and C showed smaller interparticle distances, (0.942 μm and 0.430 μm, respectively), as shown in Table 5.9.

Table 5.9. Particle size and interparticle distance of the three IPPCs

Sample	Average particle size, μm	Average interparticle distance, μm
A	0.464	0.942
B	0.431	1.265
C	0.166	0.430

The properties of IPPCs, including ESCR, can also be related to the size and distribution of the rubbery component. The difference in the amount, size and composition of rubbery materials can affect the properties of IPPCs. [24] The size of the rubber particle and the interparticle distance between these particles could be one of the most important factors in controlling the mechanical behaviour of polymers. [13] For example, the particle size significantly affects the deformation and failure processes because small particles favour shear yielding while coarser particle dispersions promote crazing. [49] Furthermore, the difference in both the size of particle and interparticle distance can counteract the effect of toughening in IPPCs. [15]

According to Lotti *et al.* [49] the best average particle size is still a matter of debate, with some setting it at 0.3-0.35 μm and others at 0.4 μm. Marcus *et al.* [15] reported that a particle size of about 0.4 μm was found to produce optimum results for a PP system. In fact, when the rubber particles are of the proper size, about 0.4 μm, they initiate many subcritical crazes that absorb significant energy during the stressing and also act to interrupt the crazes before cracking occurs. [25] Although samples A and B seem to have particle sizes closest to the predicted optimum size, sample B has the largest interparticle distance. Results from this study indicate the best range of particle sizes for toughening IPPCs seems to be about 0.4 μm. The smaller particle sizes present in C also seems to indicate that much of the ethylene in this polymer is present in crystalline areas rather than rubbery areas.

Polymers in general fail in the manner that corresponds to the lowest energy necessary to produce failure. If the energy to produce brittle failure is higher than the energy necessary to produce ductile failure, the sample will fail in a ductile manner and vice versa. [50] The reason behind the presence of EPR in IPPCs is to toughen these polymers against crack propagation by dissipating large amount of energy in the matrix material around the particle, thereby blunting the crack and inhibiting crack propagation. [16] In fact, the toughening mechanism is related to the generation of many small crazes and the interruption of a propagation crack in these polymers. [24] Toughening these polymers results in an increase in the brittle-ductility transition as well. [15,51] Toughness can be the resistance to crack growth of a material by the energy absorbed as the crack moves forward. [52] In general, the deformation process can be dependent on the toughening effect and the brittle-ductile transition. [28] The main factors in the deformation process and the fracture of all toughened plastics are rubber content, rubber particle size, and interparticle distance between rubber particles. [53] The presence of EP rubber as well as the particle size is crucial in crazing process.

According to Marcus *et al.* [15] the difference in both the size of particle and interparticle distance can counteract the effect of toughening in IPPCs. So, the large interparticle distance of sample B and small particle size of sample C seem to counteract the effect of toughness in these samples. It seems possible that the factors of the size of the rubber particle and the interparticle distance played an important role in toughening of the three IPPCs. In addition to crystallinity, these two parameters could therefore be a factor in the ESC process and therefore contributed to the difference in the values of ESCR of the three investigated IPPCs.

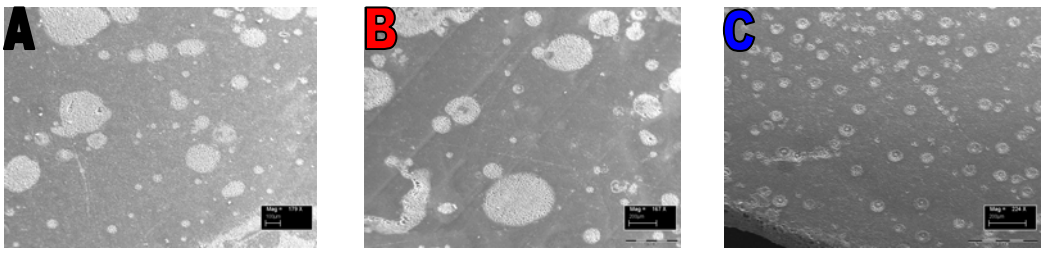

179 x 100 µm **179 x 200 µm** **224 x 200 µm**

Figure 5.13. SEM micrographs of etched IPPC samples

Sample A with 6.5% ethylene content showed the highest ESCR of the three polymers in pure isopropanol. This sample has the highest molecular weight, lowest crystallinity and closest to reported optimum particle size of rubbery particles, as well as most favorable distribution of these particle. The optimum size and distribution of EP rubber particles indicates good blendaiblity between different phases or fractions in IPPCs (poor blendaiblity prevents the rubber particles from effectively controlling craze propagation and there is little or no stress transfer from the matrix to rubber matrix). [24] On the other hand, particle size and interparticle distance of samples B and C are expected to be less effective for craze initiation and toughening. These factors are a consequence of the ethylene distribution and subsequent rubber-to-crystalline balance.

The lower crystallinity and these morphological features seem to result in A being a tougher material than B and C. The effect of the higher molecular weight of sample A must also be taken into account, but later results will indicate that molecular weight is probably not a determining factor when it comes to comparing the ESCR values for the three samples under investigation. The difference in ductility and toughness is borne out by the values presented in Table 4.2.

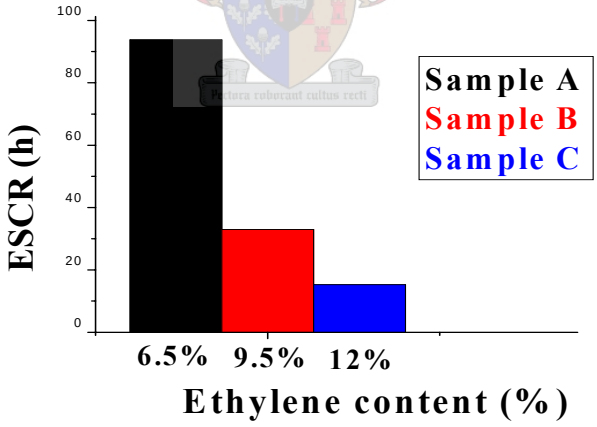

Figure 5.14. Ethylene content versus ESCR

Figure 5.14 is a graphic depiction of the effect of ethylene content on ESCR. Analyses presented in the foregoing sections have sought to reveal why this trend is prevalent. An increase in the ethylene content from 6.5% to either 9.5 or 12% appears to contribute to an increase in the overall crystallinity and affects either the rubber particle size and/or the interparticle distance between these particles. As the ethylene content increases from A to

B to C, toughness and ductility decreases. The main result that can be concluded from this study is that the ethylene content and distribution is an important variable regarding the failure process of these polymers.

5.7 Conclusions

Isopropanol can be considered as active environmental SCA that produces cracking in IPPCs, while the materials that had no affect on IPPCs such teepol, ethanol and sodium dodecylbenzene sulfonate can be considered as a low active environmental SCAs.

Although the Bell telephone test (ASRM D 1693) (ESCR test 1) was easy to use to estimate ESCR due to its simplicity and the low cost of the equipment necessary for the test, it was not aggressive enough for the investigation of Sasol IPPCs. It is difficult to use it for testing materials with high ESCR and it is even impossible to detect the precise failure time. On the other hand, the test method for determining ESCR of ethylene based plastics (ESCR test 2) was preformed without any difficulty and the exact failure time for each sample was recorded precisely by using a timer. Furthermore, the typical ESC surface (ribs and hackles) was indicated near the crack area by using optical microscopy. This test is attractive from the point of view of simplicity, inexpensive equipment is used, there is no decay in the stress with time due to stress relaxation and finally it is easy to ascertain the precise failure time. [6] In general, ESCR decreased from sample A with 6.5% ethylene content to B with 9.5% ethylene content to C with 12% ethylene content.

Although the three IPPCs that were investigated appeared to have the same general structure, they exhibited different ESCR with an important parameter being the differences in their microstructure. The difference between the three samples lie mainly in the four aspects: difference in the amount of EP rubber, EP segmented copolymer, crystalline PP and crystalline PE phase.

ESCR appears dependant on ethylene content and its distribution. For example, some of the ethylene content on sample C increased the ethylene sequences present and present as PE-like “block” crystalline structures resulting in an increase in the overall crystallinity.

The combination of lower crystallinity and higher molecular weight also could mean that more tie molecules are present in sample A. As the number of tie molecules increases there is more binding strength among different lamellae, proportional to the applied stress and ESCR increases. There is, however, a significant difference between the ESCR values of B and C, while their molecular weight values are essentially similar. This indicates that crystallinity is a far bigger factor than molecualr weight.

From the crack growth studies it appears as if there is sufficient isopropanol induced softening or plastization occurring to form crazes. Once crazes occurred, voids can then act as an easy diffusion path for the isopropanol to penetrate deeper, thus promoting craze formation. The formation of crazes does not pose immediate danger to these polymers. Crazes can continue to sustain loads after they are formed. Crazes in sample A formed after a longer period of time than the craze in samples B and C (higher percentage of crystallinity).

The mode of failure was almost the same for all three samples and the rate of the failure process was in keeping with the final failure times. The crack growth in the three samples showed two stages of velocity. These stages are a linear slow growth followed by a linear fast growth. The crack in the samples goes beyond 0.9 cm, after that the rate increases rapidly. 0.9 cm seems to be the critical length before the velocity of crack increases and crack resistance decreases. At this point, the ductile type deformation ends and brittle deformation begins “ductile-brittle transition”. The later this transition is, the better the resistance to ESC, as observed by sample A.

The most important information that easily could be extracted from studying the morphology of these polymers is that the effect of the size of rubber particles and interparticle distance between these particles. According to some studies [15,25,49] samples A and B showed to have the best particle size (~ 0.4 μm). Sample A seems to have the best particle diameter and a better interparticle distance compared to B and C. It appears that the 6.5% ethylene content is enough for interruption of crack initiation and growth and to impart more toughness. The toughening effect in sample A can be determined by two factors: the best particle size and the better distribution of the rubber particle in the polymer matrix. This indicates good blendatibility between different phases or fractions

in IPPCs. On the other hand, the small particle size of sample C and the large interparticle distance of sample B appear less effective for craze initiation and toughening.

Finally, ethylene content is an important variable regarding the failure process of these polymers. An increase in the ethylene content in the three Sasol IPPCs from 6.5 to 9.5% to 12%, tends to decease the ductility, toughness and the ESCR. An increase in the ethylene content from 6.5% to either 9.5% or 12% appear to contribute to the crystalline phase, resulting in an increase in the overall crystallinity. This also affects toughness, ductility and the brittle-ductile transition. So, these polymers seem to be normally ductile but they fail in a brittle manner when placed in an active SCA (e.g. isopropanol) under a stress.

5.8 References

1. M. Grant, Encyclopedia of Chemical Technology, Fourth Edition, Executive Editor: J. Kroschwitz, John Wiley & Sons, USA, **1996**, 7, 820-821.
2. Consulting Engineers for Plastics Products and PVC-U Windows, Tangram Technology Ltd., **2003**, http://www.tangram.co.uk/Tangram-Disclaimer.html.
3. J. DeCoste, F. Salm and V. Wallder, Industrial and Engineering Chemistry, **1951**, 43, 117-121.
4. BP Solvay Polyethylene, Environmental Stress Crack Resistance of Polyethylene, North America, **2001**, Technical Publication 9, 1-4.
5. G. Wypych, Handbook of Material Weathering, Third Edition, Chemical Technology Publishing, USA, **2003**, 686-690.
6. B. Borisova, Investigations on Environmental Stress Cracking Resistance of LDPE/EVA Blends, Ph.D. Thesis, University of Halle Wittenberg, Germany, **2004**, 23-24.
7. H. Tan, L. Li, Z. Chen, Y. Song and Q. Zheng, Polymer, **2005**, 46, 3522-3527.
8. J. Xu and L. Feng, European Polymer Journal (Review article), **2000**, 36, 867-878.
9. J. Xu, L. Feng, S. Yang, Y. Wu, Y. Yang and X. Kong, Polymer, **1997**, 38, 4381-4385.
10. H. Mark, J. Machete and D. Othmer, Encyclopedia of Chemical Technology, Second Edition, Executive Editor: A. Standen, Wiley & Sons, USA, **1967**, 14, 299-301.
11. Tangram Technology Ltd, UK, **2003**, http://www.tangram.co.uk/TI-Polymer-PP_Random-Copolymer.html.
12. C. Ou, European Polymer Journal, **2002**, 38, 467-473.
13. B. Tanem, T. Kamfjord, M. Augestad, T. Lovgren and M. Lundquist, Polymer, **2003**, 44, 4283-4291
14. N. Choo, P. Yeh, M. Gilbert and A. Birley, Polymer Communications, **1984**, 25, 250-251.
15. K. Marcus, B. Sole and R. Patil, Macromolecular Symposium, **2002**, 178, 39-53.
16. W. Tam, T. Cheung and R. Li, Polymer Testing, **1996**, 15, 363-379.
17. Y. Feng and J. Hay, Polymer, **1998**, 39, 6589-6596.
18. J. Scherirs, Compositional and Failure Analysis of Polymers: A Practical Approach, John Wiley & Sons, UK, **2000**, 176-179.
19. C. Hongjun, L. Xiaolie, M. Dezhu, W. Jeannine and T. Hongsheng, Journal of Applied Polymer Science, **1999**, 71, 93-101.
20. B. Baker, J. Bonesteel and M. Keating, Thermochimica Acta, **1990**, 166, 53-68.
21. Z. Xiao, L. Li, D. Zhou, G. Xue, Z. Yuan and Q. Dai, Thermochimica Acta, **2003**, 404, 283-288.
22. J. Prasad, Journal of Polymer Science: Part A: Polymer Chemistry, **1992**, 30, 2033-2036.
23. Y. Zhang, C. Wu and S. Zhu, Polymer Journal, **2002**, 34, 700-708.
24. A. Ibhadon, Journal of Applied Polymer Science, **1999**, 71, 579-584.
25. E. Moore, Polypropylene Handbook: Polymerization, Characterization, Properties, Processing and Applications, Chapter 6: End-Use Properties by R. Duca and E. Moore, Hanser Publisher, Germany, **1996**, 246-248.
26. H. Cheng, Macromolecules, **1984**, 17, 1950-1955.
27. Y. Feng and J. Hay, Polymer, **1998**, 39, 6723-6731.
28. P. Doshev, R. Lach, G. Lohse, A. Heuvelsland, W. Grellmann and H. Radusch, Polymer, **2005**, 40, 9411-9422.
29. J. Scherirs, Compositional and Failure Analysis of Polymer: A Practical Approach, John Wiley & Sons, UK, **2000**, 108-126.
30. D. Park, H. Kim, Y. Han, S. Seul, B. Kim and C. Ha, Journal of Applied Polymer Science, **2005**, 95, 231-237.
31. R. Paukkeri and A. Lehtinen, Polymer, **1993**, 34, 4083-4088.

32. M. Pizzoli, M. Righetti, M. Vitali and P. Ferrari, Polymer, **1998**, 39, 1445-1451.
33. W. Brostow and R. Corneliussen, Failure of Plastics, Chapter 16: Environmental Stress Cracking: The Phenomenon and its Utility by A. Lustiger, Hanser Publishers, Germany, **1986**, 305-328.
34. H. Mark, and N. Gaylord, Encyclopedia of Polymer Science and Technology, Fourth Edition, Executive Editor; N. Bikales, John Wiley & Sons, USA, **1992**, 6, 301.
35. H. Mark, and N. Gaylord, Encyclopedia of Polymer Science and Technology, Second Edition, Executive Editor; N. Bikales, John Wiley & Sons, USA, **1971**, 7, 269-289.
36. R. Portnoy, Medical Plastics: Degradation Resistance & Failure Analysis, Environmental Stress Cracking in Polyethylene by A. Lustiger, Plastics Design Library, USA, **1998**, 66-69.
37. J. Soares, R. Abbott and J. Kim, Journal of Applied Polymer Science: Part B: Polymer Physics, **2000**, 38, 1267-1275.
38. F. Billmeyer, TextBook of Polymer Science, John Wiley & Sons, USA, **1984**, 323.
39. H. Brown, Polymer, **1978**, 19, 1186-1188.
40. L. Epensdel, Journal of Applied Polymer Science, **1972**, 16, 2375-2386.
41. J. Kocsis, Polypropylene an A-Z Reference, Environmental Stress Cracking of Polypropylene by R. Chatten and D. Vesely, Kluwer Academic Publishers, UK, **1999**, 206-214.
42. A. Volynskii and N. Bakeev, Solvent Crazing of Polymers, Elsevier Science B. V., Netherlands, **1995**, 29-32.
43. X. Li, Polymer Degradation and Stability, **2005**, 90, 44-52
44. C. Hansen, Polymer Degradation and Stability, **2002**, 77, 43-53
45. W. Callister, Materials Science and Engineering, John Wiley & Sons, USA, **2000**, 193-204.
46. K. Naylor and P. Phillips, Journal of Polymer Science: Polymer Physics Edition, **1983**, 21, 2011-2026.
47. R. Olley, Science Progress, **1986**, 70, 17-43.
48. B. Jang, J. Uhlmann and J. van der Sande, Journal of Applied Polymer Science, **1984**, 29, 4377-4393.
49. C. Lotti, C. Correa and S. Canevarolo, Materials Research, **2000**, 3, 37-44.
50. R. Lenk, Plastics Rheology, Maclaren and Sons, UK, **1968**, 163-165.
51. J. Jancar, A. Dianselmo and A. Dibenedetto, Polymer, **1993**, 34, 1684-1694.
52. D. Roylance, Introduction to Fracture Mechanics, Cambridge, **2001**, 1-17.
53. B. Borisova, Investigations on Environmental Stress Cracking Resistance of LDPE/EVA Blends. Ph.D. Thesis, University of Halle Wittenberg, Germany, **2004**, 69-72.

Chapter 6

The effect of selective removal of fractions on the ESCR

Summary

The purpose of this part of this study is to determine the effect of removing selected polymer fractions on the ESCR behaviour of the IPPCs. Since IPPCs comprise multiple fractions removal of selected fractions could significantly affect the ESCR of these materials. In this part of the study (a) room temperature soluble fractions (RT) and (b) some highly crystalline fractions (eluted at 120 ^{o}C in a preparative TREF experiment) were removed from the IPPC samples in order to determine the effect of these fractions on the ESCR. Extracted fractions and the samples (without these fractions) were characterized using ^{13}C NMR, GPC and DSC. Finally, an etching process (described in Chapter 4) was applied to see the change in the morphology after removing these fractions.

6.1 Extraction of soluble fractions at room temperature

6.1.1 Procedure

The fractions that dissolve at room temperature were extracted from the three IPPCs in order to determine the effect of these fractions on the ESCR. About 3.0 g of each sample (samples A, B, and C) was dissolved in 400 ml xylene (Merck Chemicals) and boiled under reflux at 130 ^{o}C with gentle stirring. A mixture of Irganox 1010 and Irgafos stabilizers (0.08 g) was used to inhibit thermal degradation at high temperatures. Complete dissolution was achieved in 1.5 h. The solution was then cooled to ambient temperature. The precipitate (IPPC without soluble fractions) suspended in the xylene was filtered and washed with acetone. The precipitated part was dried under vacuum at 50^{o}C for 6 h. The non-precipitated or soluble part was isolated by evaporation of the solvent, then washed with acetone and dried under vacuum at 50 ^{o}C for 6 h. The precipitated and non-precipitated/soluble parts were weighed and characterized by ^{13}C NMR, GPC and DSC. The weight percent of each extracted fraction of each sample is given in Table 6.1. The extracted fractions were expected to contain rubbery ethylene-

propylene copolymer (EP) and small amounts of low molecular weight crystalline material.

Table 6.1. Soluble fractions extracted from the three IPPC samples

Sample	Ethylene content, %	Weight before extraction, g	Extracted weight, g	Weight after extraction, g	% of extracted soluble fractions
A	6.5	3.0234	0.5490	2.4744	18.16
B	9.5	3.1403	0.7760	2.3643	24.71
C	12.5	3.0051	0.8708	2.1343	28.98

6.1.2 ESCR test 2

After the above extraction, samples were prepared (as described in Sections 4.4.1 and 4.4.3) in order to perform ESCR test 2. Table 6.2 shows typical ESCR data obtained from ESCR test 2 under a predetermined constant force (calculated to give a stress of about 15 MPa) at 60 ^{o}C.

The results show a large drop in the value of ESCR of the three samples after removing the soluble fractions. Extraction of 18.16% room temperature soluble material from polymer A decreased the ESCR from 86.86 to 57.77 h (normalized values, ESCR decreased about 43.9%). More material was extracted from samples B and C, as shown in Table 6.1, so they showed a greater decrease in their ESCR. ESCR of sample B decreased from 26.12 to 02.72 h (ESCR decrease of 89.6%), while the ESCR of sample C decreased from 15.58 to 01.82 h (decrease of 88.3%). The obvious conclusion would be that the removal of the soluble fractions resulted in decreased toughness.

As shown in Table 6.2, slightly thicker specimens of the same sample took a longer time to break and showed a slight increase in the final time to failure (more ESCR) in the majority of tests. This is can be due to the dependency of stress on the sample cross-sectional area, when a constant weight is used. To illustrate this, a normalized ESCR time was calculated, based on a normalized stress of 15 MPa. While doing this changes the values, the trends remain the same.

Table 6.2. ESCR data of three samples observed after removing soluble fractions, as determined by ESCR test 2

Sample	Film thickness	ESCR* hh:mm	Average (h)	Normalized ESCR** hh:mm	Average (normalized) (h)
A1	0.15	59.07	**56.48**	59.07	**57.77**
A2	0.14	54.17		58.04	
A3	0.15	56.19		56.20	
B1	0.20	04.38	**03.14**	03.29	**2.72**
B2	0.15	02.01		02.01	
B3	0.16	03.04		02.85	
C1	0.15	01.83	**01.88**	01.83	**1.83**
C2	0.15	01.34		01.34	
C3	0.16	02.47		02.31	

*: Time to failure, ESCR test 2 conditions: isopropanol as SCA, 60 °C and 15 Mpa

**: See text for description

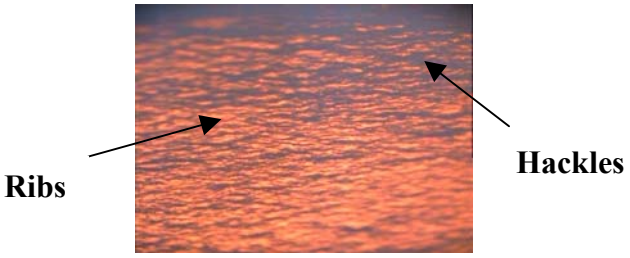

Figure 6.1. Typical ESC surface of sample B after removing soluble fractions (magnification shows area of 50 x 50μm)

The appearance of a typical ESC surface (ribs and hackles) near the crack area is shown in Figure 6.1. Figure 6.1 demonstrates the appearance of the ribs (light area) and hackles (dark area) marks in sample B after removing some soluble fractions. The number of ribs

and hackles seem to increase after removing soluble fractions, which is in concordance with the obvious decrease in crack resistance. The crack propagation seems to take place in a direction that approaches the rib marks on the concave side and leaves on the convex side.

In order to fully understand the effect of removing the soluble fractions, it was necessary to characterize both the extracted materials and the insoluble materials fully.

6.1.3 Characterization of extracted fractions

6.1.3.1 ^{13}C NMR

^{13}C NMR spectra of the three extracted fractions are shown in Figure 6.2 (solvent: 9:1 mixture of 1,2,4-trichlorobenzene:C_6D_6). It is clear from the spectra that the extracted fractions are EP copolymers but with differing tacticity and different amounts of ethylene. The peaks at 20.58-21.59, 28.65-28.66 and 46.30-46.32 ppm (peaks number 1, 2 and 4 in Figure 6.2) correspond to the CH_3, CH and CH_2 from propylene sequences respectively. The peaks at 29.78-29.86 ppm (denoted 3 in Figure 6.2) correspond to the presence of ethylene in these fractions.

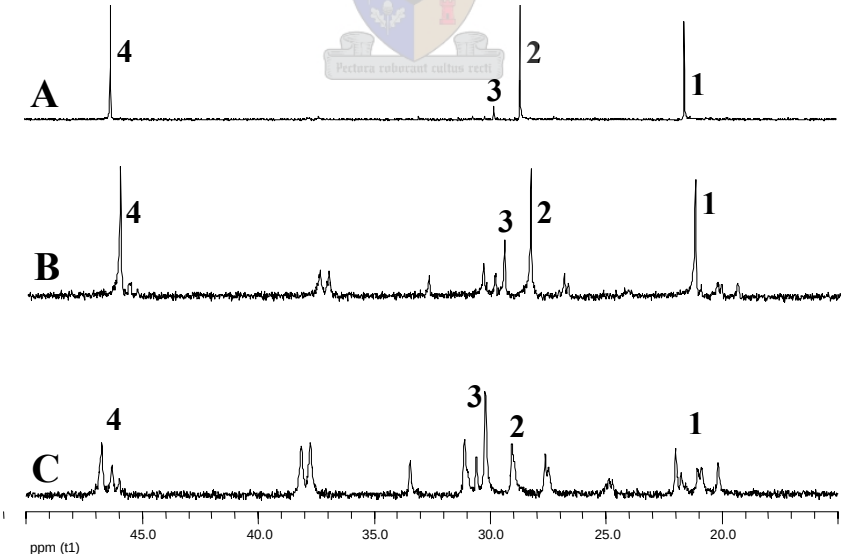

Figure 6.2. ^{13}C NMR spectra of the three extracted fractions (A) sample A, (B) sample B and (C) sample C

The tacticity relating to the polypropylene fractions of samples A, B and C were evaluated by integrating methyl peak of the ^{13}C NMR spectra, and found to increase from C (31.66%) to B (61.63%) to A (87.22%), respectively. This indicates that more crystalline material (iPP) seems to be extracted from A and B than C. The peaks at 29.49-29.84 ppm indicate that these extracted fractions seem to include some crystalline PE, or at least materials with sequences of ethylene monomer. The amount of extracted PE or sequences of ethylene monomer seems to increase from A to B to C as indicated by the integrals of the peaks at 29.49-29.84 ppm. Overall, these results indicate that more rubbery material was extracted from B and C, hence the large decrease in ESCR compared to A.

6.1.3.2 DSC

The DSC results of the three extracted fractions are presented in Table 6.3. These results include the T_m, T_c and crystallinity. The crystallinity of these fractions was measured by equation (2) as described in Section 5.3.3. As mentioned in the previous section, more crystalline material was extracted from A and B than from C. The crystallinity of these fractions decreased from fraction A (47.84%) to B (24.22%) to C (08.01%). The values of crystallinity are relative values due to using $\Delta H_{F(100\%)}$ of iPP as 100% crystalline IPPC.

Table 6.3. Characterization of extracted fractions using DSC thermograms

Extracted fractions from:	T_m (^oC)	T_c (^oC)	ΔH (J/g)	Crystallinity
Sample A	164.41	124.32	99.65	47.84
Sample B	161.52	120.13	50.45	24.22
Sample C	162.47	118.07	16.69	08.01

As shown in Figure 6.3, the DSC cooling curve for the extracted fraction of sample C shows two peaks. The strong peak at 118.07 °C is due to the crystallizing of the PP segments in this fraction, while the second peak at around 64 °C might be due to PE segments crystallizing. This peak is quite clear for sample C, but not as clear for A and B (see Appendix B). So, it is clear that some crystalline material is present in the extracted materials.

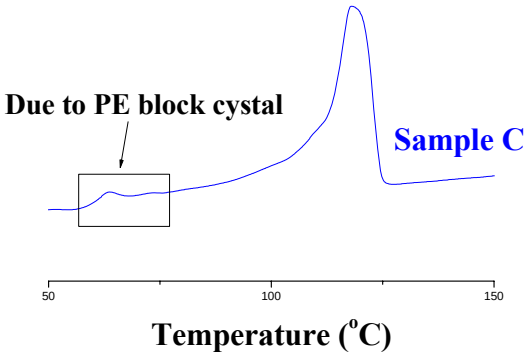

Figure 6.3. DSC crystallization curve for the extracted fraction of polymer C

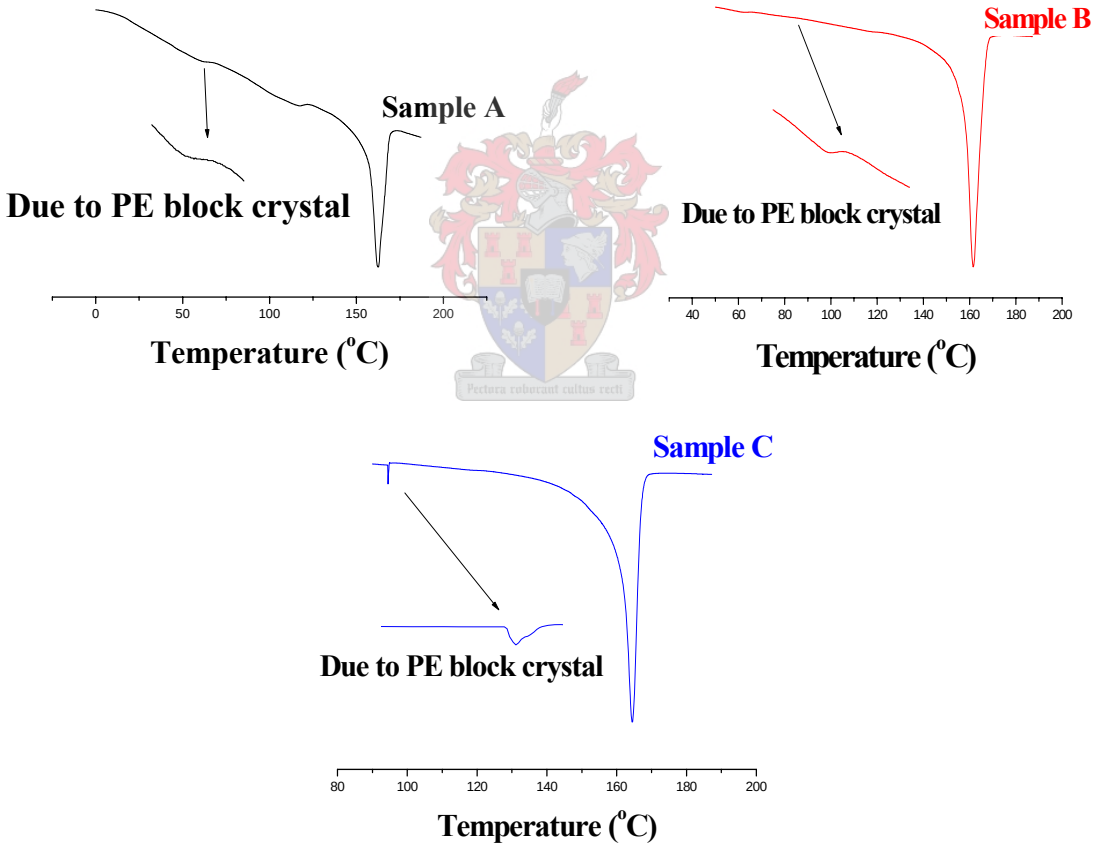

Figure 6.4. DSC melting curves for the three extracted fractions

The DSC heating curves also show clear melting endoterms, and in the case of samples B and C, it appears as if two crystalline species are present. The melting endotherms at

161.47-164.41 ^{o}C are due to PP materials, while the lower melting peaks and shoulders at 62.6-94.6 ^{o}C are possibly due to ethylene-rich materials or PE crystals. In fact, distinct shoulders in samples A and B and a tiny peak in sample C located at 63.26, 62.26 and 94.49 ^{o}C, respectively, suggests the presence of crystallizable PE sequences or long ethylene sequences. The content of a long ethylene sequence in the extracted fraction of sample C seems to be higher than that of A and B.

It can be deduced that the extracted fraction of sample A contains some iPP and some ethylene-rich copolymer, while samples B and C seem to have a more ethylene-rich copolymer and less iPP.

6.1.3.3 GPC

Table 6.4 shows the results of GPC of the three extracted fractions. The molecular weight of the extracted fraction of sample A is higher than for B an C, while the MWD is also noticeably broader.

Table 6.4. Molecular weight data for the three extracted fractions, determined by GPC

Extracted RT fraction from:	$\overline{M_w}$ x 10^3	$\overline{M_n}$ x 10^3	MWD
Sample A	394.482	78.388	5.03
Sample B	289.025	82.868	3.48
Sample C	319.789	108.408	2.95

It is uncertain if the molecular weight of the extracted fractions play any role (or at least a dominant role) in the change in ESCR. The difference in the extracted fractions can be summarized as follows: a larger amount of material was extracted from B and C than from A, more atactic or non-crystalline material was extracted from B and C than from A, and the MWD of the extracted material of samples B and C are narrower than for A.

Rubbery materials are known to toughen these polymers against crack propagation by dissipating large amount of energy in the matrix around the particle, thereby blunting the crack and inhibiting crack propagation. [(2)] They also control the craze growth and initiate numerous, small, energy absorbing crazes. They seem to provide their resistance by acting as small bumpers, absorbing energy that result in local deformation instead of

allowing cracks to propagate through the material. Also, the inclusion of EP rubbery material in the polymer matrix increases the ductility and improves the toughness. [3,4] So, removing these fractions will increase the brittleness and decrease both ductility and toughness. Furthermore, removing these fractions could cause a change in crystallinity, MW, MWD and morphology of the original IPPC samples. In order to confirm this, the three samples (without soluble fractions) were characterized (by DSC, GPC and NMR) and etched in order to see the change in the microstructure, crystallinity, MW, MWD and morphology.

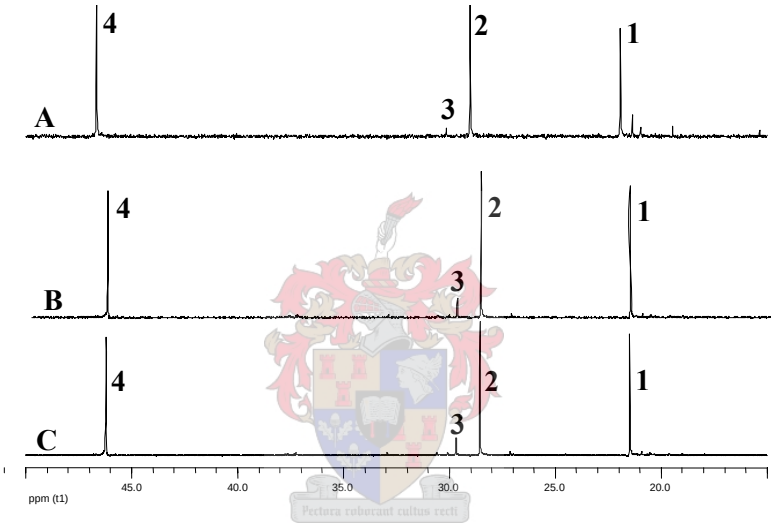

Figure 6.5. ^{13}C NMR of sample A (top), sample B (middle) and sample C (bottom) after the extraction of soluble fractions

6.1.4 Characterization of the IPPC samples after the extraction

6.1.4.1 ^{13}C NMR

The ^{13}C NMR spectra of the three samples A, B and C after extraction of soluble fractions are given in Figure 6.5 (solvent: 9:1 mixture of 1,2,4-trichlorobenzene:C_6D_6). Figure 6.5 shows that these polymers still have the structure of copolymers of PP, with different amounts of ethylene. The peaks at 29.70-30.12 ppm correspond to the presence of ethylene in these copolymers. The intensity of these peaks still increases from A to B to C, which indicates that the amount of ethylene is still higher in C than in B and A.

Comparison of the samples, based on the ^{13}C NMR spectra, before and after removal of the extractables, is summarized in Table 6.5. Some crystalline PE is still present in these samples after the extraction, as shown by the peaks of $S_{\delta\delta}$ at 29.70-30.12 ppm which correspond to the EEEEE sequence. These peaks clearly showed that the ethylene content still increases from A to B to C, respectively.

Table 6.5. Differences in the type of monomer sequences before and after extraction

^{13}C NMR Assignments	Sequences type	Peaks integration (%) of three original samples:			Peaks integration (%) of the three samples after extraction:		
		A	B	C	A	B	C
$S_{\alpha\alpha}$	**PPPPP**	18.53	21.28	19.03	35.27	31.37	38.18
$S_{\alpha\gamma}$	**PPEP**	01.02	01.68	02.13	00.04	01.26	01.18
$S_{\alpha\delta}$	**EEP**	01.60	01.70	02.09	00.23	01.48	01.25
$T_{\delta\delta}$	**EPE**	00.46	00.82	00.80	00.00	01.12	00.65
$T_{\beta\delta}$	**PPE**	00.79	01.04	01.35	00.09	01.84	01.09
$S_{\gamma\delta}$	**PEPP**	00.47	01.24	00.98	00.03	01.42	00.78
$S_{\delta\delta}$	**EEEEE**	03.74	04.35	05.78	01.61	02.87	04.74
$T_{\beta\beta}$	**PPPPP**	19.15	19.57	20.34	29.80	30.04	34.13
$S_{\beta\beta}$	**PPEPP**	00.89	01.22	00.73	00.29	01.42	01.26
$P_{\beta\beta}$	**PPPPP**	18.13	17.90	19.03	27.75	26.16	31.10
$P_{\beta\gamma}$	**PPPPE**	01.55	00.21	00.96	04.25	00.95	01.02
$P_{\gamma\gamma}$	**PPPEP**	01.01	00.43	00.16	01.99	00.66	00.68

The four strong assignments $S_{\delta\delta}$, $S_{\alpha\alpha}$, $T_{\beta\beta}$ and $P_{\beta\beta}$, which result from long and continuous PE and PP segments, respectively, still exist in these spectra. As shown in Table 6.5, the integrals of $S_{\alpha\alpha}$, $T_{\beta\beta}$ and $P_{\beta\beta}$ increased and the integrals of $S_{\delta\delta}$ which is due to PE segments decreased compared with the original samples. This indicates that some PE segments are extracted from the three samples. On the other hand, the integrals of some

peaks such as $S_{\alpha\delta}$, $S_{\alpha\gamma}$, $T_{\delta\delta}$ and $T_{\beta\delta}$ are significantly decreased. This means that some percentage of the extractable materials contain segments such as EEP, PPEP, EPE and PPE. The peak of $T_{\delta\delta}$ is absent in sample A after the extraction of the soluble fraction. It seems that the EPE segment is totally extracted from sample A, as shown in Table 6.5 and Figure 6.6.

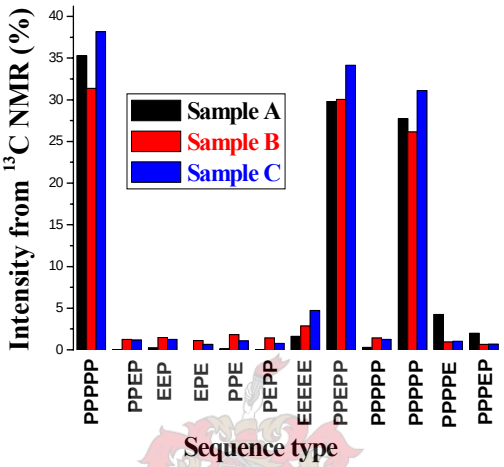

Figure 6.6. The percentage of types of monomer sequences of sample A, after the extraction of soluble fractions

6.1.4.2 DSC

Table 6.6 shows the T_m, T_c and crystallinity of the three IPPC samples after the extraction of soluble fractions. The crystallinity of IPPC samples after the extraction of soluble fractions was measured by equation (2) as described in Section 5.3.3. The values of crystallinity in Table 6.6 are relative values (using $\Delta H_{F(100\%)}$ of iPP as 100% crystalline for IPPC).

Table 6.6 Characterization of IPPC samples after removing soluble fractions, using DSC

Sample	T_m (^{o}C)	T_c (^{o}C)	ΔH (J/g)	Crystallinity, %
Sample A	164.50	123.39	74.34	35.69
Sample B	163.28	122.30	91.20	43.78
Sample C	162.91	121.98	41.90	20.12

Crystallinity of sample A increased from 25.06 to 35.69% and from 36.12 to 43.78% for sample B. On the other hand, crystallinity of sample C decreased from 40.50 to 20.12%.

There was a negligible decrease in T_m and T_c from sample A to B to C, as shown in Table 6.6.

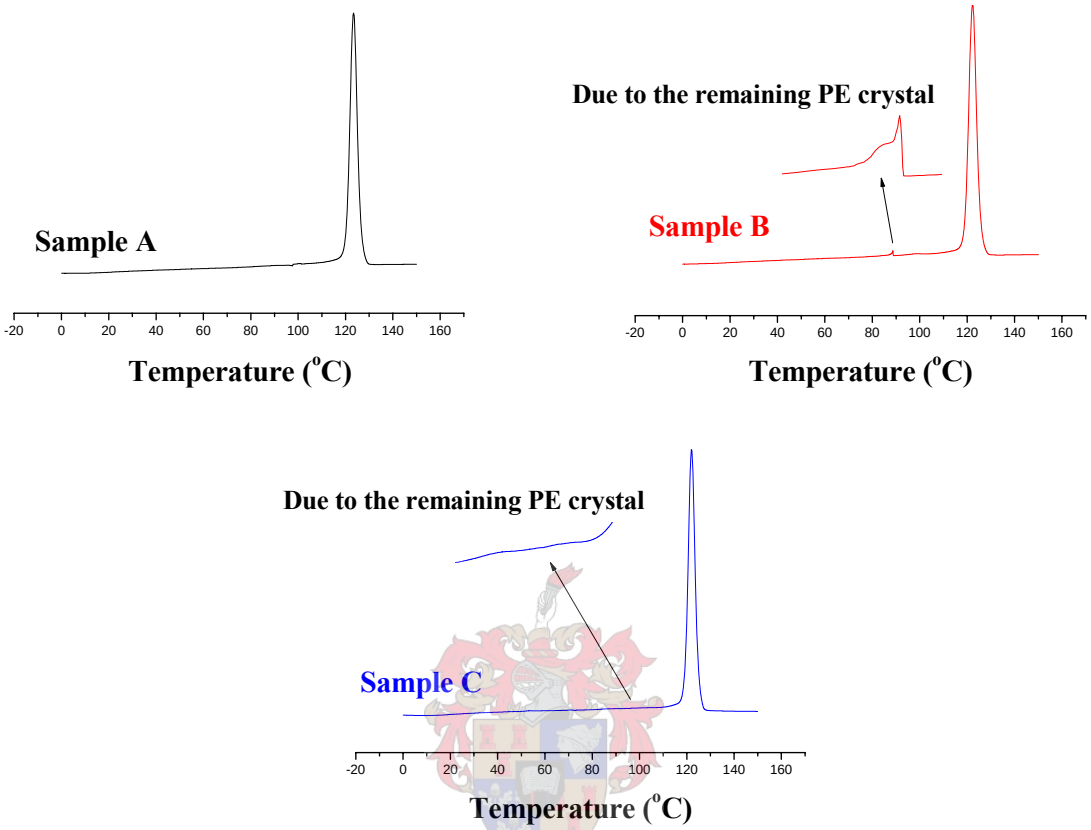

Figure 6.7. DSC crystallization curves for the three samples after extraction of soluble fractions

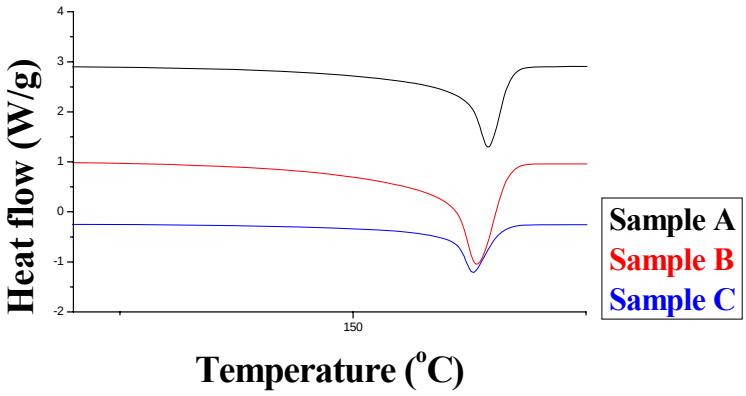

Figure 6.8. DSC melting curves for the three samples after the extraction of soluble fractions

Cooling DSC curves of samples B and C (without soluble fractions) in Figure 6.7 show two exothermic peaks for the crystallization, while the cooling DSC curve of sample A shows just one exothermic peak. The strong peaks at 121.98-123.39 ^{o}C in the three samples are due to the crystallizing of the PP homopolymer. The average PP sequence length is high enough to be detected and only a single peak can be detected in the melting endotherms at 162.91-164.50 ^{o}C for each sample, as shown in Figure 6.8. The weak crystallization peaks in the DSC cooling curves of samples B and C at 85.17-88.68 ^{o}C are due to the remaining polyethylene-like materials. This peak is absent in the cooling curves of sample A. This means that the remaining polyethylene-like material in sample A is not enough to be detected. Overall, these crystalline areas are not large enough to be detected in the melting endotherms in the three samples, as shown Figure 6.8.

6.1.4.3 GPC

$\overline{M_n}$, $\overline{M_w}$ and MWD of the three IPPCs after the extraction of soluble fractions are presented in Table 6.7. In general, there are increases in $\overline{M_n}$ (except in sample C) and decreases in $\overline{M_w}$ of the three samples, while there is a little change in MWD. Sample A still has the highest $\overline{M_n}$ (111.180 x 10^3) and the narrowest MWD (2.77) than other samples. On other hand, sample C still has the lowest $\overline{M_n}$ (51.418 x 10^3) and broadest MWD (4.79), while sample B has $\overline{M_n}$ and MWD values between those of A and C (71.864 x 10^3 and 3.19, respectively).

Table 6.7. Molecular weight data of the three samples after removing soluble fractions, determined by GPC

Sample	$\overline{M_w}$ x 10^3	$\overline{M_n}$ x 10^3	MWD
Sample A	307.487	111.180	2.77
Sample B	229.553	71.864	3.19
Sample C	246.353	51.418	4.79

As expected, removing these fractions affected the MW, MWD, crystallinity, and microstructure, and subsequently caused a dramatic change in ESCR of the three IPPCs.

The changes in the original IPPCs properties are presented in Table 6.8. These changes can be summarized as a follows:

1. Change in the microstructure due to a decrease/increase and absence of some sequences (e.g. absence of EPE sequence from sample A after removing the soluble fraction), as shown in Table 6.5.
2. A decrease in $\overline{M_w}$ of the three samples.
3. An increase in $\overline{M_n}$ of samples A and B and decrease in $\overline{M_n}$ of sample C.
4. The MWD becomes narrower in cases of samples A and B and broader in sample C,
5. An increase in crystallinity of samples A and B and decrease in crystallinity of sample C.
6. All these changes reduced the ESCR.

Table 6.8. Changes in IPPC sample properties before and after the extractions

Sample	% of extracted material	$\overline{M_w}$	$\overline{M_n}$	MWD	Crystallinity	ESCR
A	18.16	-	+	-	+	-
B	24.71	-	+	-	+	-
C	28.98	-	-	+	-	-

+ Increase and – Decrease

The role of MW, MWD and crystallinity of the three samples after the extraction on ESCR behaviour seem a bit perplexing. For example, although there are increases in the crystallinity of sample A, it showed less of a decrease in ESCR than the other two samples (about 43.6% from 86.86 to 57.7 h). This effect on ESCR of samples A and C cannot be ascribed to the effect of $\overline{M_n}$ and crystallinity alone. Sample B showed the highest decrease in the values of ESCR. It decreased from 26.1 to 2.7 h (about 89%), although there is a slight increase in $\overline{M_n}$. In this case, the increase in crystallinity of sample B seems to be the main reason for the highest drop in the ESCR, especially when the change in MWD was not significant. On the other hand, although there was large decrease in the crystallinity of sample C after the extraction, it showed a decrease in ESCR more than A and about the same as B (about 88% from 15.3 to 1.82 h). In general the MW effect on ESCR of these samples seems to be a small, while crystallinity seems to be a strong factor compared with molecular weight.

It is concluded that the drop in the values of ESCR of the three samples is simply due to the effect of the extractables materials. The level of effect depends strongly on the type, the amount and finally the properties (e.g. crystallinity, MW) of these extractables. It would also remain dependant on the remaining rubber particles size and interparticle distance between these particles because removing some EP rubbery materials might affect the rubber particles size and interparticle distance of the original samples and counteract the effect of toughening as shown in the previous chapter. This effect is discussed later in Section 6.1.7.

6.1.5 The formation of crazes

Optical microscopy showed craze formation in all the three samples after extraction of soluble fraction (see Figure 6.9). Craze formation was seen during the first hour in samples B and C, as shown in Table 6.9. This indicates that there is deformation in these samples in the stress direction during the first hour (crazing is related to the speed at which the test specimen is deformed) [5]. On the other hand, sample A showed no deformation during the first five hours and deformed only in the sixth hour when crazes were formed. Sample C still has a lowest resistance to crazing, while sample A still has the highest resistance to crazing. Figure 6.9 shows the early stage of craze formation. It is believed that the main cause of ESC in these polymers (even after removing the soluble fractions) after immersion in isopropanol is related to craze formation. Once crazes occurred, voids can then act as an easy diffusion path for the isopropanol, thus promoting craze formation.

Table 6.9. Time of the craze formation of the three tested samples after removing the soluble fractions

Sample	**Craze formation**							
	0.5 h	**1 h**	**1.5 h**	**2.5 h**	**3 h**	**4 h**	**5 h**	**6 h**
A	No	No	No	No	No	No	No	**Yes**
B	No	**Yes**	----	----	----	----	----	----
C	**Yes**	----	----	----	----	----	----	----

It is believed that the main cause of ESC in these polymers (even after removing the soluble fractions) after immersion in isopropanol is related to craze formation.

Isopropanol induced softening or plastization, led to initiation of crazes, and finally to ESC. Similar to the situation before the extraction, the breakdown stage seems to be the governing stage in the craze mechanism. This is reported to be dependant upon molecular weight. [6] The effect of molecular weight on the craze process is discussed in the previous chapter (Section 5.4). The effect of molecular weight on the craze mechanism can be said to have made a difference between the craze and crack formation and propagation of sample A and crack formation and propagation of either in samples B or C, while it made a little or no difference between samples B and C because the difference in MW is not significant between them. So, the breakdown stage gets shorter in samples B and C, as the MW decreased, resulting in a decrease in the time of crack formation and propagation.

Figure 6.9. Optical micrograph of crazes in the three samples after removing soluble fractions (magnified to 50 x 50μm)

6.1.6 Crack growth

The crack length increased with time in all IPPC samples after removing the soluble fractions, as shown in Table 6.10. Although the mode of failure in three samples seems to be the same and similar to failure in the original samples, the velocity of crack growth increased and final time to failure decreased compared to original samples.

As in the case before the extraction, the three samples showed two stages of cracks, a linear slow growth followed by a linear fast growth, as shown in Figure 6.10. In sample C, we could make a case for stating that there are three, and not two stages of breakdown, but as we see a rapid increase in crack growth only at the end (sharp increase in slope), the initial crack growth is regarded as a single stage. The discontinuity arises from the

fact that the effective stress is increased, as the stressed area is decreased due to the crack formation, but the force remains the same. The force remains constant while the crack length increases in a controlled manner, until eventually a critical length is reached. It also might be due to the effect of the remnants of the crazed material which holds together the polymer surface before the crack propagates through it as discussed in Section 5.5.

Table 6.10. Time under stress versus the crack growth of the three samples after removing soluble fractions

Sample A							
Time under stress, min	0	600	1080	2040	2520	3600	~ 62
Crack growth, cm	0.5	0.6	0.7	0.9	1.3	1.6	2.0 (Final failure)
Sample B							
Time under stress, min	0	40	100	130	180	220	~ 250
Crack growth, cm	0.5	0.6	0.7	0.8	1.2	1.6	2.0 (Final failure)
Sample C							
Time under stress, min	0	20	40	60	90	120	~180
Crack growth, cm	0.5	~ 0.5	0.6	0.7	0.8	1.6	2.0 (Final failure)

The critical crack length before the velocity of crack increases in the three samples after the extraction decreased from 0.9 cm (for the original samples) to 0.8 cm (for the samples after the extraction). At this point, the ductile type deformation ends and brittle deformation begins. The ductile-brittle transition occurred therefore in early stage compared to the same transition of the original samples. Also, the final stage of failure seems to be more brittle in this case than in the case of original samples, since the crack speed is higher, which resulted in reduction of toughness. This means there was a more dramatic drop in the energy absorbed by the stressed samples and the ability for deformation in the tested specimens is more reduced in this case. [3]

Sample A has the highest ESCR and the ductile-brittle transition occurs later than in the case of samples B and C. The later this transition is, the better the resistance to ESC, [7] as shown in Figure 6.10. Although Figure 6.10 shows that samples B and C have only one stage of crack, it is believed that the above two stages of crack are present in these samples. The first stage in samples B and C is so short that it was not measurable and can thus not be seen in Figure 6.10.

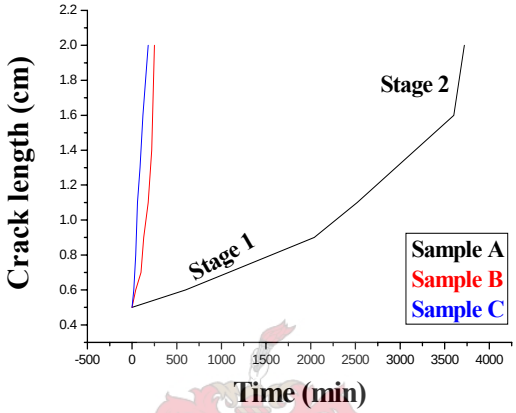

Figure 6.10. Crack length versus time for the three samples after the extraction.

6.1.7 Morphology

Etched samples (samples without the soluble fractions) showed that some rubber particles are still present in these samples, as shown in Figure 6.11. The difference in both the particle size and interparticle distance between these particles in the three samples after removing the soluble fractions is shown in Table 6.11. The average particle size in sample C (0.191 μm) is smaller than in samples B (0.193 μm) and A (0.331 μm). The large average interparticle distance can be seen in the micrograph of sample B (1.499 μm), while samples A and C showed less interparticle distance (0.721 μm) and (0.739 μm), respectively, as shown in Table 6.11.

In general, there are decreases in the average particle size and average interparticle distance in the three samples after the extraction. This resulted in a decrease in the toughness and the ductility of these samples. Sample A still has a uniform size and

distribution of these particles (the interparticle distance is almost twice the particle size). These results in increased toughness and ductility compared to samples B and C.

Table 6.11. Particle size and interparticle distance of the three samples after removing the soluble fractions

Sample	Average particle size, µm	Average interparticle distance, µm
A	0.331	0.712
B	0.193	0.739
C	0.191	1.499

The large interparticle distance of sample C and small particle size of samples B and C seem to counteract the effect that the rubber particles has on the toughness. Toughness and ductility decreased dramatically in the cases of these samples and the compatibility between different phases or fractions is very poor after removing the soluble fractions. This prevents the remaining rubber particles from effectively controlling craze propagation. The particle size and interparticle distance of samples B and C would expected to be less effective for craze initiation and toughening. It is clear now that the size of the rubber particles and the interparticle distance between these particles can be important factors in controlling the mechanical behaviour of IPPCs; they have a significant effect on the deformation and failure processes and, therefore, influence the ESCR.

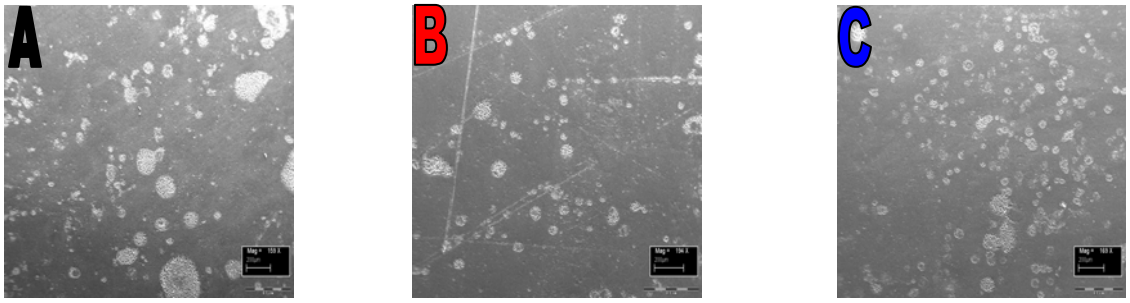

Figure 6.11. SEM micrographs of etched IPPC samples after removing the soluble fractions

From the above results it can be concluded that the high ESCR of stressed sample A in pure isopropanol, even after removing the soluble fraction is related to the better molecular weight and molecular weight distribution, the lower crystallinity, the optimum particle size of the rubber domains, critical interparticle distance and uniformity in the size and distribution of rubber particles compared to samples B and C. Results in this study agree with that found by Marcus *et al.,* [3] Lotti *et al.* [8] and Moore [9] concerning the best average particle size needed to produce optimum ESC results for a PP system.

6.2 Removing a crystalline fraction

6.2.1 Introduction

High temperature or crystalline fractions were removed by using preparative temperature rising elution fractionation (TREF) as the primary technique. It is a technique which fractionates semi-crystalline polyolefins from solution according to the solubility-temperature relationship which relates directly to crystallinity, and thus to their molecular structure. [10] It is the most effective technique for investigating the microstructure of semi-crystalline polymers, especially polyolefins. The wide application of TREF in polyolefins is related to two main facts: most polyolefins are crystallizable and polyolefins dissolve in solvents at high temperature (above 100 ^{o}C). The fractionation can be performed without any special cooling equipment and the temperature is easy to control. [11] The experimental TREF apparatus can be analytical or preparative. In an analytical TREF, TREF is linked with other techniques such as IR and GPC to determine the properties of polymer fractions. These fractions can be characterized by any other techniques such as NMR, etc., by off-line characterization "Preparative TREF". Preparative TREF usually provides more information than analytical TREF but it is a time-consuming technique. [11]

The fractionation of IPPC by TREF has been carried out by many workers. [12-14] In general, in TREF the polymer is dissolved in a suitable solvent at elevated temperatures. Afterward the solution is slowly cooled down to crystallize the sample onto a suitable inert support. Subsequently the sample is eluted by fresh solvent at successively increased temperatures. Then fractions can be collected and characterized. In this part of

our study, preparative TREF was used to fractionate samples A and C to remove some of the crystalline fractions (eluting at 120 ^{o}C in order to see the effect of this on ESCR.

6.2.2 Procedure

Fractionation of samples A and C were done by a preparative TREF procedure that was developed in our laboratory, the details of the technique are described in Reference 15. Typically, about 3.0 g of polymer (samples A or C) was dissolved in 300 ml xylene and heated under reflux, at 130 ^{o}C with gentle stirring in a glass reactor. Four reactors were used for each sample in order to obtain enough polymer to make film or test specimens. Irganox 1010 and Irgafos stabilizers (a mix of 0.06 g per reactor) were used in this step to inhibit thermal degradation at high temperatures. A period of 1.5 h was employed for complete dissolution. The solutions were mixed with preheated washed sea sand (Aldrich, as an inert support). Solutions were cooled in a programmable bath at 1.5 ^{o}C/h from 130 ^{o}C to 20°C, as shown in Figure 6.12 (temperature reached 130 ^{o}C in 3 h, was then kept constant at 130 ^{o}C for 4 h, cooled to 80 ^{o}C in 50 h and finally cooled to RT in 60 h). Afterwards, a steel elution column was prepared by placing some glass wool in the bottom, followed by some glass beads to avoid any flow currents in the column, followed again by more glass wool. Then the mixture of solution-sand was loaded into the column, followed by more glass wool and glass beads to fill up the column. The column was securely closed with a stainless steel lid and transferred to a GC-oven (Variant, model 3700), used for the controlled temperature environment. The entire GC-oven was inside a fume hood. The column was heated by a stepwise heating profile (2 ^{o}C/min), to a predetermined elution temperature for each fraction. A nitrogen bottle with a regulator and a gas flow valve was coupled to the solvent reservoir, to deliver a nitrogen flow rate of 20 ml/min. The fractions were eluted by fresh xylene, delivered by nitrogen gas pressure, at successively rising temperatures. Subsequently the fractions (about 200 ml from each fraction) were collected in 300 ml beakers and transferred to a rotary evaporator to remove the solvent (xylene) at 60 ^{o}C. The fractions were washed with acetone and placed in pre-weighed glass vials. Then the fractions were dried in a vacuum oven at 50 ^{o}C overnight. The glass vials were re-weighed to determine the weight of each fraction.

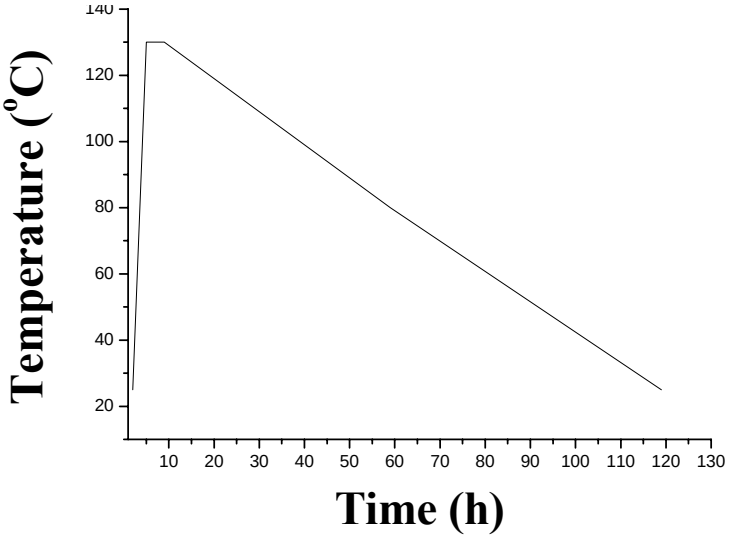

Figure 6.12. The cooling program used in preparative TREF.

6.2.3 TREF results

Eleven fractions from each polymer (A and C) were obtained by elution in the temperature range 25 to 150 °C. The preparative TREF results of samples A and C are shown in Tables 6.12 and 6.13. These tables show the fractionation data, including the weight percentage of each fraction in each sample. TREF results showed that the solvent-extracted fractions described in Section 6.1 were not exactly the same as the "soluble" fraction (what remains behind in solution after the cooling crystallization step) obtained by TREF. The latter comprised only 10.80%, of the sample, while the solvent extractables were 18.16% for sample A, and 18.27% as opposed to 28.98% for sample C. This indicates that the solvent-extracted soluble fractions included some material that will co-crystallize onto an inert support under slow cooling from solution.

Figures 6.13 and 6.14 are TREF curves of samples A and C, respectively. The derivative curves show that the summation of weight% (ΣW%) increase with the increase in the elution temperature. The ΣW% and W% /ΔT versus the TREF elution temperature curves show two main peaks. The small peaks between 25-60 °C are due to the less crystalline fractions. Less crystalline fractions elute first (after the fractions that soluble at RT). The highly crystalline PP fractions in samples A and C elute at a higher and in a narrower temperature range (compared with the fractions at low temperature), as shown by the strong peaks between 100 to 130 °C in Figures 6.13 and 6.14. This is in agreement with

the finding of Soares *et al.*, [10] they found that homopolymer PP is obtained in the higher temperature fractions while EP copolymer is obtained in the lower temperature fractions. Some crystalline EP copolymer seems to exist in the fractions between 80 to 100 ^{o}C, as shown in the Figures 6.13 and 6.14 of samples A and C. 18% and 28% (about 0.140 and 0.203 g) from fractions at 120 ^{o}C were removed from samples A and C, respectively.

These amounts were selected to correspond with the amounts of soluble materails extracted during the first part of this study. The rest of the fractions at 120 ^{o}C (about 0.6350 g of sample A and 0.5218 g from sample C) were added back to the other fractions and test specimens were prepared from these fractions as described in Sections 4.4.1 and 4.4.3. Subsequently, the ESCR test 2 was performed to determine the change in the ESCR of two IPPC samples (sample A and C) after removing some crystalline materials from the eluting fractions at 120 ^{o}C.

Table 6.12. Raw data of sample A obtained after fractionation by preparative TREF

Fraction number	Elution temperature (^{o}C)	W[a] (g)	W% [b]	ΣW% [c]	ΔT [d] (^{o}C)	(W% /ΔT) [e]
1	25	0.3288	10.80	10.80	0	0.000
2	40	0.1801	05.92	16.72	15	0.395
3	60	0.0763	02.51	19.23	20	0.126
4	80	0.0786	02.58	21.81	20	0.129
5	90	0.1666	05.47	27.28	10	0.547
6	100	0.2493	08.19	35.47	10	0.819
7	110	0.8253	27.11	62.58	10	2.711
8	120	0.7750	25.46	88.04	10	2.526
9	130	0.2693	08.85	96.89	10	0.885
10	140	0.0443	01.46	98.35	10	0.146
11	150	0.0272	00.89	99.24	10	0.089

[a] weight of each fraction
[b] weight /total weight of sample A x 100, total weight of sample A about 3.0438 g
[c] summation of the [(weight /total weight of sample A x 100)]
[d] the elution temperature range between each fraction
[e] weight fraction percentage divided by the elution temperature range between each fraction

Table 6.13. Raw data of sample C obtained after fractionation by preparative TREF

Fraction number	Fraction temperature (^oC)	W* (g)	W%	ΣW %	ΔT (^oC)	W% /ΔT
1	25	0.5658	18.27	18.27	0	0
2	40	0.0982	03.17	21.44	15	0.211
3	60	0.0712	02.30	23.74	20	0.115
4	80	0.0805	02.60	26.34	20	0.130
5	90	0.1415	04.57	30.91	10	0.457
6	100	0.2910	09.40	40.31	10	0.940
7	110	0.8690	28.06	68.37	10	2.806
8	120	0.7248	23.40	91.77	10	2.340
9	130	0.1972	06.37	98.44	10	0.637
10	140	0.0312	01.01	99.45	10	0.101
11	150	0.0142	> 0.01	99.46	10	>0.001

Total weight of sample C (3.0968 g)

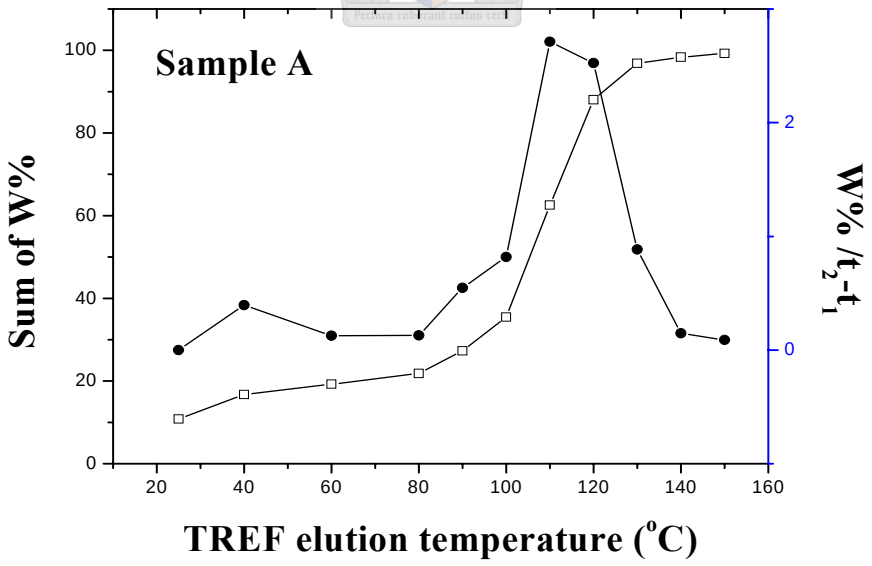

Figure 6.13. The ΣW% and W% /ΔT versus the TREF elution temperature (sample A)

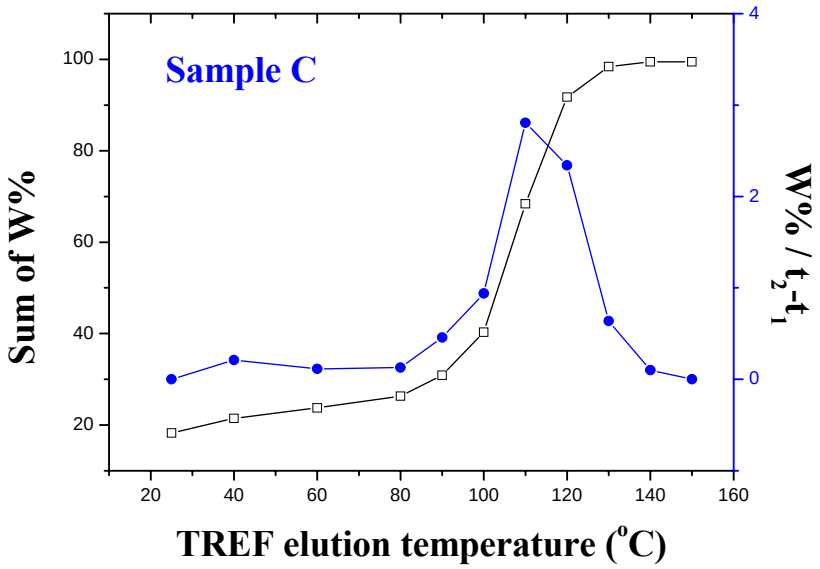

Figure 6.14. The ΣW% and W% /ΔT versus the TREF elution temperature (sample C)

6.2.4 ESCR test 2

The results from this test are summarized in Table 6.14. The Table shows typical ESCR data obtained from ESCR test 2 under a predetermined, constant applied stress (15 MPa) at 60 °C after removing part of one crystalline fraction. The results showed that the value of ESCR increased to double of the original samples. The average ESCR increased dramatically in both samples A and C. ESCR of sample A increased from 86.86 to 128.63 h (increased about 48% compared with the original sample), while in sample C increased from 15.30 to 26.03 (increased about 70% compared with the original sample). In general, this increase is probably due to the removal of the readity crystalline fractions which can cause a decrease in the overall crystallinity of the two samples, and minimizing the weaker interspherulite boundaries.

Thicker specimens required longer times to break and showed a slight increase in the final time to failure (more ESCR) in the majority of tests, as shown in Table 6.14. This is because the stress is normally depending on the sample cross-sectional area, when a constant weight is used. So, thicker samples experience as lower stress. This decreases the crack propagation rate and increases the final time to failure. In order to get a clearer

picture, the final time to failure was normalized, by calculating the failure time based on a film thickness of 0.15 cm. A typical ESC surface (ribs and hackles) near the crack area was detected by optical microscopy, as shown in Figure 6.15.

Table 6.14. ESCR data of three samples after removing some crystalline fractions, obtained by ESCR test 2

Sample		ESCR for each specimen after extraction (time to failure) hh:mm	Average ESCR, (h)	Average ESCR Normalized (h)*
Sample A				
	Thickness (cm)			
Specimen 1	0.22	182.21	**176.0**	**128.6**
Specimen 2	0.20	175.59		
Specimen 3	0.18	170.34		
Sample C				
Specimen 1	0.19	30.75	**30.1**	**26.0**
Specimen 2	0.20	31.51		
Specimen 3	0.14	28.20		

* See text

Figure 6.15. Typical ESC surface of sample A after removing 18% crystalline material (magnification 50 x 50μm)

Once again, as mentioned early when the soluble fractions were removed, whatever the change in the values of ESCR of IPPCs might be (increase/decrease), it is strongly dependent on the type and the amount of the material removed (MW, its MWD and its crystallinity). For this reason, ^{13}C NMR, GPC and DSC were used to characterize the

removed fractions in order to see the difference between these extracted fractions. Then, the same techniques were applied on the IPPC samples (A and C) after removing the above-mentioned materials to determine the change in their microstructure and properties such as MW, MWD and crystallinity. Then formation of crazes and crack growth were studied and finally, these samples were etched in order to see the change in their morphology.

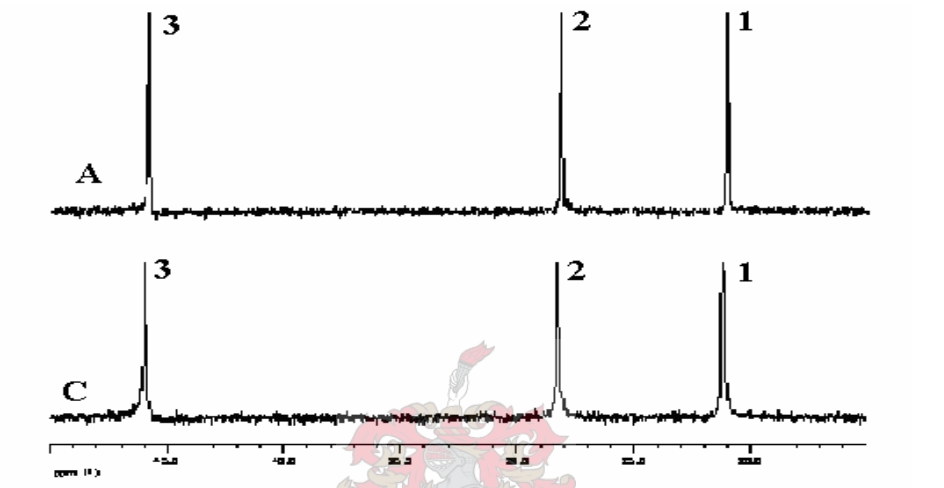

Figure 6.16. ^{13}C NMR of fractions removed at 120 ^{o}C in samples A and C

6.2.5 Characterization of extracted fractions

6.2.5.1 ^{13}C NMR

As expected, high temperature fractions (eluted at 120 ^{o}C during preparative TREF) in both samples A and C are homopolymer PP, as shown in Figure 5.16 (NMR solvent a 9:1 mixture of 1,2,4-trichlorobenzene and C_6D_6).

6.2.5.2 DSC

Table 6.15 shows the T_m, T_c and crystallinity of the two fractions removed from samples A and C. The crystallinity of the extracted fractions was measured by equation (2) as described in Section 5.3.3. In general, these fractions are highly crystalline, as shown in Table 6.15. The crystallinity in both fractions is the same (about 71% for each fraction). The melting and crystallization temperatures are essentially identical for both fractions. Just one endothermic peak appeared at 163.22-164.67 ^{o}C in both samples, which due to

the melting of the PP homopolymer, and similarly only a single exothermic crystallization peak was detected at 119.49-120.89 ^{o}C for both samples (see Appendix B).

Table 6.15. Characterization of extracted fractions using DSC thermograms

Sample	T_m (^{o}C)	T_c (^{o}C)	Δ H (J/g)	Crystallinity, %
Sample A	163.22	120.89	148.13	71.11
Sample C	164.67	119.49	148.50	71.29

6.2.5.3 GPC

GPC results of the 120 ^{o}C TREF fractions that were removed from samples A and C are shown in Table 6.16. These are high molecular weight materials with similar molecular weight distribution.

We conclude that these fractions are crystalline PP homopolymers (71%) with almost the same MWD. The main difference between these fractions lies in the difference in $\overline{M_w}$ and $\overline{M_n}$, as shown in Table 6.16. Now, it is important to see the effect of extracting these fractions had on the properties of samples A and C (e.g. microstructure, molecular weights and crystallinity).

Table 6.16 Molecular weight data of the two extracted fractions of samples A and C, obtained by GPC

Sample	$\overline{M_w}$ x 10^3	$\overline{M_n}$ x 10^3	MWD
Sample A	417.140	128.766	3.24
Sample C	658.620	199.702	3.03

6.2.6 Characterization of the two samples after removing a crystalline fraction

6.2.6.1 ^{13}C NMR

The ^{13}C NMR spectra of samples A and C after removing some high temperature or crystalline materials are given in Figure 6.17. There is not much change in the spectra of both samples after removing these crystalline fractions. The peaks at 21.58-21.59, 28.64-28.65 and 46.29-46.30 ppm correspond to the CH_3, CH and CH_2 respectively (peak numbers 1, 2 and 4 in Figure 6.17). The peaks at 29.75-29.78 ppm (peak number 3 in Figure 6.17) correspond to the presence of ethylene in these copolymers.

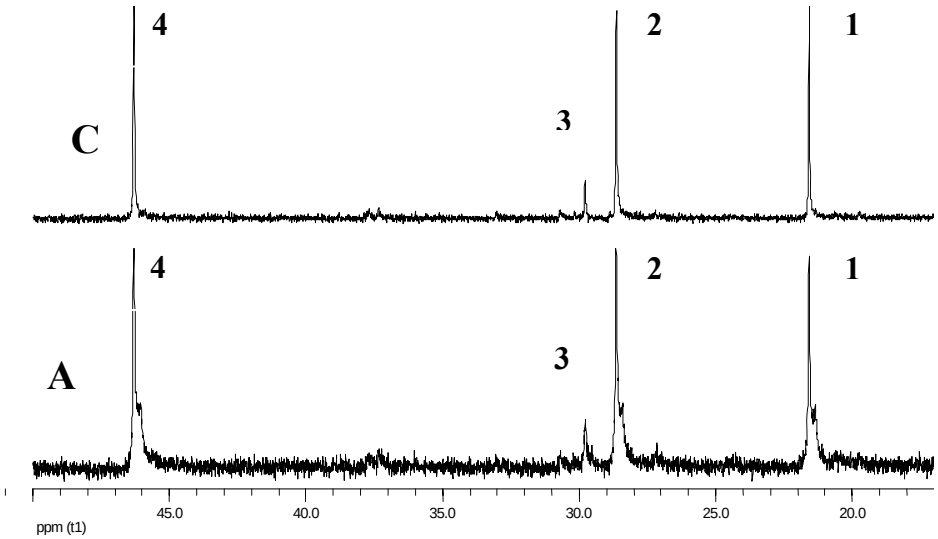

Figure 6.17. ^{13}C NMR spectra of samples A and C after removing some crystalline materials

All the sequences that appeared in the ^{13}C NMR spectra of the original samples (Figure 5.6) are still exist in above ^{13}C NMR spectra (Figure 6.17). This means that the segments such as PPPPP, PPPEP, PPPPE, EEEEE, PPEP, PEPP, EEP, EPE and PPE are still present in samples A and C even after removing some high temperature fractions. The major change happened to samples A and C is a small, but noticeable the decrease in the tacticities of both samples. For example, after removing about 18% from the fraction at 120 ^{o}C of sample A, tacticity decreased from 60.26 to 56.86%, while the tacticity of sample C decreased from 67.36 to 65.90%. This indicates that some amount of PPPPP (iPP) was removed from these samples, and this should decrease the overall crystallinity of the samples.

6.2.6.2 DSC

The DSC results of samples A and C after removing some crystalline materials are shown in Table 6.17. The crystallinity was measured by equation (2) as described in Section 5.3.3. The values of crystallinity in Table 6.18 are relative values (using $\Delta H_{F(100\%)}$ of iPP as 100% crystalline IPPC). As expected, removing some crystalline materials or PPPPP sequences (iPP) decreased the overall crystallinity from 25.06% to 23.81% of sample A and from 40.50% to 32.39% of sample C. The larger decrease in the case of sample C is due to the larger amount of crystalline materials that were removed from sample C (0.203 g) than A (0.140 g). Although sample C showed more decrease in its crystallinity, it is

still a higher crystallinity (32.39%) than A (23.81%). This can be one of the reasons why sample A is still has a higher ESCR than C.

Table 6.17. Characterization of samples A and C after removing some crystalline materials by TREF, using DSC

Sample	T_m (°C)	T_c (°C)	Δ H (J/g)	Crystallinity, %
Sample A	162.86	121.19	49.60	23.81
Sample C	162.66	121.26	67.47	32.39

DSC cooling curves of the two samples A and C after removing some crystalline materials show two exothermic peaks for the crystallization (Figure 6.18). The strong ones at (121.19-121.26 °C) are due to the crystallizing of the PP homopolymer. This is also evident in the melting endotherms as a single peak at (162.66-162.86 °C) for each sample, as shown in Figure 6.19. The other weak cooling DSC curves at 96.6-97.3 °C are due to the polyethylene-like material (PE block crystal), as shown in Figure 6.18. This structure is not reflected in the melting endotherms in the two samples, as shown Figure 6.19. Finally, removing these crystalline materials resulted negligible decrease in T_m and T_c values compared to T_m and T_c of the original samples.

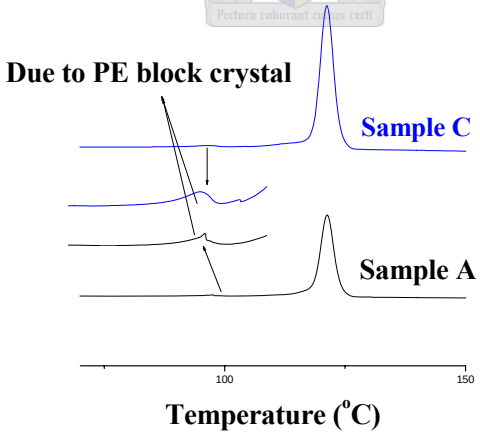

Figure 6.18. DSC crystallization curves of samples A and C after removing a fraction of crystalline material

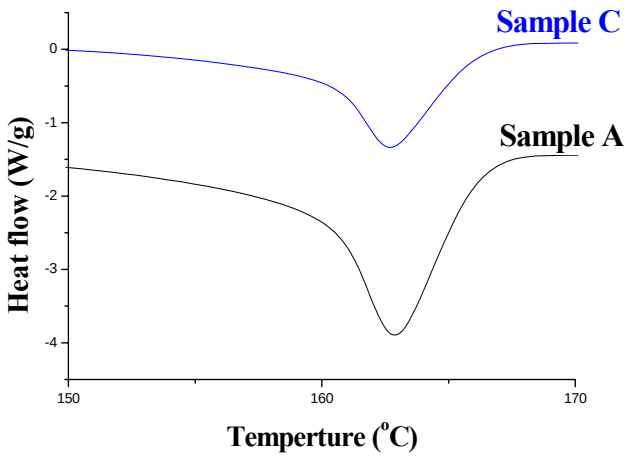

Figure 6.19. DSC melting curves of samples A and C after removing a fraction of crystalline material

6.2.6.3 GPC

Table 6.18 shows the $\overline{M_n}$, $\overline{M_w}$ and MWD of samples A and C after removing the part of a fractions of high temperature or crystalline materials (from fractions at 120 °C). We see a decrease in $\overline{M_w}$ of samples A and C, and an increase in MWD for sample A and a decrease in MWD for sample C.

Table 6.18. Molecular weight data for samples A and C after removing crystalline fractions

Sample	$\overline{M_w}$ x 10^3	$\overline{M_n}$ x 10^3	MWD
Sample A	319.909	71.19	4.49
Sample C	201.742	49.60	4.30

While we see a decrease in molecular weight for the 2 samples, we see an improvement in their ESCR. This indicates that with these materials, the more important factor is crystallinity. Sample C showed more improvement in ESCR than A. Crystallinity of sample A decreased about 04.9% (from 25.06% (original one) to 23.81% (after removing the crystalline part)), while the crystallinity of sample C decreased about 20.0%. We can conclude that the difference in ESCR between samples A and C after removing some crystalline materials is partly due to the difference in crystallinity and that the difference

in $\overline{M_n}$ and MWD is not significant. As the crystallinity decreases, ESCR generally increases. [15-18] The effect of crystallinity on ESCR is discussed in Section 5.3.3. In summary, we can see that removing highly crystalline material from the IPPCs resulted in (see also Table 6.19):

1. A drop in isotacticity of the remaining material, compared to the original material.
2. A decrease in the crystallinity of the remaining material, compared to the original material.
3. A decrease in molecular weight for both samples, and an increase in the molecular weight distribution for A and a decrease for C.
4. The removal of the crystalline material resulted in an increase in ESCR for both polymers.
5.

Table 6.19. Changes in properties of the IPPCs A and C after removing crystalline materials

Sample	% of extracted material	Changes in Properties				
		$\overline{Mw}$	$\overline{Mn}$	MWD	Crystallinity	ESCR
A	**18**	**-**	**+**	**+**	**-**	**+**
C	**28**	**-**	**+**	**-**	**-**	**+**

+ Increase and – Decrease

6.2.7 The formation of crazes

The crazes in samples A and C after removing the fractions at 120 ^{o}C were detected by the optical microscopy, as shown in Figure 6.20. This experimental was done as described in Section 4.5 in order to investigate the time of craze formation. Crazing in sample A seems to be in the early stage, while crazing of sample C seems to be at a later stage of breakdown (see Section 5.4). Sample A deformed after twenty-two hours when crazes were formed, while sample C deformed after twelve hours when crazes were formed.

Figure 6.20. Optical micrograph of crazes in samples A and C after removing the fractions at 120 ^{o}C

Craze formation was observed long before final failure. This means that craze formation does not pose immediate danger to these polymers. Crazes can continue to sustain loads after they are formed. For example, crazes in sample A were formed after 22 hours and final failure was observed after about 176 hours. While craze formation in general is highly dependent upon molecular weight, [6] crazing in this case is retarded due to the decrease in the crystallinity of the tested samples which resulted in a decrease in the percentage of weak interphase regions.

Figure 6.21. Optical micrographs of the crack regions in samples A and C after removing some crystalline materials

6.2.8 Crack growth

The crazes shown in Figure 6.20 broke down and formed a crack, as shown in Figure 6.21. Crack length of both samples A and C increased with time as shown in Table 6.19. The crack propagation rate in sample A is lower than the crack propagation in C. That is why the final time to failure in sample C (33 h) was observed earlier than that in A (189 h).

Table 6.20. Time under stress versus the crack growth of samples A and C after removing crystalline fractions

Sample A							
Time under stress, (h)	0	40	80	110	150	170	189
Crack growth, (cm)	0.5	0.6	0.7	0.9	1.1	1.5	2.0 (Final failure)
Sample C							
Time under stress, (h)	0	10	15	18	24	28	33
Crack growth, (cm)	0.5	0.6	0.7	0.8	1.0	1.4	2.0 (Final failure)

The crack growth in both samples (A and C) showed the same two general stages of velocity found in the original samples after removing the soluble fractions. Samples A and C showed two stages of crack growth, a linear slow growth followed by a linear fast growth, as shown in Figure 6.22. This is because the effective stress is increased as the stressed area is decreased, but the force remains the same. The force remains constant while the crack length increases in a controlled manner, until eventually a critical length is reached. The critical crack length seems to be higher than that in the original samples.

As shown in Figure 6.22, the critical crack length before the velocity of crack increases in the two samples after removing part of a fractions of crystalline materials showed an increase from 0.9 cm (for the original samples) to somewhere between 1.0-1.1 cm (for the samples after the removing some crystalline materials). At this point, the ductile type of deformation ends and brittle deformation begins. The final stage of failure seems to be less brittle in this case compared to the original ones, since the crack speed is very much lower, which resulted in a large increase in the toughness of these samples. Even after removing these crystalline materials, sample A still has the highest ESCR because it is still has a better ductile-brittle transition and lower cystallinity. The later this transition is, the better the resistance to ESC. [(7)]

The interphases between the crystalline and the amorphous regions seem to have a large impact on the failure process of these polymers, especially when the other factors such molecular weight is less important. This is probably because at these interphases stresses

are the highest in the polymer structure. This means that these areas are more susceptible to initiating stress cracking because cracks start at the interphases of these materials, and this increases with an increase in crystallinity. [19] Therefore a decrease in the amount of stressed interphase regions which results from a decrease in crystallinity results in turn in an increase in the ESCR of samples A and C. Since the size of EP rubber particle and interparticle distances are also important, it was necessary to study the change in the morphology of these samples after removing these crystalline materials.

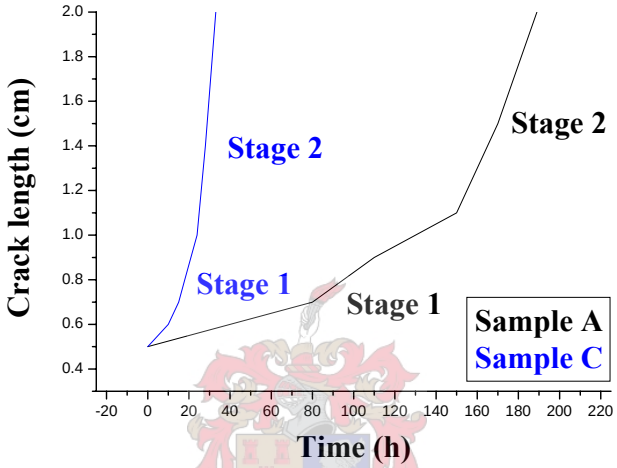

Figure 6.22. Crack lengths versus time for samples A and C after removing some crystalline materials

6.2.9 Morphology

Etched samples (samples without the extracted crystalline material removed) are shown in Figure 6.23. The difference in both the size of particle and interparticle distance between these particles is shown in Table 6.21.

Table 6.21. Particle size and interparticle distance of samples A and C after removing crystalline fractions

Sample	Average particle size, µm	Average interparticle distance, µm
A	0.419	0.924
C	0.259	0.806

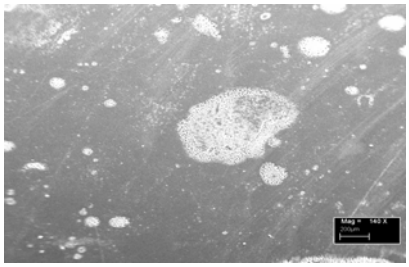

140 x 200 μm

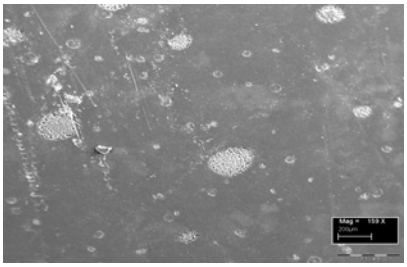

159 x 200 μm

Figure 6.23. SEM micrographs of etched IPPC samples after removing some crystalline materials

The average particle size in sample C (0.259 μm) is significantly smaller than in sample A (0.419 μm). The average interparticle distance showed by sample A (0.924 μm), is somewhat more than for C (0.806 μm). This means there is negligible change in the average particle size and the average interparticle distance in sample A (after removing some crystalline materials) compared to the original material. On the other hand, sample C showed an apparent change in the average particle size and the large average interparticle distance comparing with the original one (the average particle size increased from 0.104 to 0.259 μm, while the average interparticle distance increased from 0.386 to 0.806 μm). This could be a result of agglomeration or coalescing of the rubber particles due to the extraction.

The particle size and interparticle distance of samples A and C may be more effective for craze initiation and toughening when compared to the original samples. Although there are increases in the average particle size and the average interparticle distance in sample C (also became slightly more uniform), sample A still has the optimum particle diameter and interparticle distance. The particle size of about 0.4 μm was found to produce optimum results for the PP system. [3,8,9] The particle size and interparticle distance of sample C is still less effective for craze initiation and toughening than sample A. In spite of more crystalline material being removed from sample C, sample C still has a overall higher crystallinity than A, which obviously indicates that the latter is tougher.

From the above results we can conclude that the high ESCR of stressed sample A in pure isopropanol after removing some crystalline materials can be related to the lower

crystallinity, while maintaining optimum particle size and critical interparticle distance and uniformity in the size and distribution of rubber particles. Although sample A still shows more ductility and toughness than C, both samples seemed to have higher ductility than the originals.

6.3 Conclusions

IPPCs are complicated copolymers which have multi-fraction copolymeric structures. Each of these fractions has significantly different average properties. These fractions are EP rubber, EP block copolymers, block crystalline PE and PP homopolymer. The difference in properties of the polymers originates from differences in these fractions, for example, the different weight percentage of EP rubber and/or PP homopolymer and/or EP blocky copolymer and/or the ethylene content and its distribution. This means the properties of IPPC are dependent on the microstructure rather than the overall structure.

Removing some soluble fractions (fractions that dissolve at RT) from these polymers resulted a large drop in the values of ESCR of the three samples. This is probably because these fractions, which are soluble at RT, contain EP rubbery materials. EP rubbery materials are known to toughen PP against crack propagation by dissipating a large amount of energy in the matrix around the particle, thereby blunting the crack and inhibiting crack propagation. [(1)] In addition, they control the craze growth and initiate numerous, small energy absorbing crazes. They also lower the ductile to brittle transition, leading the material to fail in a ductile manner. [(2)] Removing these fractions affected the properties such as crystallinity, MW, MWD, morphology and finally microstructure of the three original samples. This was clearly shown by ^{13}C NMR, GPC and DSC. ^{13}C NMR results showed that some percentage of various segments such as EEP, PPEP, EPE and PPE were extracted from these samples. EPE segments were totally extracted from sample A. DSC results showed increase in crystallinity of samples A and B and decrease in crystallinity of sample C, while GPC results showed decrease in $\overline{M_w}$ of the three samples, increase in $\overline{M_n}$ of samples A and B and decrease in $\overline{M_n}$ of sample C and finally MWD becomes narrower in cases of samples A and B and broader in sample C.

Removing crystalline material from samples A and C increased the ESCR in both samples significantly. As shown by ^{13}C NMR, GPC, and DSC, removing some of the crystalline material from these samples resulted in a decrease in the crystallinity, a decrease in the molecular weight, an increase in MWD of sample A and a decrease in MWD of sample C. This decrease in molecular weight coupled with a large increase in ESCR seems to indicate that molecular weight is not a dominant factor in the ESCR of these polymers. Removing some crystalline material reduced the overall crystallinity and seems to make the material tougher and more resistant to ESC.

The main cause of ESC in IPPCs either after removing the rubbery materials or after removing the crystalline materials is related to craze formation when immersed in isopropanol. In the case of removing the rubbery materials, isopropanol induced more softening or plastization at the time before crazes appeared than the original samples. In the case of removing the crystalline materials (compared to the original samples (samples before the extraction)) less softening or plastization was induced at the time before crazes appeared. In both cases, once crazes occurred, voids can then act as an easy diffusion path for the isopropanol, thus promoting craze formation. Also, the formation of crazes in both cases does not pose an immediate danger to these polymers. Crazes can continue to sustain loads after they are formed.

Results showed that the crack growth showed two stages of velocity, a linear slow growth followed by a linear fast growth. After removing the soluble fractions, the crack length before the velocity of crack increases was 0.8 cm (critical crack length), while it is somewhere between 1.0-1.1 cm after removing the crystalline material. At these critical lengths, the ductile type deformation ends and brittle deformation begins. The ductile-brittle transition occurred at an early stage in the case when soluble fractions were removed. It occurred in a later stage in the case of removed crystalline material (both compared to original samples). After removing soluble fractions, the final stage of failure seems to be more brittle than in the case of original samples, since the crack speed is higher, which resulted more reduction in toughness. This means there was more dramatic drop in the energy absorbed by the stressed samples and the ability for deformation in the tested specimens is reduced more in this case (decrease in ductility and toughness). On

the other hand, removing some crystalline materials had the opposite effect (increase in ductility and toughness). Most importantly, the later the ductile-brittle transition is, the better the resistance to ESC as observed in the case of removing the crystalline materials.

Permanganic etching can be useful technique for studying the morphology of IPPCs even after removing some fractions from these copolymers. Good quality SEM images proved to be useful for determining average particle size and interparticle distance for the rubbery material in the polymer. Not only is the rubber content important, but rubber particle size, and the interparticle distance are important factors in the deformation and fracture of all toughened plastics. Results from this study indicate the best average particle size to be 0.4 μm, in accordance with the results of Marcus *et al.,* [(2)] Lotti *et al.* [(8)] and Moore. [(9)]

Overall we can conclude that the most important factors that influence ESCR of IPPC polymers are the crystallinity and the morphology (particle size and interparticle distance of the rubbery particles). Molecular weight has a lesser effect on the ESCR of these samples.

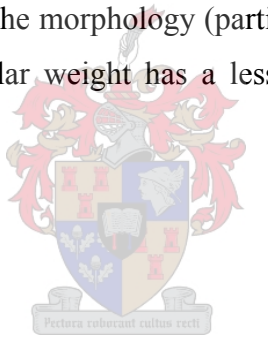

6.4 References

1- J. Soares and A. Hamielec, Polymer, **1995**, 36, 1639-1654.
2- W. Tam, T. Cheung and R. Li, Polymer Testing, **1996**, 15, 363-379.
3- K. Marcus, B. Sole and R. Patil, Macromolecular Symposium, **2002**, 178, 39-53.
4- J Jancar, A. Dianselmo and A. Dibenedetto, Polymer, **1993**, 34, 1684-1694.
5- M. Mark, N. Bikales, C. Overberger and G. Menges, Encyclopedia of Polymer Science and Engineering, John Wilely & Sons, USA, **1986**, 4, 313-314.
6- J. Kocsis, Polypropylene an A-Z Reference, Environmental Stress Cracking of Polypropylene by R. Chatten and D. Vesely, Kluwer Academic Publishers, UK, **1999**, 206-214.
7- R. Portnoy, Medical Plastics: Degradation Resistance & Failure Analysis, Environmental Stress Cracking in Polyethylene by A. Lustiger, Plastics Design Library, USA, **1998**, 66-69.
8- C. Lotti, C. Correa and S. Canevarolo, Materials Research, **2000**, 3, 37-44.
9- E. Moore, Polypropylene Handbook: Polymerization, Characterization, Properties, Processing and Applications, Chapter 6: End-Use Properties by R. Duca and E. Moore, Hanser Publishers, Germany, **1996**, 246-248.
10- J. Soares and A. Hamielec, Polymer, **1995**, 36, 1639-1654.
11- J. Xu and L. Feng, European Polymer Journal, **2000**, 36, 867-878.
12- M. Francis and J. Mirabella, Journal of Applied Polymer Science: Applied Polymer Symposium, **1992**, 51, 117-134.
13- M. Francis and J. Mirabella, Journal of Liquid Chromatography, **1994**, 17, 3201-3219.
14- P. Zacur, C. Golzueta and N. Caplati, Polymer Engineering and Science, **2000**, 40, 1921-1930.
15- W. Brostow and R. Corneliussen, Failure of Plastics, Chapter 16: Environmental stress cracking: The Phenomenon and its Utility by A. Lustiger, Hanser Publishers, Germany, **1986**, 305-328.
16- H. Mark, and N. Gaylord, Encyclopedia of Polymer Science and Technology, Fourth Edition, Executive Editor: N. Bikales, John Wiley & Sons, USA, **1992**, 6, 301.
17- H. Mark, and N. Gaylord, Encyclopedia of Polymer Science and Technology, Second Edition, Executive Editor: N. Bikales, John Wiley & Sons, USA, **1971**, 7, 269-289.
18- J. Soares, R. Abbott and J. Kim, Journal of Applied Polymer Science: Part B: Polymer Physics, **2000**, 38, 1267-1275.
19- R. Al-Zubi, A. Strong and M. Lampson, Understanding Environmental Stress Crack Resistance (ESCR) in Rotomolded Polyethylene Tanks, Innovation and Technology Poly Processing Company, **2001**, 1-9.

Chapter 7

Conclusions

7.1 Conclusions

In this study, three different impact copolymer polypropylenes (IPPCs) were evaluated in terms of their resistance to environmental stress cracking. During this study, the following was achieved, and conclusions reached.

1. A suitable stress crack agent for testing ESCR was determined to be neat isopropanol.
2. A test apparatus was designed and built that could provide quantitative data for the ESCR of polymer films or thin sheets.
3. The three copolymers were fully characterized and then tested for ESCR.
4. TREF and NMR analysis showed that IPPCs are complicated, multi-fraction copolymeric materials. The fractions comprise EP rubber, EP block copolymers, crystalline ethylene-rich materials, and PP homopolymer.
5. As the ethylene content of the copolymers increased, the ESCR decreases. This is not as straightforward as it might appear as characterization revealed that:
    a. The increase in ethylene content corresponded with an increase in overall crystallinity.
    b. This indicates that materials with apparently higher impact strength might in fact be less resistant to ESC.
    c. The ethylene content, and the distribution of ethylene in the molecular species present, is also a determining factor in the size and distribution of rubber-like particles in the copolymers. The polymer with the lowest ethylene content had the closest to optimum rubber particle size and interparticle distance for high ESCR.
6. Molecular weight and MWD might be a contributing factor in the ESCR, but is within the limits of the polymers evaluated, not a determining factor.
7. The use of solvent extraction removed some rubbery materials and some ethylene rich (polyethylene-like) materials from all the polymers. This resulted in large

decreases in the ESCR. This indicates that the soluble rubbery materials do play a role in toughening the materials.

8. Preparative TREF was used to fractionate two of the polymers (high and low ethylene content), and a crystalline fraction obtained by elution at 120°C was removed from each polymer (the amount removed being equal to the amount of soluble or rubbery material removed in the previous experiment). As expected, the removal of crystalline material increased the ESCR of the samples, and the extent of the increase was directly related to the amount of crystalline material removed. In both cases, removal of the crystalline fractions (18 – 25% of the total polymer) decreased the average molecular weight significantly, yet the ESCR increased, indicating again that the crystallinity is a dominating factor, and that molecular weight was, in this case, not.
9. Removal of the crystalline material had the effect of improving rubber particle size and distribution in the case of the more crystalline polymer, while it had little effect on the less crystalline polymer.
10. Craze formation, crack growth as a function of time and morphology were successfully studied. Morphology studies revealed that, even after extraction experiments, rubber particle size and interparticle distance are important factors in controlling the failure process of IPPCs.
11. As a final conclusion it can be stated that the ESCR is dependent on crystallinity as well as the distribution and structure of the rubbery materials in the polymer. The latter is dependent on the arrangement and make-up of the molecular species present in the polymer.

APPENDIX A: GPC DATA

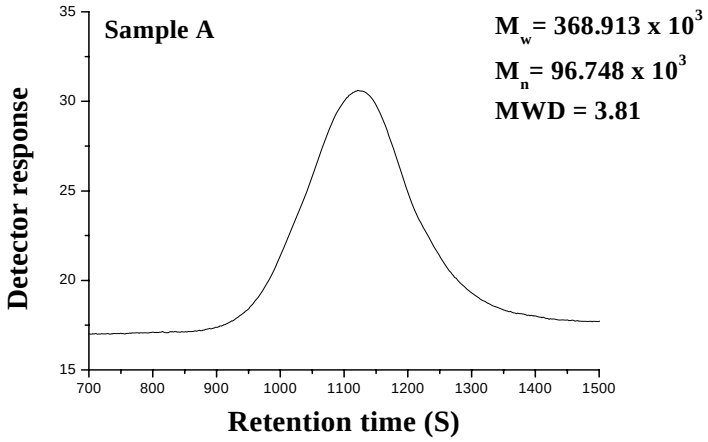

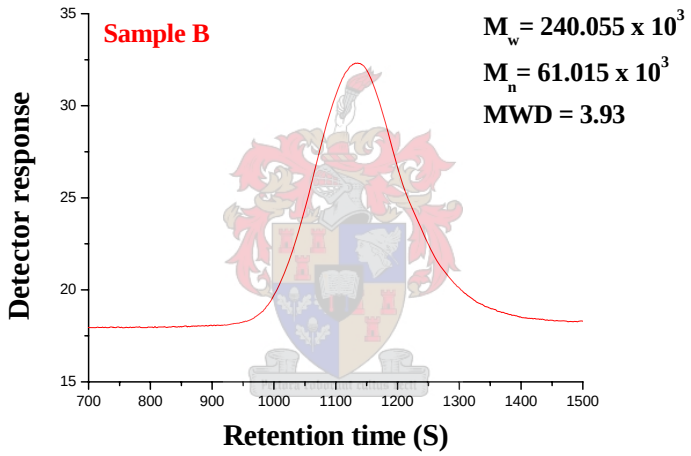

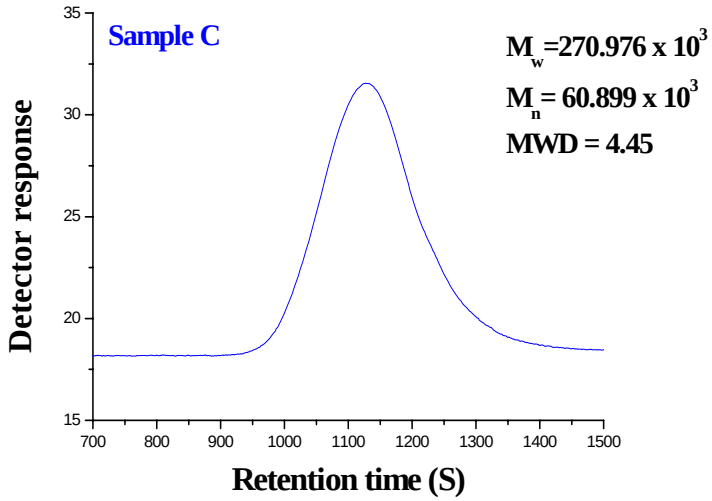

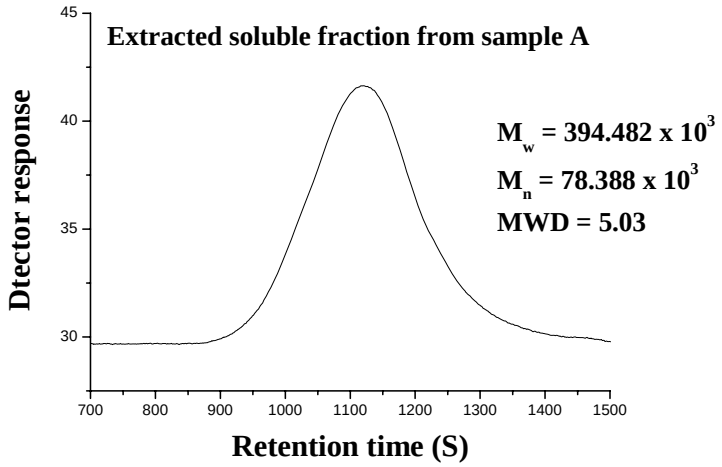
Extracted soluble fraction from sample A
Dtector response
Retention time (S)
M_w = 394.482 x 10^3
M_n = 78.388 x 10^3
MWD = 5.03

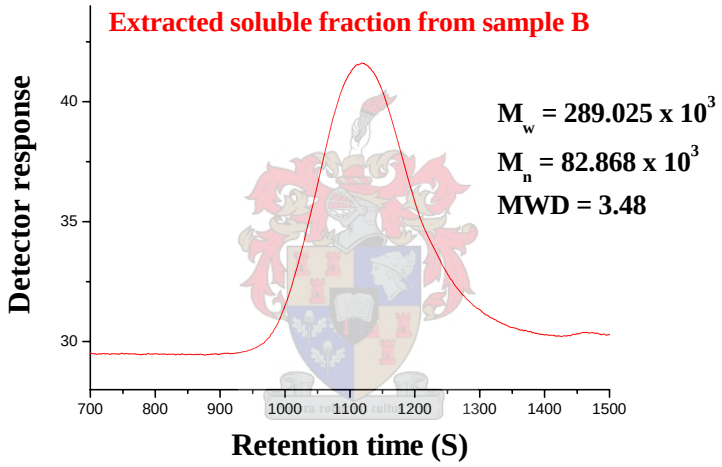
Extracted soluble fraction from sample B
Detector response
Retention time (S)
M_w = 289.025 x 10^3
M_n = 82.868 x 10^3
MWD = 3.48

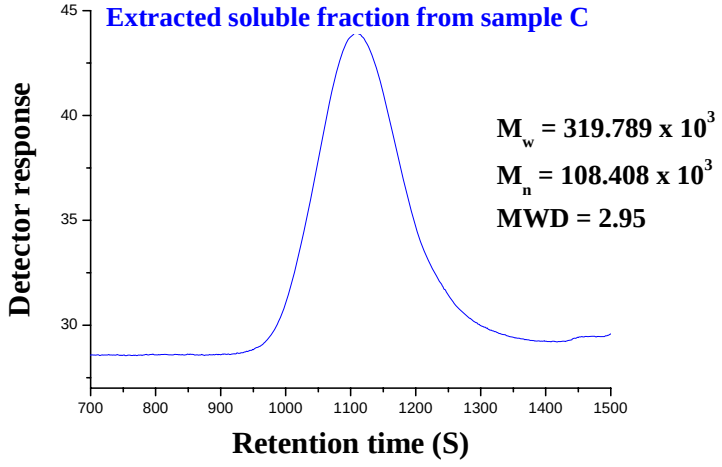
Extracted soluble fraction from sample C
Detector response
Retention time (S)
M_w = 319.789 x 10^3
M_n = 108.408 x 10^3
MWD = 2.95

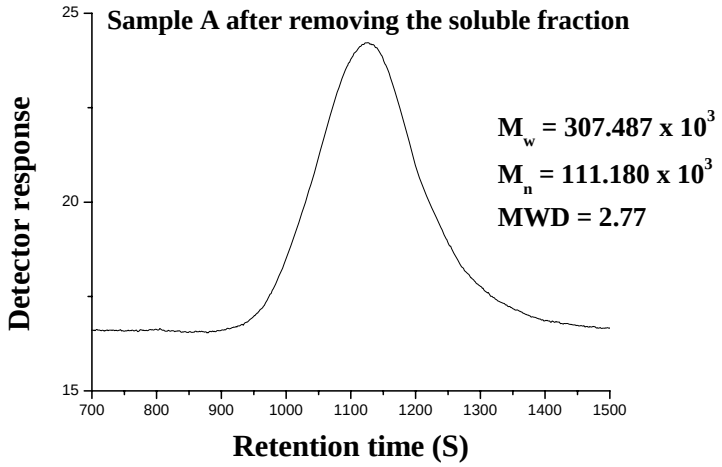
Sample A after removing the soluble fraction
Detector response
Retention time (S)
M_w = 307.487 x 10^3
M_n = 111.180 x 10^3
MWD = 2.77

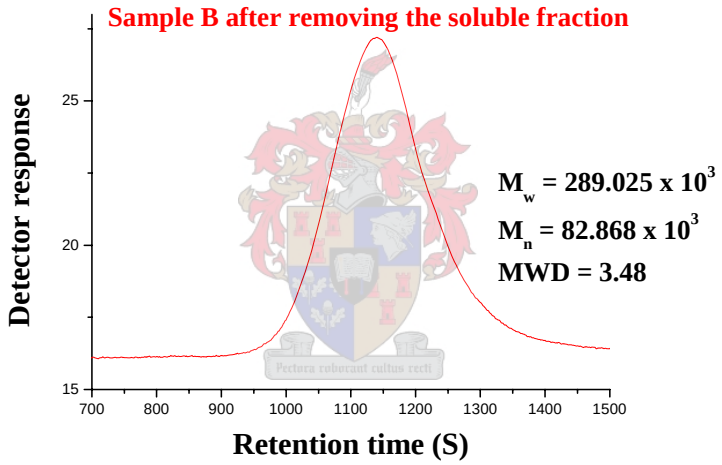
Sample B after removing the soluble fraction
Detector response
Retention time (S)
M_w = 289.025 x 10^3
M_n = 82.868 x 10^3
MWD = 3.48

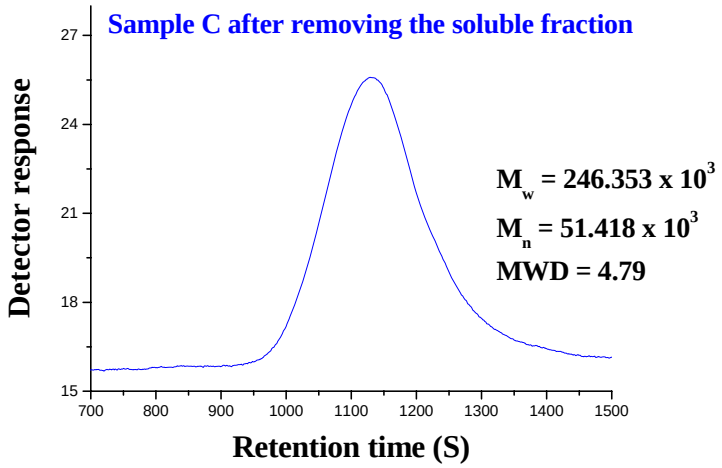
Sample C after removing the soluble fraction
Detector response
Retention time (S)
M_w = 246.353 x 10^3
M_n = 51.418 x 10^3
MWD = 4.79

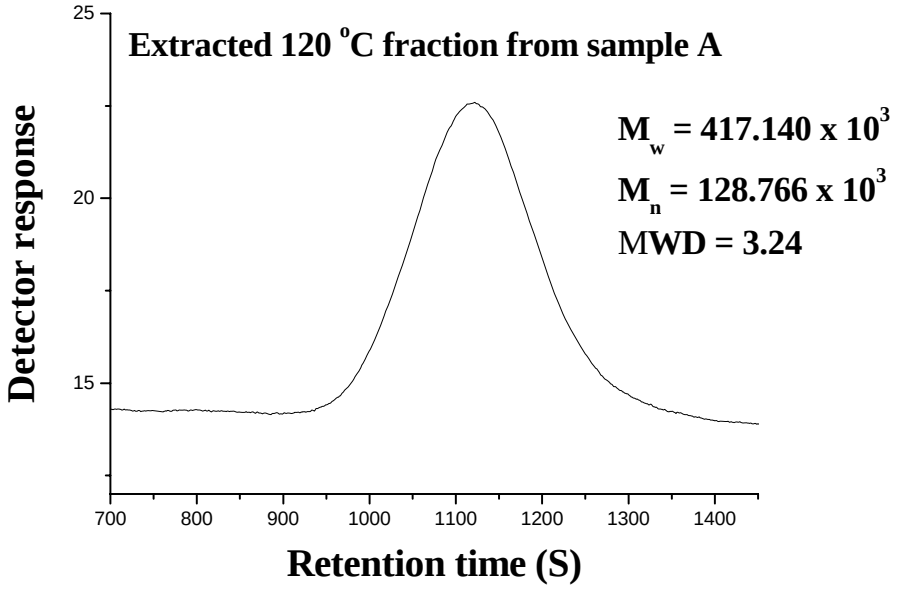
Extracted 120 °C fraction from sample A
M_w = 417.140 x 10^3
M_n = 128.766 x 10^3
MWD = 3.24
Detector response
Retention time (S)
25
20
15
700
800
900
1000
1100
1200
1300
1400

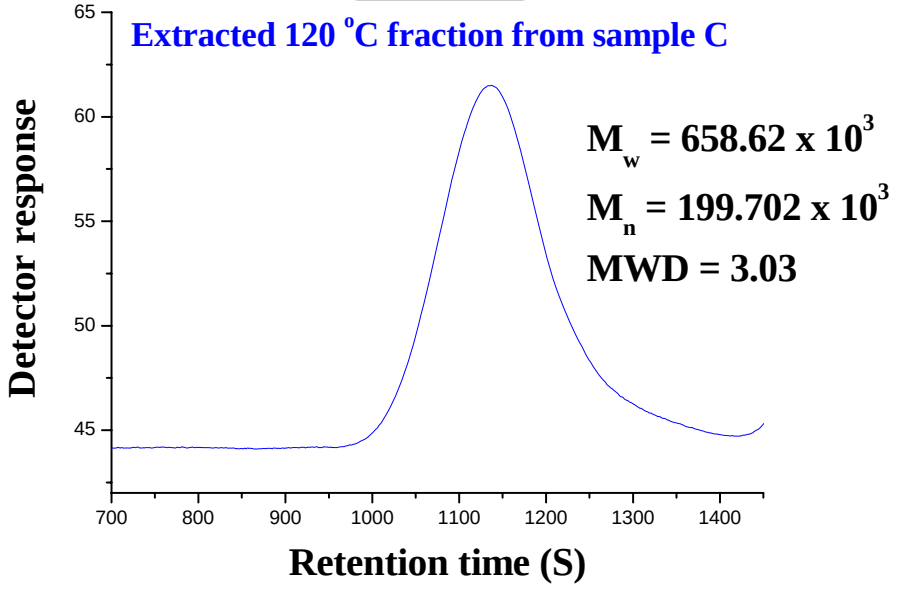
Extracted 120 °C fraction from sample C
M_w = 658.62 x 10^3
M_n = 199.702 x 10^3
MWD = 3.03
Detector response
Retention time (S)
65
60
55
50
45
700
800
900
1000
1100
1200
1300
1400

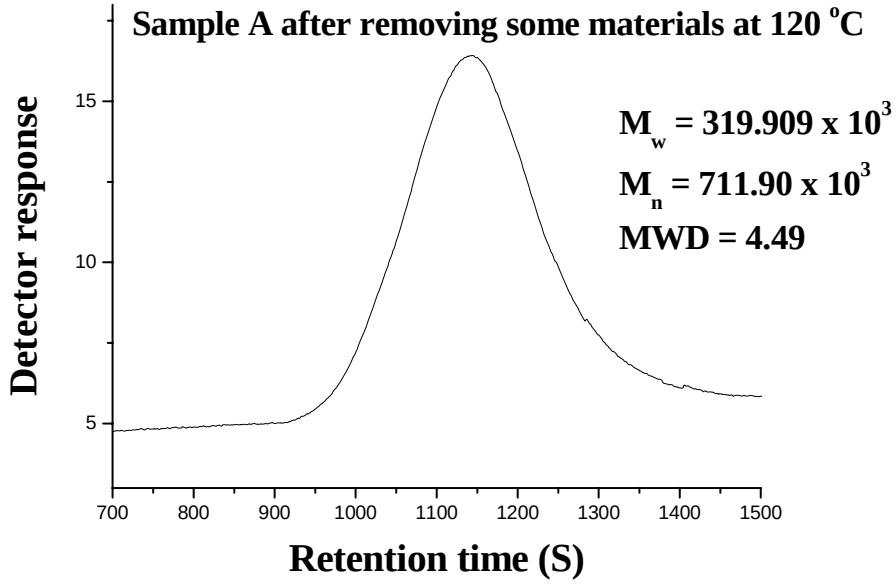
Sample A after removing some materials at 120 °C
Detector response
15
10
5
700
800
900
1000
1100
1200
1300
1400
1500
Retention time (S)
M_w = 319.909 x 10^3
M_n = 711.90 x 10^3
MWD = 4.49

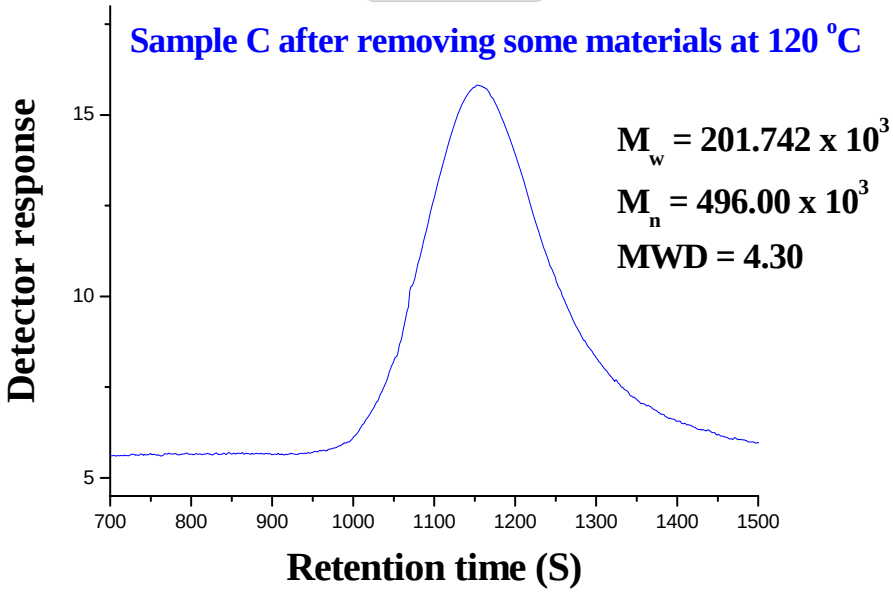
Sample C after removing some materials at 120 °C
Detector response
15
10
5
700
800
900
1000
1100
1200
1300
1400
1500
Retention time (S)
M_w = 201.742 x 10^3
M_n = 496.00 x 10^3
MWD = 4.30

APPENDIX B: DSC DATA

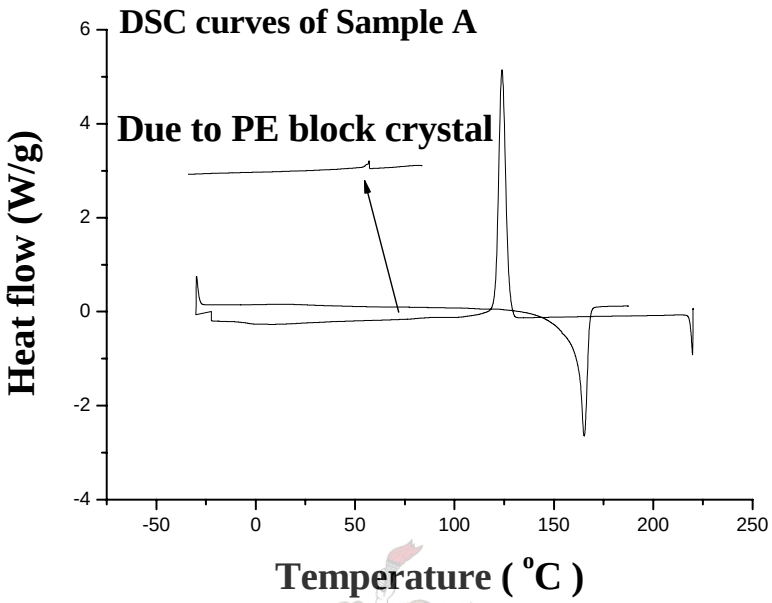

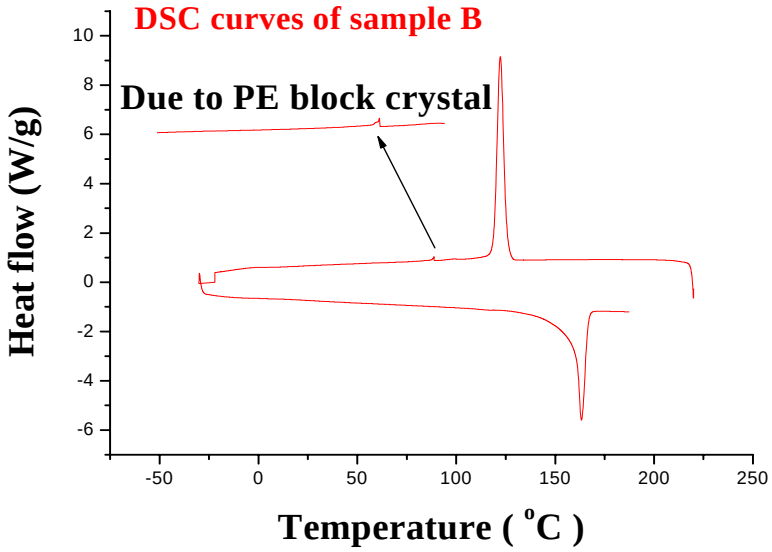

DSC curves of the extracted crystalline fraction from sample A

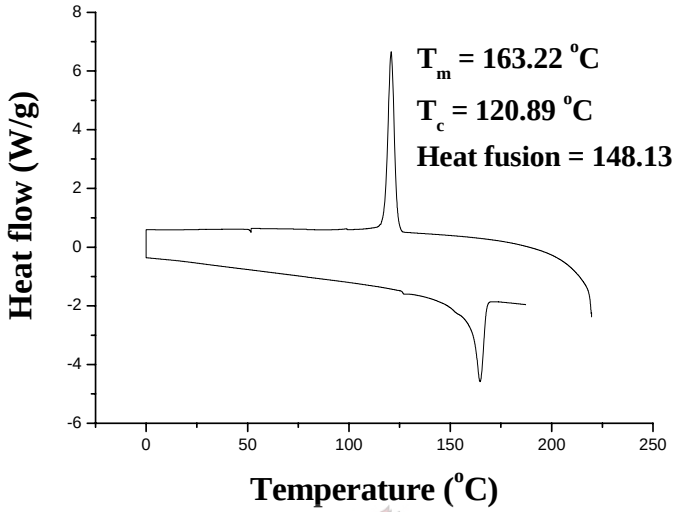

DSC curves of the extracted crystalline fraction from sample C

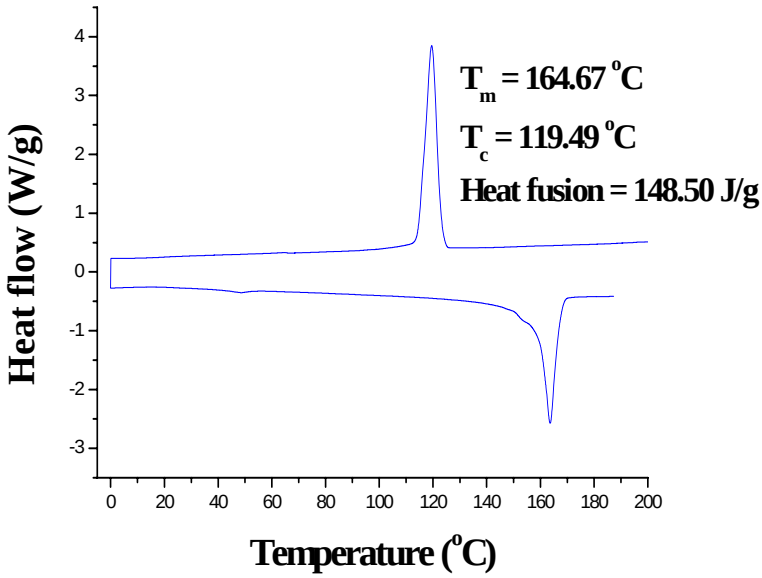

DSC curves of the extracted crystalline fractions from sample C.

DSC crystallization curve for the extracted soluble fraction from sample A

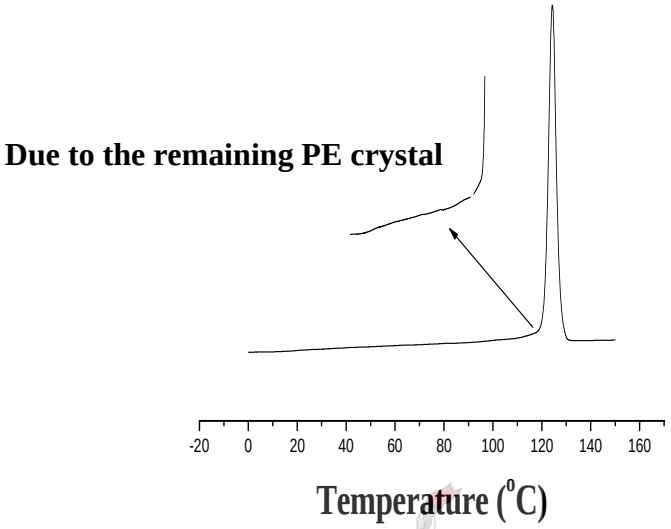

DSC crystallization curve for the extracted soluble fraction from sample B

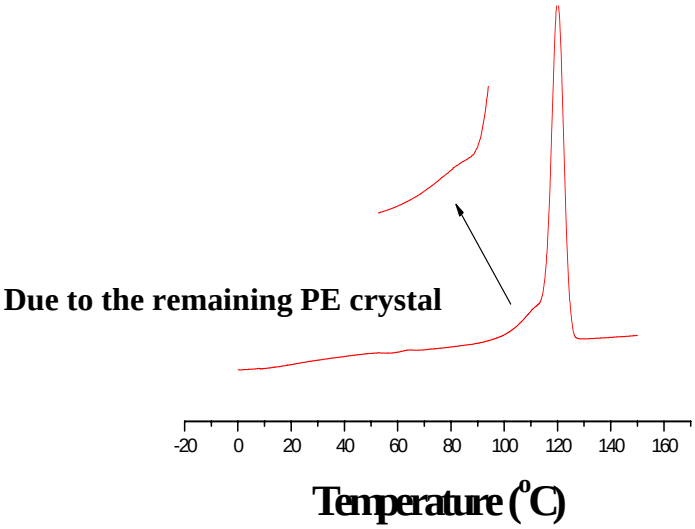

APPENDIX C: SEM IMAGES

SEM Magnifications of each tested sample

Sample	Magnification, μm			
	1	**2**	**3**	**4**
Sample A	179 x 100	179 x 100	179 x 100	-----
Sample B	176 x 200	142 x 200	176 x 200	-----
Sample C	224 x 200	224 x 200	224 x 200	-----
Sample A after removing the soluble fractions	140 x 200	159 x 200	159 x 200	-----
Sample B after removing the soluble fractions	135 x 200	194 x 200	194 x 200	-----
Sample C after removing the soluble fractions	169 x 200	169 x 200	169 x 200	-----
Sample A after removing some crystalline or high temperature fractions	140 x 200	140 x 200	126 x 200	-----
Sample C after removing some crystalline or high temperature fractions	159 x 200	159 x 200	204 x 200	204 x 200

- **Particle size and interparticle distance in sample A**

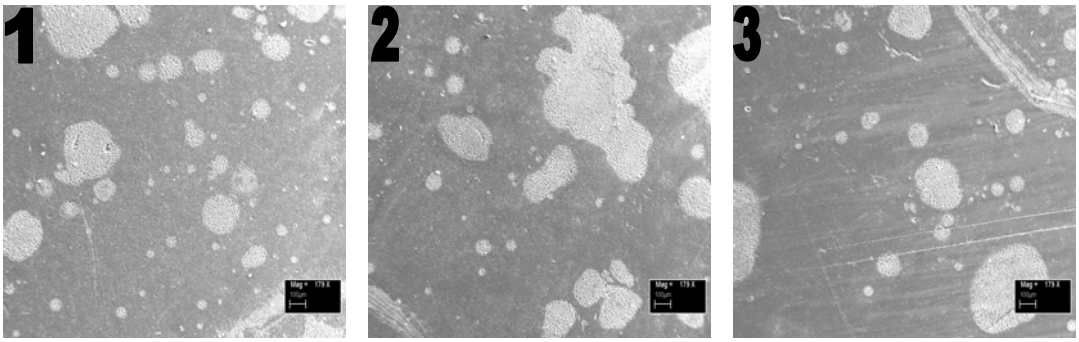

- **Particle size and interparticle distance in sample B**

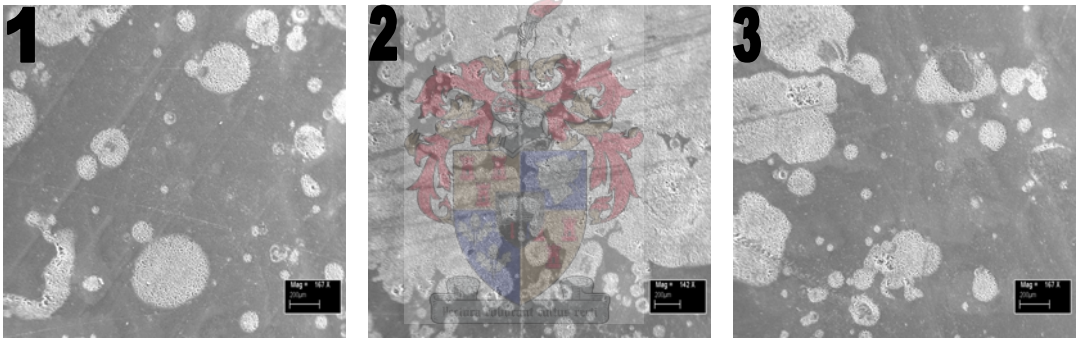

- **Particle size and interparticle distance in sample C**

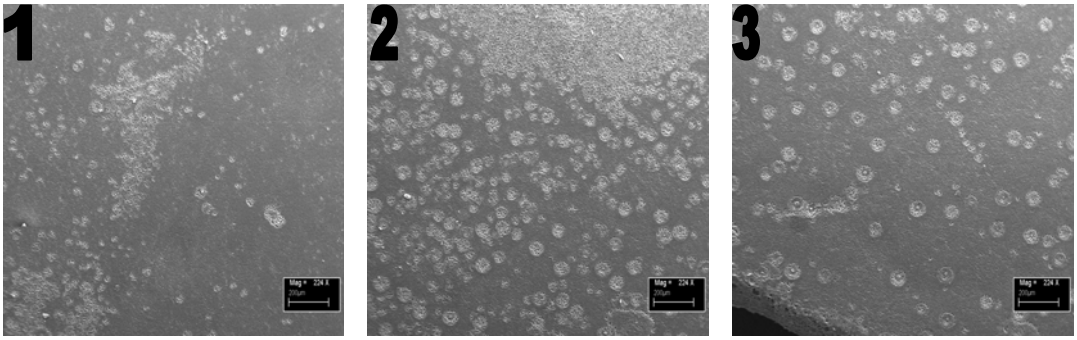

- **Particle size and interparticle distance in sample A after removing the soluble fractions**

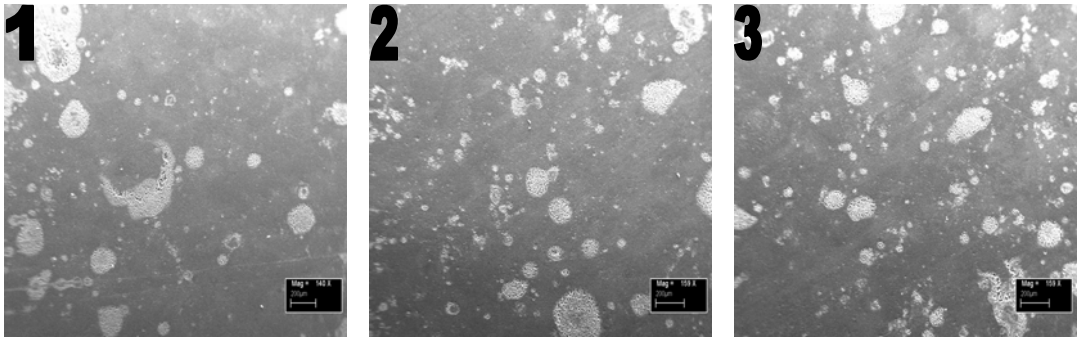

- **Particle size and interparticle distance in sample B after removing the soluble fractions**

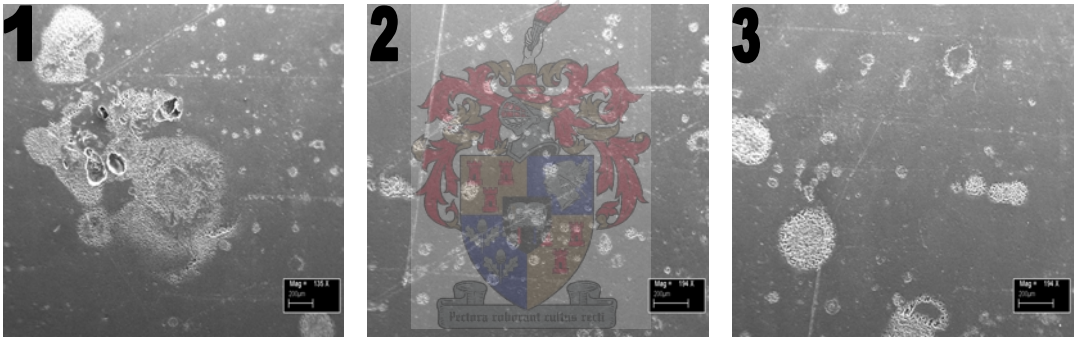

- **Particle size and interparticle distance in sample C after removing the soluble fractions**

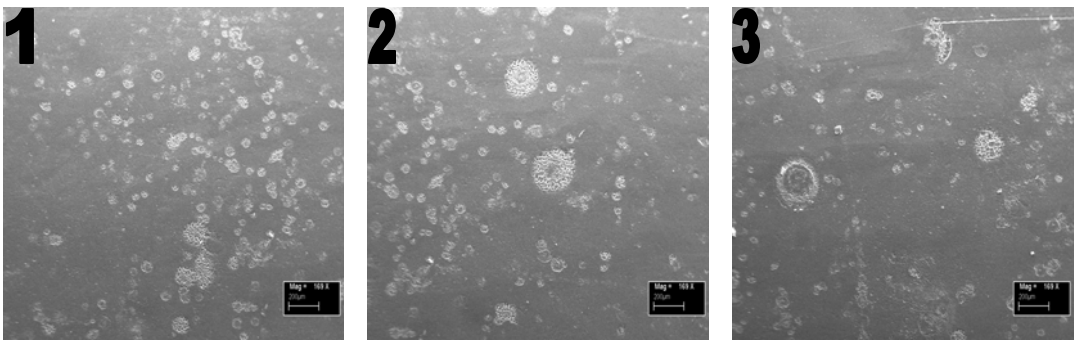

- **Particle size and interparticle distance in sample A after removing some crystalline or high temperature fractions (fraction at 120 oC)**

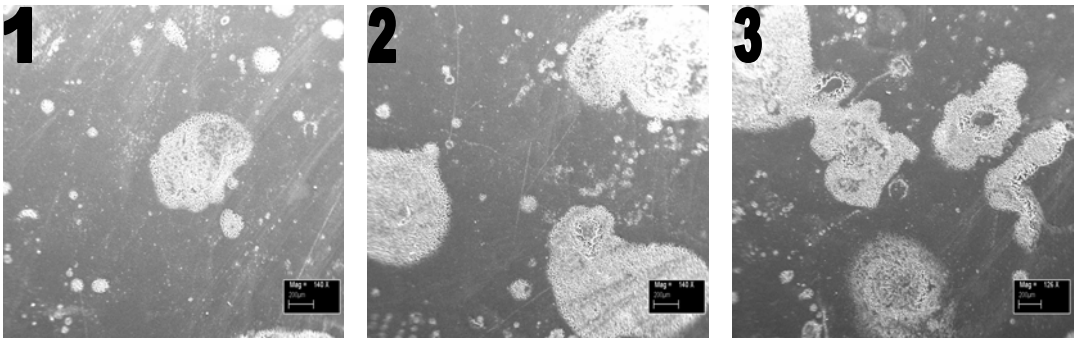

- **Particle size and interparticle distance in sample C after removing some crystalline or high temperature fractions (fraction at 120 ^{o}C)**

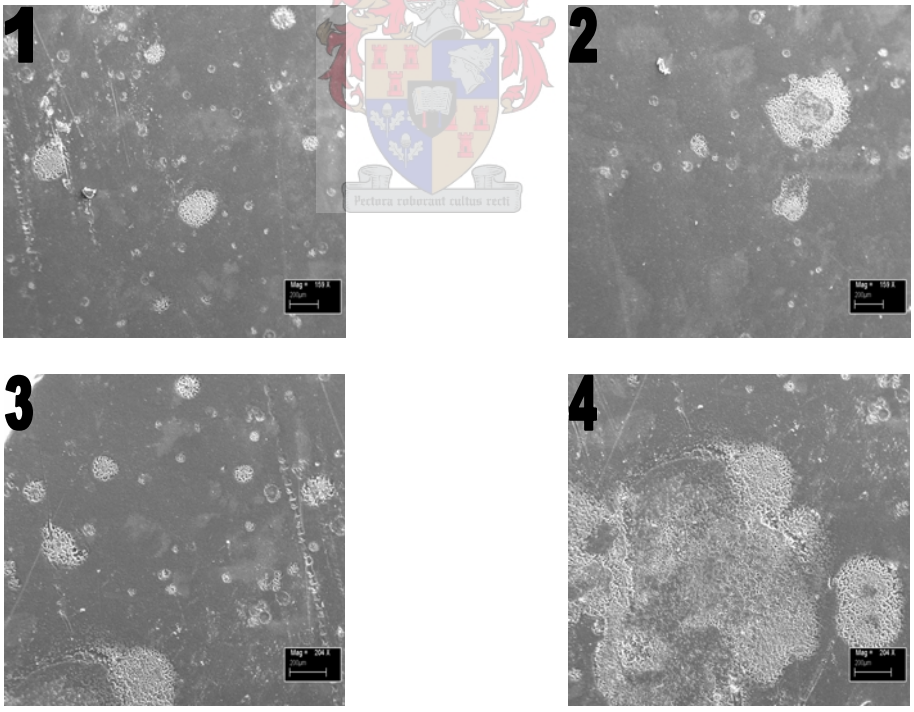

APPENDIX D: OPTICAL MICROSCOPY IMAGES

- **Particle size and interparticle distance in sample A (mag x 50 μm)**

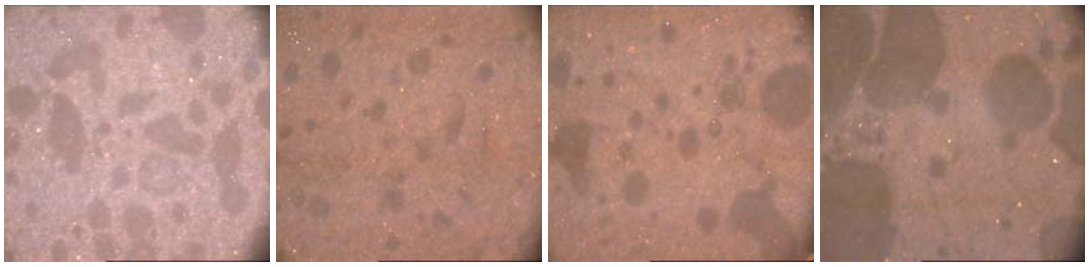

- **Particle size and interparticle distance in sample B (mag x 50 μm)**

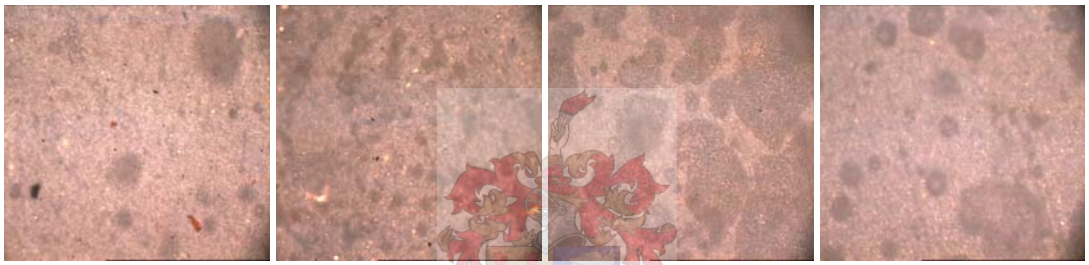

- **Particle size and interparticle distance in sample C (mag x 50 μm)**

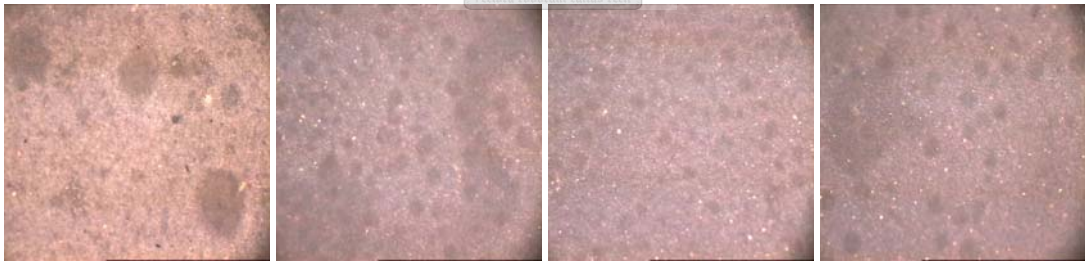

- **Particle size and interparticle distance in sample A after removing the soluble fractions (mag x 50 μm)**

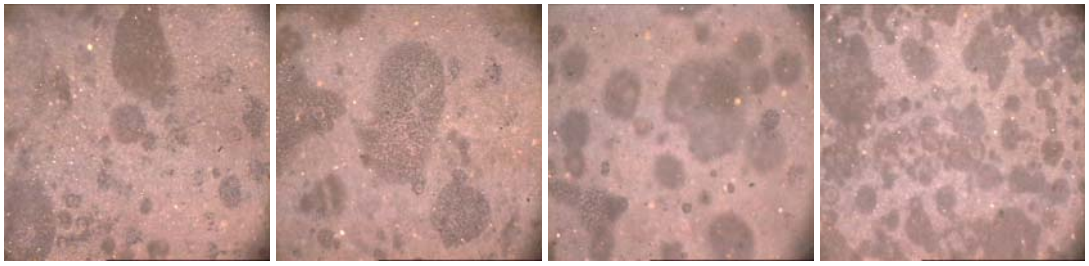

- **Particle size and interparticle distance in sample B after removing the soluble fractions (mag x 50 μm)**

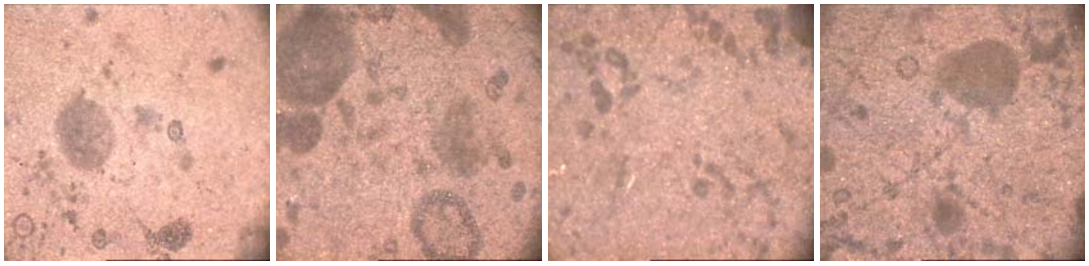

- **Particle size and interparticle distance in sample C after removing the soluble fractions (mag x 50 μm)**

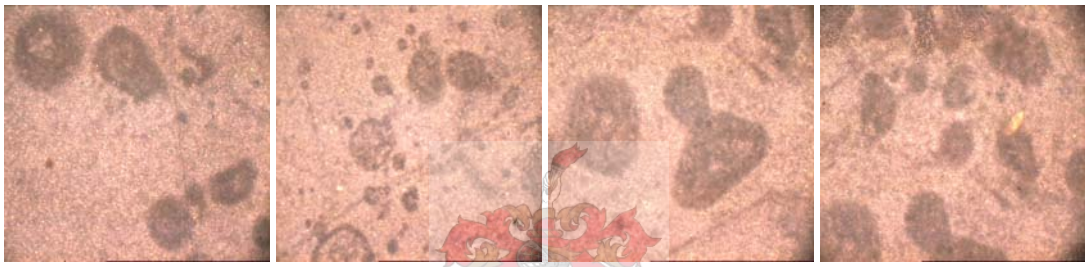

- **Particle size and interparticle distance in sample A after removing the high temperature fractions (120 ^{o}C fraction) (mag x 50 μm)**

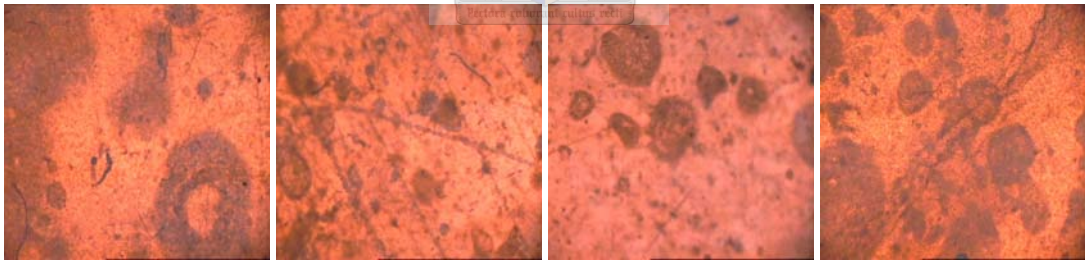

- **Particle size and interparticle distance in sample C after removing the high temperature fractions (120 ^{o}C fraction) (mag x 50 μm)**